

© 2014

Hetalben Patel

ALL RIGHTS RESERVED

DETECTION OF THE TIME-COURSE OF THIAMIN-BOUND INTERMEDIATES
ON ENZYMATIC PATHWAYS USING STEADY STATE AND TIME-RESOLVED
SPECTROSCOPY

By

HETALBEN PATEL

A Dissertation submitted to the
Graduate School-Newark
Rutgers, The State University of New Jersey

in partial fulfillment of the requirements

for the degree of

Doctor of Philosophy

Graduate Program in Chemistry

written under the direction of

Professor Frank Jordan

and approved by

Newark, New Jersey

January, 2014

THESIS ABSTRACT

Detection of the Time-course of Thiamin-bound Intermediates on Enzymatic Pathways

Using Steady State and Time-resolved Spectroscopy

By

Hetalben Patel

Thesis Advisor: Professor Frank Jordan

Since the discovery of thiamine diphosphate (ThDP, active form of vitamin B1) as active cofactor in 1937 by Lohmann and Schuster, its catalytic mechanism has become an interest of many enzymologist. The ThDP-dependent enzymes catalyze a variety of enzymatic reactions including decarboxylation, condensation, ligation etc.

Here is reported a mechanistic study carried out with multiple ThDP enzymes: *Escherichia coli* 1-deoxy- D-xylulose-5-phosphate (DXP) synthase, *E. coli* E1 component (E1o) of the 2-oxoglutarate dehydrogenase complex (OGDHc), yeast pyruvate decarboxylase (YPDC) and benzaldehyde lyase (BAL) by using state-of-the art instruments: the circular dichroism (CD) method can monitor events on the enzyme itself followed by pre-steady state rate determination by stopped-flow (SF) CD, the NMR method monitors ThDP-bound intermediates after release from the enzyme (fortuitously all the major ones are stable in acid), and is also useful to provide positive identification of the species seen in the CD spectrum. Several of these enzymes have in common initial pyruvate decarboxylation to form aldehyde or carboligation products. Steady state and pre-steady state analysis with the enzyme DXP synthase, enabled observation of remarkable stabilization of ThDP-bound pre-decarboxylation intermediate C2 α -

lactylThDP (LThDP) on the enzyme with pyruvate, and subsequent LThDP decarboxylation greatly accelerated by the second substrate D-glyceraldehyde-3-phosphate (GAP) by at least 600-fold. Further stabilization of LThDP was observed on DXP synthase variants Y392F, R478A and R420A which are shown to be essential for binding of D-GAP, without affecting the LThDP decarboxylation rates in the presence of GAP.

While DXP synthase stabilizes pre-decarboxylation intermediate LThDP, the enzyme E1o from *E. coli* on decarboxylation of 2-oxoglutarate stabilizes the resulting enamine intermediate followed by hydroxy-carboxypropylidene-ThDP radical formation (with both substrates 2-oxoglutarate and 2-oxoadipate), characterized by CD, SFCD, NMR and electron paramagnetic resonance (EPR) spectroscopy.

The *E. coli* E1o was also used in the chiral synthesis of α -hydroxy ketones with good yield and high enantiomeric excess, by varying both the 2-oxoacid substrates and exogenous aldehydes.

Next, The conjugated 2-oxoacid substrates acetyl pyruvate, its methyl ester and (*E*)-4-(4 chlorophenyl)-2-oxo-3-butenoic acid (CPB) with thiamin enzymes YPDC, BAL and E1o led to formation of charge transfer bands on the enzymes which are attributed to transitions between the thiazolium ring of thiamin and a C2- β , γ double bond.

ACKNOWLEDGEMENTS

First and foremost I want to thank my mentor and now my idol Professor Frank Jordan for his kind support and guidance throughout my research work. It has been an honor to be his Ph.D. student and a cause of countless pride. He patiently provided the vision, encouragement, and great freedom to pursue independent research work. I could not have imagined having a better advisor for my Ph. D. study.

Besides my advisor, I would also like to thank the rest of my thesis committee members for their encouragement and insightful comments in pre-oral, thesis defense and for their time in reviewing my thesis.

I am really thankful to Dr. Natalia Nemeria for her kind support and for teaching me basic biochemistry techniques. Studies with wt DXP synthase were carried out with her help. I am grateful to Dr. Anand Balakrishnan for the training during my initial year of graduate study.

This work would not have been possible without great collaborators from various areas. It's my great pleasure to acknowledge all the collaborators, Prof. Caren Freel Meyers from Johns Hopkins University for DXP synthase protein, Prof. Michael J. McLeish from IUPUI for BAL, Prof. David Chipman from Beer Sheva for GCL, Prof. Gary Gerfen at Albert Einstein College of Medicine for running EPR experiment with E1o.

My hearty thanks to my friend Dr. Sowmini Kumaran for being all the time with me. It was such an enjoyable period of time we spent together. I express my gratitude to

all the colleagues at chemistry department and staff members for their help in so many helpful aspects.

Finally, financial support of research on thiamin enzymes by the NIH (currently GM050380) is gratefully acknowledged.

Last but not the least, I would like to thank my family: my parents, incredibly wonderful husband Dr. Dinesh Manvar and my beautiful princess Ania for their love, patience and abundant sacrifices throughout this four years. This thesis and pursuit to reach this success would not have been possible without each of them. Two people deserves tons of thank you, my lovable husband Dinesh for everything and my beautiful daughter Ania who taught me how to enjoy the life along with learning.

DEDICATIONS

Heartily dedicated to my family, M. Sc. Advisor Prof. Anamik Shah, and in fond memory of my grandparents.

TABLE OF CONTENTS

THESIS ABSTRACT.....	ii
ACKNOWLEDGEMENTS.....	iv
LIST OF SCHEMES.....	xiii
LIST OF FIGURES.....	xiv
LIST OF TABLES.....	xvii
ABBREVIATIONS.....	xviii
CHAPTER 1. Introduction and overview of thiamin diphosphate-dependent enzyme mechanisms and potential intermediates on the pathways	
1 Detection of ThDP-related intermediates and their kinetic fates.....	2
1.1 ThDP-related intermediates prior to substrate addition.....	2
1.1.1 The canonical 4'-aminopyrimidine (AP) form of ThDP.....	3
1.1.2 The 1',4'-iminopyrimidine (IP) form of ThDP.....	3
1.1.3 The 1'H,4'-aminopyrimidinium (APH ⁺) form.....	4
1.1.4 Determination of the pK _a for the enzyme-bound APH ⁺ form.....	4
1.1.5 The C2-carbanion/ylide/carbene.....	5
1.2 Thiamin-bound intermediates with substrate or substrate analogue present.....	6
1.2.1 The Michaelis-Menten complex (MC).....	6
1.2.2 The covalent substrate-ThDP pre-decarboxylation complex (LThDP and analogues).....	7
1.2.3 Observation of LThDP analogues from chromophoric substrate analogues.....	7

1.2.4	The first post-decarboxylation intermediate: the enamine/C2 α -carbanion.....	7
1.2.5	The second post-decarboxylation intermediate, the product-ThDP complex (HEThDP, HBThDP).....	8
1.2.6	2-Acetylthiamin diphosphate, the 2-electron oxidation product of the enamine.....	9
1.2.7	The C2 α -hydroxyethylideneThDP radical, the 1-electron oxidation product of the enamine.....	9
1.3	Determination of rate-limiting steps and microscopic rate constants on ThDP enzymes	10

CHAPTER 2. Observation of thiamin-bound intermediates and determination of microscopic rate constants on 1-deoxy- D-xylulose 5-phosphate synthase.

2.1	Introduction.....	14
2.2	Materials and Methods.....	18
2.2.1.	Materials.....	18
2.2.2.	General methods.....	18
2.2.3.	Enzyme activity measurements.....	19
2.2.4.	Steady-state CD measurements.....	21
2.2.5.	Stopped-flow CD measurements.....	22
2.2.6.	NMR measurements.....	24
2.3	Results and Discussion.....	26
2.3.1	CD spectroscopy gives evidence of an elevated pK _a of the APH ⁺ form of ThDP on DXP synthase	26

2.3.2	Pyruvate analogues on DXP synthase form stable ThDP-bound pre-decarboxylation intermediates.....	27
2.3.3	Direct observation of the pre-decarboxylation LThDP intermediate formed from pyruvate on DXP synthase.....	30
2.3.4	pH dependence of steady state formation of DXP by DXP synthase.....	32
2.3.5	Time-resolved spectroscopic studies leading to key microscopic rate constants for DXP synthase mechanism.....	33
2.3.6	NMR confirmation of DXP formation by DXP synthase from pyruvate and D-GAP.....	37
2.3.7	The rate of enzyme-bound enamine reacting with alternative acceptors...	38
2.3.8	Arg-478 is essential for D-GAP binding.....	39
2.3.9	The R420A substitution stabilizes LThDP in the absence of D-GAP but does not reduce the rate of D-GAP promoted decarboxylation.....	43
2.3.10	The R420A substitution reduces affinity for D-GAP and stabilizes LThDP in the absence of D-GAP but does not reduce the rate of D-GAP promoted decarboxylation	43
2.3.11	Tyr-392 contributes to D-GAP affinity.....	45
2.3.12	Y392F stabilizes LThDP in the absence of D-GAP but does not affect D-GAP promoted decarboxylation.....	46
2.3.13	DXP product formation by R420A, R478A and Y392F DXP synthase...	48
2.3.14	Behavior of CD ₃₁₃ under in stopped-flow CD experiments of LThDP decarboxylation in the presence of GAP	50
2.4	Conclusions.....	51

CHAPTER 3. Detection of an enamine intermediate and C2 α - hydroxy-carboxypropylidene-ThDP radical on E1 component of 2-oxoglutarate dehydrogenase complex from *Escherichia coli*

3.1	Introduction.....	54
3.2	Materials and Methods.....	57
3.2.1	Materials.....	57
3.2.2	Activity Measurements.....	57
3.2.3	Circular dichroism experiments with substrates.....	59
3.2.4	Stopped-flow CD.....	59
3.2.5	Rapid chemical quench and NMR experiments.....	60
3.2.6	Sample preparation for EPR spectroscopy.....	61
3.3	Results and Discussion.....	61
3.3.1	ThDP on E1o	61
3.3.2	Formation of post decarboxylation intermediate on E1o with substrates OG and 2-OA	62
3.3.3	Pre-steady state rates of formation of ThDP-bound intermediates on E1o with substrates 2-OG and 2-OA.....	66
3.3.4	What is the origin of CD signal ~350 nm?	68
3.3.5	Identification of hydroxy-carboxypropylidene-ThDP radical with 2-OG and 2-OA.....	73
3.4	Conclusions.....	74

CHAPTER 4. Investigation of the donor and acceptor range for chiral carboligation catalyzed by the E1 component of the 2-oxoglutarate dehydrogenase complex

4.1	Introduction.....	75
4.2	Materials and Methods.....	77
4.2.1	Materials.....	77
4.2.2	CD spectroscopy to monitor the carboligase product formation	78
4.2.3	NMR spectroscopy to characterize the carboligase product.....	78
4.2.4	Chiral GC analysis for <i>ee</i> measurement.....	79
4.3	Results and Discussion.....	79
4.3.1	The ThDP-dependent enzyme E1 α can catalyze carboligase reactions not only with acid but also with ester as acceptor substrate.....	80
4.3.2	Characterization of chiral product and <i>ee</i> calculation by using CD spectroscopy and chiral GC.....	81
4.4	Conclusions.....	88

CHAPTER 5. Identification of charge transfer transitions related to thiamin-bound intermediates on enzymes provides a plethora of signatures useful in mechanistic studies

5.1	Introduction.....	90
5.2	Materials and Methods.....	94
5.2.1	Materials	94
5.2.2	Synthesis of 4-hydroxy-2-oxopent-3-enoic acid.....	94
5.2.3	Enzyme purification and activity assays.....	94
5.2.4	Circular Dichroism Experiments.....	95

5.2.5	Rapid-Scan Stopped-Flow Photodiode Array (PDA) Experiments of BAL with CPB.....	96
5.3	Results and Discussion.....	97
5.3.1	ThDP on YPDC	97
5.3.2	Studies with ACP and MACP.....	98
5.3.3	Reaction of fluoropyruvate with E1p	100
5.3.4	Studies with a longer conjugated system CPB	100
5.4	Conclusions.....	103
	REFERENCES.....	105
	APPENDIX.....	113
	CURICULUM VITAE.....	134

LIST OF SCHEMES

- Figure 2.1 Mechanism of yeast pyruvate decarboxylase YPDC
- Scheme 2.1 The catalytic cycle of DXP synthase
- Scheme 2.2 Formation of covalent adduct of ThDP with pyruvate and analogues MAP, BAP and AcPhi
- Scheme 2.3 Alternative acceptors for the enamine reactions under steady state conditions
- Scheme 3.1 A. Mechanism of pyruvate and 2-oxoglutarate dehydrogenase complexes
B. Formation of one electron oxidation product ThDP radical
- Scheme 4.1 E1o catalyzed reaction mechanism of carboligase product
- Scheme 5.1 Mechanism of CT band formation on ThDP enzymes using ACP, MACP, fluoropyruvate and CPB
- Scheme 5.2 Mechanism of benzaldehyde lyase, BAL with benzoylformate decarboxylase side reaction

LIST OF FIGURES

- Figure 2.1 pH titration of the AP form of ThDP on DXP synthase
- Figure 2.2 CD titration of DXP synthase with MAP
- Figure 2.3 Formation of 1',4'-iminopyrimidinyl tautomer on DXP synthase with BAP
- Figure 2.4 Formation of 1',4'-iminopyrimidinyl tautomer on DXP synthase with AcPhi
- Figure 2.5 Formation of LThDP on DXP synthase with pyruvate
- Figure 2.6 Dependence of (*R*)-acetolactate production on pyruvate concentration
- Figure 2.7 pH dependence of DXP product formation using CD spectroscopy
- Figure 2.8 Rates of 1', 4'-iminoLThDP formation by DXP synthase with pyruvate under pre-steady state conditions and characterization of LThDP by ¹H NMR
- Figure 2.9 Rate constant of 1', 4'-iminoLThDP decarboxylation by DXP synthase with pyruvate in the presence of D-GAP
- Figure 2.10 DXP product formation by DXP synthase
- Figure 2.11 Active site residues of interest highlighted on *D. radiodurans* DXP synthase
- Figure 2.12 Steady state and pre-steady state study with R478A DXP synthase
- Figure 2.13 NMR detection of [1-¹³C]-DXP formation by R478A DXP synthase during pre-steady state, D-GAP promoted decarboxylation of pre-formed [C2β-¹³C]-LThDP
- Figure 2.14 Steady state and pre-steady state study with R420A DXP synthase

- Figure 2.15 Steady state and pre-steady state study with Y392F DXP synthase
- Figure 2.16 Pre-steady state rate of DXP formation by the DXP synthase variants R478A, R420A and Y392F
- Figure 3.1 Observation of IP and AP form of ThDP on E1o without substrate
- Figure 3.2 Formation of intermediates and/or hydroxy-carboxypropylidene-ThDP radical on E1o-ec with 2-OG and 2-OA
- Figure 3.3 NMR spectrum of acid quench reaction of [C₂,C₆'-¹³C₂]ThDP labeled E1o with 2-OG in the absence and presence of DCPIP and formation of hydroxy-carboxypropylidene-ThDP by reacting E1o with succinic semialdehyde
- Figure 3.4 Pre-steady state rate determination of post-decarboxylation intermediate, an enamine and/or hydroxy-carboxypropylidene-ThDP radical on E1o
- Figure 3.5 Stopped-flow CD behavior at 365 nm using different concentration of 2-OG with E1oec
- Figure 3.6 Effect of different enamine acceptors on CD at 365 nm
- Figure 3.7 Radical detection on E1oec with 2-OG and 2-OA by EPR spectroscopy
- Figure 4.1 Substrates and acceptors for carboligase reaction
- Figure 4.2 E1o catalyzed formation of acetoin-like chiral product
- Figure 4.3 Structure and nomenclature of the chiral products produced from the E1o catalyzed reaction by using variety of acceptors and substrates
- Figure 4.4 CD and chiral GC analysis of compounds **1-9**

- Figure 4.5 Characterization of compounds **1-9** by ^1H NMR
- Figure 5.1 pH dependence of IP form of ThDP formed by titration of YPDC variant E477Q with pyruvate
- Figure 5.2 Formation of charge transfer band on E1o and E477Q YPDC
- Figure 5.3 Formation of enamine by reacting YPDC with CPB and CT band by CD titration of BAL with CPB
- Figure 5.4 Time-dependent formation of a CT band on BAL with CPB

LIST OF TABLES

Table 1.1	Detection of ThDP-related intermediates
Table 1.2	The pK_a of enzyme-bound APH^+ on ThDP enzymes
Table 2.1	Assignment of the 1', 4'-iminopyrimidine tautomeric form of ThDP-bound pre-decarboxylation intermediates from substrate and analogues on DXP synthase using CD spectroscopy
Table 2.2	Microscopic rate constants for LThDP formation and decarboxylation and DXP formation on R478A, R420A and Y392F DXP synthase
Table 3.1	K_m determination from DCPIP and overall activity of E1o with substrates
Table 3.2	Pre-steady state rate determination on E1o with 2-OG in the presence of enamine acceptors
Table 4.1	Enantiomeric excess of acetoin-like product formation by E1o using chiral GC
Table 5.1	Steady state detection of CT band related to ThDP on enzymes by CD spectroscopy

ABBREVIATIONS

ThDP, thiamin diphosphate

DXP synthase, 1-deoxy- D-xylulose-5-phosphate synthase enzyme

GAP, D-glyceraldehyde-3-phosphate

DXP, 1-deoxy- D-xylulose-5-phosphate, condensation product of pyruvate and D-glyceraldehyde-3-phosphate

DXS, 1-deoxy- D-xylulose-5-phosphate, condensation product of pyruvate and D-glyceraldehyde

LThDP, C2- α -lactylthiamin diphosphate

MAP, methyl acetylphosphonate

AcPhi, acetyl phosphinate

BAP, butyl acetylphosphonate

NADH, nicotinamide adenine dinucleotide

YADH, yeast alcohol dehydrogenase

DCPIP, 2,6-dichlorophenolindophenol

IP, 1', 4'-iminopyrimidine form of ThDP

AP, 4'-aminopyrimidine form of ThDP

APH⁺, 4'-aminopyrimidinium conjugate acid form of ThDP

HEThDP, C2 α -hydroxyethyl-ThDP, the adduct of acetaldehyde and ThDP

HBThDP, C2 α -hydroxybenzylThDP, the adduct of benzaldehyde and ThDP

TCA, trichloroacetic acid

HEPES, 4-(2-hydroxyethyl)-1-piperazineethanesulfonic acid

Tris, tri(hydroxymethyl)aminomethane

DTT, dithiothreitol

YPDC, yeast pyruvate decarboxylase from *Saccharomyces cerevisiae*

OGDHc, 2-oxo glutarate dehydrogenase complex

E1o, the first E1 component of the *E. coli* OGDHc

E2o, E2 component of OGDHc

LDo, lipoyl domain of E2o

DDo, didomain of E2o-ec¹⁻¹⁷⁶

E1p, the E1 component of the *E. coli* pyruvate dehydrogenase complex

IPTG, isopropyl- β -D-thiogalactopyranoside

2-OG, 2-oxoglutarate

2-OA, 2-oxoadipate

gCHSQC, gradient carbon heteronuclear single quantum coherence

EPR, electron paramagnetic resonance spectroscopy

BAL, benzaldehyde lyase

GCL, glyoxylate carboligase

TK, transketolase

POX, pyruvate oxidase from *Lactobacillus plantarum*

BFDC, benzoylformate decarboxylase

CD, circular dichroism

SF, stopped-flow

PDA, photodiode array

YI, the C2-carbanion/ylide/carbene form conjugate base of ThDP

3-PKB, (*E*)-4-(pyrid-3-yl)-2-oxo-3-butenoic acid

CT, charge transfer

ACP, acetyl pyruvate

MACP, methyl acetyl pyruvate

CPB, (*E*)-4-(4 chlorophenyl)-2-oxo-3-butenic acid

MES, 2-(N-morpholino) ethanesulfonic acid

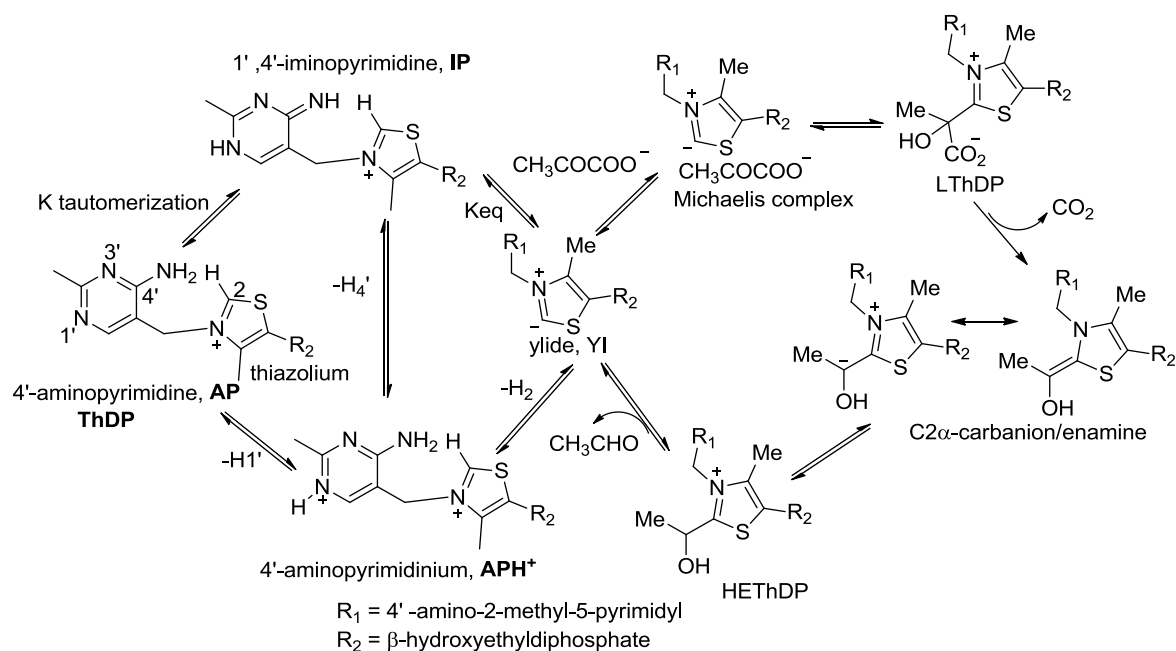
CHAPTER 1

Introduction and overview of thiamin diphosphate-dependent enzyme mechanisms and potential intermediates on the pathways

Thiamin (vitamin B1) is a water soluble vitamin with chemical formula $C_{12}H_{17}N_4OS$. Its diphosphate derivative or active form, thiamin diphosphate (ThDP) is a coenzyme involved in sugar and amino acid catabolism. The ThDP-dependent enzymes are multifunctional biocatalysts, involved in metabolic pathways and catalyze a variety of enzymatic reactions including C-C bond formation to form chiral α -hydroxy ketones (Chapter 4). The chemistry and enzymology of ThDP is intimately dependent on three chemical moieties comprising the coenzyme: a thiazolium ring, a 4-aminopyrimidine ring and the diphosphate side chain (Scheme 1.1, Left). From the large number of high-resolution X-ray structures available for the past 20 years (starting with transketolase (TK)⁽¹⁾, pyruvate oxidase (POX)⁽²⁾ from *Lactobacillus plantarum* and pyruvate decarboxylase (YPDC)^(3, 4) from the yeast *Saccharomyces cerevisiae*, it has become clear that the diphosphate serves to bind the cofactor to the protein.

Chemically, the thiazolium ring is central to catalysis as reported in seminal studies by Breslow⁽⁵⁾, due to its ability to form a key nucleophilic center, the C2-carbanion/ylide/carbene resonance forms. The 4'-aminopyrimidine moiety has gained more recognition as an important contributor to catalysis since the appearance of the X-ray structures showing its conserved proximity to the C2 thiazolium atom and the possibility for its participation in acid-base catalysis.⁽⁶⁾ This makes ThDP a truly unique and bi-functional coenzyme.

Scheme 1.1 Mechanism of yeast pyruvate decarboxylase YPDC.



1. Detection of ThDP-related intermediates and their kinetic fates.

The presentation of thiamin-related and thiamin-bound intermediates represent pre-, or post-substrate (or substrate analogue) binding states, an important distinction needed with the recent identification of several forms of ThDP on the enzymes.

1.1 ThDP-related intermediates prior to substrate addition. During the past decade, our laboratory with collaborators (whose enzymes enable generalization of the findings) established the presence of various tautomeric and ionization states of ThDP (Scheme 1.1). A need arose to identify spectral signatures for various tautomeric and ionization states of the 4'-aminopyrimidine ring of ThDP (Table 1.1).

1.1.1 The canonical 4'-aminopyrimidine (AP) form of ThDP. The signature for this species is a negative circular dichroism (CD) band centered near 320-330 nm as illustrated with the enzyme benzaldehyde lyase (BAL). A number of studies on YPDC and E1ec and their variants, as well as chemical model studies in our laboratory suggest that this UV/CD band is due to a charge transfer transition between the 4'-aminopyrimidine ring as donor and the thiazolium ring as acceptor. The band has been observed on 10 ThDP enzymes, and its observation depends both on the pH and also on the specific enzyme environment.

1.1.2 The 1',4'-iminopyrimidine (IP) form of ThDP. The notion that the 4'-aminopyrimidine could exist in its 1',4'-iminopyrimidine tautomeric form was suggested by models attempting to mimic the reactivity of such a tautomer. The N1'-methyl analogue of both the 4-aminopyrimidine ring and of thiamin was synthesized and gave evidence of two relevant points: (i) in this N1'-methylpyrimidinium the pK_a of the exocyclic amine was reduced to ca. 12-12.5^(7, 8), offering a rationale for the presence of a conserved glutamate as a catalyst for the amino \rightleftharpoons imino tautomerization, and (ii) with the positive charge on the ring, the amino protons undergo differential exchange rates and the exchange is buffer catalyzed.⁽⁹⁾ A spectroscopic signature for the 1',4'-iminopyrimidylThDP tautomer was first identified on the slow E477Q variant of YPDC. The CD bands corresponding to the AP and IP forms have different phases, enabling observation of both bands simultaneously, making the CD method useful. The electronic absorption characteristics of the APH⁺ and the ylide (Yl) forms are yet to be established.

1.1.3 The 1'H, 4'-aminopyrimidinium (APH⁺) form. The existence of the protonated 4'-aminopyrimidinium ion APH⁺ received positive confirmation by solid state NMR measurements on three enzymes: YPDC, and the E1 components of both the pyruvate dehydrogenase and 2-oxoglutarate dehydrogenase complexes from *E. coli*, on the basis of the characteristic ¹³C and ¹⁵N chemical shifts. The need for solid state NMR is due to the large molecular mass of all ThDP enzymes (at least 120 kDa).⁽¹⁰⁾

Table 1.1 Detection of ThDP-related intermediates.

Prior to substrate addition	With substrate present
-AP form of ThDP (-CD at 320-330 nm)	-Michaelis complex (- CD at 325-335 nm)
-IP form of ThDP (+CD at 300-314 nm)	-Pre-decarboxylation intermediate
-APH ⁺ form of ThDP (no CD signature)	(CD+300-314nm) ^a
-C2-carbanion/ylide/carbene (no CD signal)	-Enamine/C2 α carbanion (290-295 nm for aliphatic & ~380 nm for aromatic substrate)
	-HEThDP
	-2-acetylThDP
	-C2 α -HEThDP radical

^awith chromophoric substrate ~400 nm.

1.1.4 Determination of the pK_a for the enzyme-bound APH⁺ form. By lowering the pH, the amplitude of the band for the AP or IP form diminishes with an apparent pK_a value for the ([AP]+[IP])/[APH⁺] equilibrium. This pK_a in water for ThDP is 4.85⁽¹¹⁾, while on the enzymes it ranges from 5.6 to 7.5 (Table 1.2). It was concluded from data in Table

1.2, that the pK_a for the APH^+ coincides with the pH of optimum activity for each enzyme, indicating that all three forms IP, AP and APH^+ must be readily accessible during the catalytic cycle. The pK_a elevation on the enzymes could be rationalized by the presence of the highly conserved glutamate near the N1' position of ThDP that would tend to make the 4'-aminopyrimidine ring more basic.

Table 1.2 The pK_a of enzyme-bound APH^+ on ThDP enzymes.⁽¹²⁾

<i>Enzyme</i>	<i>pK_a for the ([AP]+[IP])/(APH⁺)</i>
BAL	7.42 ± 0.02
BFDC	7.54 ± 0.11
POX	5.56 ± 0.03
E1h	7.07 ± 0.07
E1o	7.2 ± 0.01
GCL V51D	6.1 ± 0.02
DXP synthase	7.5 ± 0.09

1.1.5 The C2-carbanion/ylide/carbene. According to Breslow's findings, proton loss at the thiazolium C2 position is required to initiate the catalytic cycle. In 1997 there were two reports with significant implications regarding this issue: (i) A 1H NMR-based method was presented for measuring the rate of H/D exchange at the C2 position of bound ThDP, providing the rate constant for the dissociation of the C2H to the ylide.⁽¹³⁾ (ii) Arduengo and colleagues showed that the conjugate bases of imidazolium and indeed

of thiazolium salts could be generated and their structure evaluated by NMR methods.⁽¹⁴⁾ The ^{13}C chemical shift of the C2 resonance shifted from 157 to 253 ppm on conversion of their model thiazolium compound to its conjugate base ylide.⁽¹⁴⁾

1.2 Thiamin-bound intermediates with substrate or substrate analogue present.

What makes detailed mechanistic studies of ThDP enzymes feasible is a powerful array of methods to monitor the kinetic fate of each intermediate along the catalytic cycle of all ThDP enzymes. An important method was developed for determination of the rate constants for individual steps by Tittmann and Hübner ('TH method').⁽¹⁵⁾ The TH method takes advantage of the known acid stability of the intermediates in Schemes 1.1, so that using either rapid quench or manual quench methods one can 'freeze' the intermediates under acidic conditions while also precipitating the enzyme. The chemical shifts of the C6'H resonances of each intermediate are sufficiently distinct from each other and from that of the unsubstituted ThDP, making ^1H NMR an efficient method for evaluation of the relative concentrations of the intermediates under steady state conditions, which in turn enable calculation of rate constants for individual reaction steps.

1.2.1 The Michaelis-Menten complex (MC). The earliest detection of an MC was on addition of a substrate analogue methyl acetylphosphonate (MAP) and acetylphosphinate to several ThDP enzymes. An example is shown with acetylphosphinate added to YPDC leading to a negative CD band at ca. 325-335 nm, reminiscent of the band observed for the AP form. In this example, addition of ThDP alone did not display the AP form, the

negative CD band only appeared after addition of substrate analogue, and hence the band must pertain to a MC.⁽¹⁶⁾

1.2.2 The covalent substrate-ThDP pre-decarboxylation complex (LThDP and analogues).

Observation of the intermediate analogues derived from substrate analogue phosphonates and phosphinates. The IP form (positive CD band, 300-314 nm) on ThDP enzymes, resulted from formation of a stable pre-decarboxylation adduct not a MC of ThDP with (a) MAP or acetylphosphinate($\text{CH}_3\text{C}(\text{C}=\text{O})\text{P}(\text{H})\text{O}_2\text{Na}$) and (b) the aromatic 2-oxoacid analogue methyl benzoylphosphonate (MBP). With 10 enzymes tested so far, the IP form appeared on the stopped-flow time scale (either absorption or CD mode): the reaction is efficiently catalyzed by all of the enzymes.

In some favorable cases, the CD band for the true pre-decarboxylation intermediate (via the IP form) could be observed from the slow substrates. More recently, formation of surprisingly stable LThDP was observed on the enzyme 1-deoxy-D-xylulose 5-phosphate synthase (DXP synthase, condenses the enamine derived from pyruvate with the acceptor D-glyceraldehyde-3-phosphate, GAP) in the absence of GAP (Chapter 2).⁽¹⁷⁾

1.2.3 Observation of LThDP analogues from chromophoric substrate analogues. On three enzymes, YPDC, E1o and BAL, formation of the pre-decarboxylation adduct formed with ThDP from a chromophoric substrate analogue was observed on CD at unexpected longer wavelength (Chapter 5).

1.2.4 *The first post-decarboxylation intermediate: the enamine/C2 α -carbanion.*

According to Scheme 1.1 the enamine is the only conjugated covalent ThDP-bound intermediate. UV-VIS observation of enzyme-bound enamine derived from aliphatic substrates is difficult due to the expected λ_{max} near 290-295 nm, according to thiazolium-based models and ~380 nm with aromatic substrates. The enamine is chiral on the enzyme, even though it is planar and conjugated; hence all intermediates here discussed are chiral on the enzymes, both pre- and post-substrate addition. The CD measurements nicely confirm this expectation for all intermediates, both covalently bound and even non-covalent ones such as the MC.

1.2.5 *The second post-decarboxylation intermediate, the product-ThDP complex (HEThDP, HBThDP).*

Evidence for formation of this intermediate can be confirmed by using the TH method. As mentioned above that C6'-H has different chemical shift for all the intermediates. The HEThDP was observed on E1o-ec with its substrate 2-OG at 7.35 ppm (Chapter 3). While HEThDP is not usually considered to be on the reaction pathway of ThDP-dependent oxidative decarboxylases, groups working with POX and the PDHc's have long used HEThDP as an alternate substrate. Based on previous studies at Rutgers, HEThDP cannot be oxidized directly by either FAD or lipoic acid as oxidizing partners. Instead, oxidation must be preceded by ionization at the C2 α position to generate the enamine, which is then prone to oxidation by even molecular dioxygen from air. However, the pK_a at the C2 α position is very high, estimated at ca. 17-18 for HEThDP derived from pyruvic acid.

1.2.6 2-Acetylthiamin diphosphate, the 2-electron oxidation product of the enamine.

This compound is the product of oxidation of the enamine by any one of the following oxidizing agents on enzymes: the dithiolane ring of lipoic acid covalently amidated to a lysine side chain in the 2-oxoacid dehydrogenase multienzyme complexes; less frequently by FAD in the pyruvate oxidases; finally by NAD^+ . The POX reaction has been studied for many years and evidence suggests that the oxidation takes place via single electron transfers with the likely intermediacy of the radical cation species delocalized onto the thiazolium ring. Our group published evidence indicating that in the presence of an artificial oxidizing agent 2,6-dichlorophenoindophenol the enamine produced by E1p is converted to 2-acetylThDP, while in the presence of the E2p component, there is no apparent 2-acetylThDP on the way to reductive acetylation. This could signal that both pathways may be available to the enzymes.

1.2.7 The $\text{C2}\alpha$ -hydroxyethylideneThDP radical, the 1-electron oxidation product of the enamine. Early and clear evidence for a free-radical mechanism on ThDP enzymes was obtained on pyruvate-ferredoxin oxidoreductase, an enzyme that converts pyruvate to acetylCoA in anaerobes. In addition to ThDP, the enzyme has three Fe_4S_4 clusters forming a 40-50Å long electron transfer chain. The stability of the free radical was manifested by the fact that the crystal structure also displayed an electron paramagnetic resonance signal. A chemical model was generated for the electrochemical oxidation of the enamine leading to dimerization at the $\text{C2}\alpha$ atom, suggesting significant electron spin density at this atom. Subsequent detailed work on pyruvate-ferredoxin oxidoreductase clearly showed that the spin density is delocalized into the thiazolium ring, but there

indeed is a significant fraction at the C2 α atom. The enzyme pyruvate oxidase using both ThDP and FAD as cofactors also uses a free radical mechanism. Recently, the ThDP radical was reproduced on E1 α -ec with substrates 2-oxoglutarate and 2-oxoadipate (Chapter 3). At the same time, there are ThDP enzymes with no known redox role for the bound FAD, such as glyoxylate carboligase (GCL). This enzyme carries out decarboxylative carboligation, similar to DXP synthase. Perhaps the most striking feature of glyoxylate carboligase is the replacement of the virtually universally conserved Glu residue opposite the N1' atom of ThDP by a hydrophobic residue. GCL and BAL are of particular interest since on neither enzyme is there an acid-base residue within hydrogen bonding distance of the ThDP to assist with proton transfers. There is perhaps no alternative to water carrying out the proton transfers on these two enzymes. Of course, these enzymes also provide strong support for an obligatory catalytic role of the 4'-aminopyrimidine ring of the ThDP.

1.3 Determination of rate-limiting steps and microscopic rate constants on ThDP enzymes.

Starting with the 1970s, both solvent and heavy-atom kinetic isotope effects (KIE) were employed to probe the rate-limiting steps in ThDP enzymes, especially on YPDC. $^{13}\text{C}/^{12}\text{C}$ KIEs used natural abundance ^{13}C label at the pyruvate C1 atom by measuring the mass ratio of $^{45}\text{CO}_2/^{44}\text{CO}_2$ using an isotope ratio mass spectrometer. Supported by a model study in which the decarboxylation step could be isolated, the results of such studies could inform about the partitioning of the LThDP intermediate reverting to pyruvate and free coenzyme or going forward to decarboxylation to the enamine (Scheme 1.1). The

earlier quoted TH method is based on the observations of covalent ThDP-bound intermediates (Schemes 1.1) after their release from the enzyme by acid-quench of a reaction mixture resulting from rapid mixing of enzyme and substrate on a chemical quench instrument. Fortuitously, HEThDP, LThDP and 2-acetylThDP all (a) are stable under these conditions, and (b) have distinct ^1H chemical shifts for their C6'-H resonances. Integration of these resonances provides the relative steady-state distribution of intermediates, and, with the turnover number of the enzyme, the forward rate constants could be calculated for the pathway (rate constants for formation of LThDP, its decarboxylation and acetaldehyde release.⁽¹⁵⁾ The method has been applied to a number of ThDP enzymes.

The method has some limitations: (a) It measures intermediate distribution once those are released from the enzyme; (b) It cannot differentiate the level of enamine and HEThDP, since under acid quench the former is converted to the latter. Therefore, the HEThDP measured in the quench corresponds to the sum of the relative concentration of enamine and HEThDP; and (c) Given that the method depends on the observation of the aromatic C6'-H resonances, many aromatic cofactors would interfere with the observations.

Balakrishnan and Chakraborty from our laboratory addressed the NMR issue and extended the power of the TH method by synthesizing ThDP specifically labeled at both the C2 and C6' positions with ^{13}C ([C2, C6'- $^{13}\text{C}_2$] ThDP). Using 1D-gradient HSQC NMR methods only protons attached to these two ^{13}C -labeled atoms were detected. This enabled detection of C2H and C6'H in the aromatic region of the ^1H NMR spectrum even in the presence of other cofactors with aromatic resonances.

To observe directly the time-course of enzyme-bound intermediates, a method was developed which is a combination of CD methods and the TH method: the time-course of intermediate formation/depletion is assessed by stopped-flow CD, by looking at the intermediates with signatures identified as above. If there is ‘degeneracy’ in the CD assignments (an important case in point is that all ThDP-bound intermediates with tetrahedral substitution at C2 α appear to exist in their IP tautomeric forms at pH values above the pK_a of the APH⁺ form), we rely on the TH method to identify the intermediate after acid quench under identical reaction conditions.

This combined approach is applied in this thesis research to DXP synthase, which catalyzes condensation of pyruvate and D-glyceraldehyde-3-phosphate (GAP) to form DXP. It was found that DXP synthase and its Y392F, R478A, R420A variants stabilize the ThDP-bound pre-decarboxylation intermediate C2 α -lactylThDP (LThDP) upon addition of pyruvate in the absence of D-GAP, while addition of D-GAP enhanced the rate of LThDP decarboxylation. This appears to be the first study of a ThDP enzyme where the individual rate constants could be evaluated by time-resolved CD spectroscopy, and the results have relevance to other ThDP enzymes in which decarboxylation is coupled to a ligation reaction. Also, the observed pre-steady state rates suggests that formation of LThDP is the rate-limiting step in DXP synthase catalytic cycle (Chapter 2). On the other hand, the E1 component of OGDHc from *E. coli* stabilizes the enamine intermediate followed by ThDP radical formation with its real substrate 2-OG and the longer analogue 2-OA. The rate of its formation and disappearance were measured in the absence and presence of various enamine acceptors. Further, formation of the radical on *E. coli* E1o was observed using EPR spectroscopy (Chapter 3). Reaction of the enamine with an

acceptor substrate, such as an aldehyde can lead to a carbonylase (C-C bond formation) reaction. We have synthesized chiral α -hydroxy ketones with good yield and 60-95 % *ee* by varying donor and acceptor substrates, making E1o an utmost candidate for protein engineering. The chiral α -hydroxy ketones can be used in natural product and fine chemical synthesis (Chapter 4).

By using CD and stopped-flow photo diode array experiments, we assigned new spectral signatures related to ThDP-bound intermediates on enzymes with conjugated substrates, at longer wavelength than expected, which was never explained before even with model studies. Our experimental evidence suggests that the interaction between the positive charge on the thiazolium ring and π bond of substrates covalently attached to the thiazolium C2 position could be responsible for the long wavelength of the charge transfer transitions (Chapter 5).

A major conclusion from these studies is that the rate of individual steps can be assessed directly from detailed time course studies, providing a virtually unprecedented opportunity to gain insight into ThDP-dependent reactions, including interrogation of individual enzyme residues regarding their catalytic roles.

CHAPTER 2

Observation of thiamin-bound intermediates and determination of microscopic rate constants on 1-deoxy- D-xylulose 5-phosphate synthase

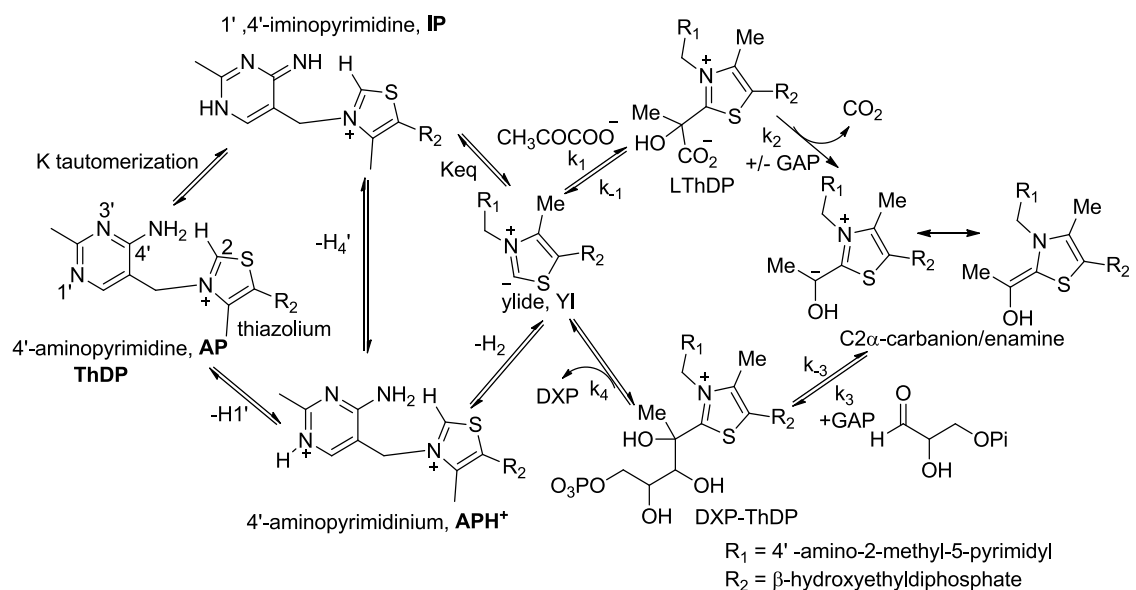
2.1 INTRODUCTION

The enzyme 1-deoxy- D-xylulose-5-phosphate (DXP) synthase generates the first crucial intermediate in the biosynthesis of both thiamin (vitamin B1) and pyridoxal (vitamin B6), as well as in isoprenoid biosynthesis essential in human pathogens. ⁽¹⁸⁻²⁰⁾ DXP synthase uses thiamin diphosphate (ThDP) as coenzyme and pyruvate and D-glyceraldehyde-3-phosphate (GAP) as substrates. Mechanistically, the initial reaction can be anticipated to parallel typical ThDP-dependent pyruvate and other 2-oxoacid decarboxylase enzymes, the pyruvate molecule forming a pre-decarboxylation covalent intermediate with ThDP (C2 α -lactylThDP or LThDP) followed by decarboxylation to an enamine/C2 α -carbanion/C2 α -hydroxyethylidene-ThDP, followed by carboligation of the enamine with the aldehyde functional group of GAP, and finally release of DXP (Scheme 2.1). The results reveal not only the rate-limiting step for the enzyme, but perhaps more surprisingly, the dramatic effect that addition of second substrate GAP has on the decarboxylation step.

We first explored the substrate specificity of the reaction regarding the 2-oxoacid, by using 2-oxophosphonates and a 2-oxophosphinate that form dead-end but stable LThDP analogs readily recognizable by the positive CD band centered near the 300-310 nm region and attributed to the 1',4'-iminopyrimidine tautomer (IP form) of ThDP.

Previous mechanistic studies of DXP synthase were performed under steady-state conditions. ⁽²¹⁻²⁴⁾ We initiated the first study of DXP synthase using tools capable of observing and determining the time-resolved behavior of ThDP-bound covalent intermediates (Scheme 2.1, right): stopped-flow circular dichroism (CD) and chemical quench followed by NMR detection. The CD studies can be used for (a) identification of an electronic absorption for the 1',4'-iminopyrimidine (IP form, Scheme 2.1 left) of ThDP at 300-310 nm⁽²⁵⁾ and (b) demonstration on ten ThDP enzymes so far, that at pH values at or above the pK_a of the 4'-aminopyrimidinium form (APH⁺) of ThDP, the IP tautomer predominates in ThDP-bound covalent intermediates where the C2 α -carbon carries four substituents. ⁽²⁶⁾

Scheme 2.1 The catalytic cycle of DXP synthase.



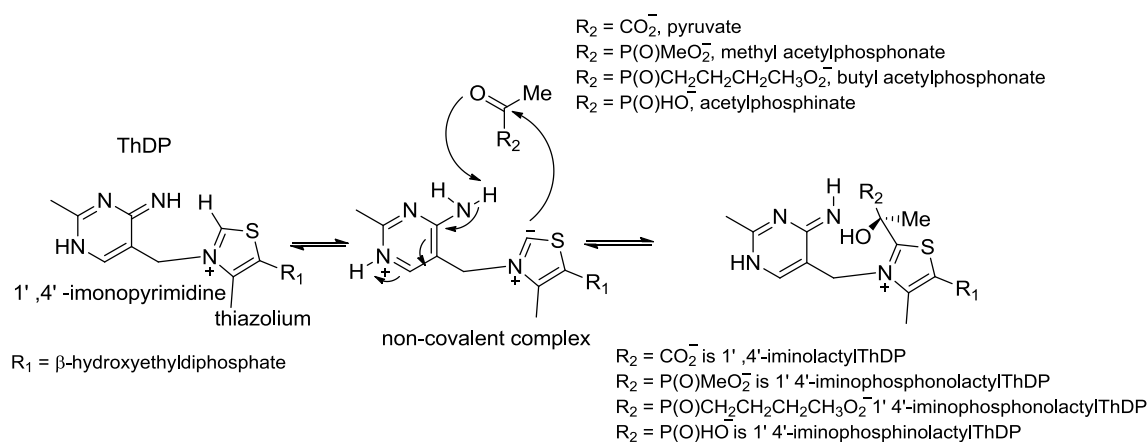
k_1 formation of S~ThDP.DXP synthase, the Pre-decarboxylation intermediate ; k_2 is decarboxylation to enamine; k_3 is carbonylation to provide the Post-decarboxylation intermediate P~ThDP.DXP synthase; k_4 is release of DXP product from ThDP.DXP

Indeed, as expected, LThDP analogues are readily formed from the substrate analogues (Scheme 2.2) creating a positive CD band at ~300-310 nm. While carrying out preliminary CD experiments on the mutual effects of the two substrates on binding and catalysis, the following surprising and very useful observation was made: on addition of pyruvate to DXP synthase in the absence of GAP at 5 °C, a positive CD band centered at 313 nm developed and persisted with as much as 1 mM pyruvate, indicating that the alternative conversions, such as protonation followed by acetaldehyde release, or carboligation with a second molecule of pyruvate yielding acetolactate take place very slowly (see Scheme 4.1 for the alternative fates of the enamine). Next, we needed to establish the nature of the intermediate with the positive CD band at 313 nm. It turned out to be the pre-decarboxylation LThDP thiamin-bound intermediate in the IP tautomeric form. Apparently, decarboxylation in the absence of GAP is sufficiently slow to allow determination of all microscopic rate constants for this enzyme using time-resolved CD experiments. In the presence of GAP the LThDP decarboxylation rate was accelerated by at least 600-fold.

We next investigated other factors important for substrate binding. Based on the previous structural studies on DXP synthase and in comparison with other ThDP enzymes, a few active site DXP synthase variants R478A, R420A and Y392F were created at JHU. The evidence from protein fluorescence experiments at JHU revealed the roles of active site residues to be critical for substrate binding. Further CD and time-resolved studies were carried out at Rutgers with the all three variants. The CD (RU) and fluorescence (JHU) results demonstrate that Arg-420 and Arg-478 are critical active site residues for binding of the acceptor substrate D-GAP, but are not essential for catalysis of

LThDP formation or D-GAP promoted decarboxylation. In addition, we have investigated the importance of Tyr-392, analogous to Tyr-599 of the PDHc E1 component⁽²⁷⁾, which is known to interact via hydrogen bonding to a phosphono-LThDP mimic of the enzyme-bound LThDP intermediate.⁽²⁸⁾ Contrary to our expectations, the results of protein fluorescence, CD and kinetic analyses suggest Tyr-392 contributes to D-GAP binding, but is not required for formation of LThDP on DXP synthase, or for D-GAP-promoted decarboxylation of LThDP. We note stabilizing effects of R420A and Y392F on LThDP in the absence of acceptor substrate, which suggest that Arg-420 and Tyr-392 could play a role to create a barrier to decarboxylation in the absence of D-GAP, a barrier that is even larger on R420A and Y392F. The implications of the findings to ThDP-dependent enzymes carrying out decarboxylation coupled to carbonylation are substantial to inhibitor design.

Scheme 2.2 Formation of covalent adduct of ThDP with pyruvate and analogues MAP, BAP and AcPhi.



2.2 MATERIALS and METHODS

2.2.1 Materials

Thiamin diphosphate (ThDP), pyruvate, dithiothreitol, yeast alcohol dehydrogenase, nicotinamide adenine dinucleotide, 2,6-dichlorophenolindophenol (DCPIP), 1-deoxy- D-xylulose 5-phosphate (DXP), D, L-GAP (L-GAP would not affect DXP synthase activity^(18, 22, 23)) were from Sigma-Aldrich (St. Louis, MO). The concentration of D-GAP was calculated as one-half of the D, L-GAP concentration. The enzymes DXP synthase wt and all variants, AcPhi and BAP were from Dr. Meyers lab at Johns Hopkins University. *Methyl acetylphosphonate (MAP)* was synthesized according to Kluger et al.⁽²⁹⁾

2.2.2 General methods

1. To adjust the pH, a sympHony pH electrode (VWR) was used. UV spectra were acquired on a Varian DMS 300 spectrophotometer.
2. CD spectra were recorded on an Applied Photophysics Chirascan CD Spectrometer (Leatherhead, U.K.) in 2.4 ml volume with 1 cm path length cell. Buffer A is defined as 50 mM Tris pH 8.0, 100 mM NaCl, 0.5 mM ThDP, 2 mM MgCl₂, 1 mM DTT, 1% glycerol. The titration experiments with substrates and analogues were carried out in 100 mM HEPES (pH 8.0) containing 100 mM NaCl, 1 mM MgCl₂ and 0.2 mM ThDP (buffer B).
3. Kinetic traces were recorded on a Pi*-180 stopped-flow CD spectrometer (Applied Photophysics, U.K.) using 10 mm path length. The ThDP-bound intermediates were detected by dissolving enzyme or substrates in buffer A at 313 nm, product DXP at 297 nm, as dictated by the high sensitivity of the lamp at those wavelengths. Data from ten

repetitive shots were averaged and fit to the appropriate equation using Sigma Plot v.10.0.

4. NMR spectra were acquired on a Varian INOVA 500 or 600 MHz instruments. The water signal was suppressed by pre-saturation.

2.2.3 Enzyme activity measurements

DXP forming activity measurement by CD spectroscopy. The assay was carried out by direct detection of DXP formation at 290 nm at 37 °C. The assay medium (2.4 ml) contained in 100 mM HEPES (pH 8.0), 100 mM NaCl, 0.1 mM ThDP, 2 mM MgCl₂, 1 mM DTT, D-GAP (0.0075 – 1.25 mM, 0.25-2 mM, 0.15-2 mM, 0.025-1.25 mM for wt, R420A,R478A and Y392F respectively) and 1 mM pyruvate. The reaction was initiated by adding DXP synthase (20 µg). The rate of DXP formation was calculated from the slope of $\Delta mdeg$ vs time plot. The K_m value for D, L-GAP was calculated by fitting the data to a Hill function (Eq 1).

$$CD_{\lambda} = CD_{\lambda}^{\max} \cdot [Ligand]_{H}^{n_H} / (K_{d, app})_{H}^{n_H} + [Ligand]_{H}^{n_H} \quad (1)$$

where CD_{λ} is the observed CD signal at a particular wavelength, CD_{λ}^{\max} the maximum CD signal at saturation with ligand, $[Ligand]$ is the concentration of substrate, and n_H is the Hill coefficient.

Molar ellipticity of DXP was determined by recording CD spectrum of commercial DXP in water at 25 °C and calculated using Eq 2:

$$[\theta] = 100 \cdot \theta_{\text{obsd}} / c \cdot l \quad (2)$$

where $[\theta]$ is the molar ellipticity in $\text{deg cm}^2 \text{ dmol}^{-1}$, θ_{obsd} is the observed ellipticity at a given wavelength in deg, c is the concentration of an optically active compound in M, and l is the cuvette path length in cm.

Acetaldehyde forming activity measurement. The acetaldehyde-forming activity of wild type DXP synthase was measured in a coupled assay using yeast alcohol dehydrogenase (YADH) by monitoring the depletion of NADH at 340 nm using a Varian DMS 300 spectrophotometer. The assay medium contained in buffer A (see General methods), 1 mg/ml BSA, YADH (0.08 mg/ml), NADH (0.2 mg/ml), D, L-GAP (0.1-0.4 mM) and 0.5 mM pyruvate at 37 °C. The reaction was initiated by adding the DXP synthase (100 μg). One unit of activity is defined as the amount of NADH depleted per minute per mg DXP synthase ($\mu\text{mol}/\text{min}/\text{mg}$ of DXP synthase).

Evidence for decarboxylation from DCPIP reduction. The rate for DCPIP-induced oxidation of the enamine (resulting from decarboxylation of LThDP) was carried out by monitoring the reduction of DCPIP at 600 nm. The reaction medium contained in buffer A (see General methods), 0.1 mM DCPIP, 0.4 mM D, L-GAP and 2 mM pyruvate at 37 °C. The reaction was initiated by adding DXP synthase (30 μg). One unit of activity is defined as the amount of DCPIP reduced per minute per mg DXP synthase ($\mu\text{mol}/\text{min}/\text{mg}$ of DXP synthase).

Acetolactate formation by DXP synthase monitored by CD. The assay medium (2.4 ml) contained in 100 mM HEPES buffer (pH 8.0), 100 mM NaCl, 0.1 mM ThDP, 2 mM MgCl_2 , 1 mM DTT and DXP synthase (33.33 μM active sites concentration). The reaction was initiated by adding pyruvate (1-90 mM) and acetolactate formation was monitored at 300 nm. The slope was calculated using the Pro-Data Viewer program

supplied by the manufacturer which was used to calculate the rate of formation of acetolactate using molar ellipticity of $3600 \text{ deg cm}^2 \text{ dmol}^{-1}$.⁽³⁰⁾ In parallel, the rate of formation of (*R*)-acetolactate was also measured by CD at 300 nm. The K_d^{app} was calculated by fitting the data to a Hill function (Eq 1).

2.2.4 Steady-state CD measurements

pH titration of the AP form of ThDP on DXP synthase. DXP synthase (36.3 μM active sites concentration) in 100 mM HEPES buffer containing 100 mM NaCl, 0.5 mM ThDP and 2 mM MgCl_2 was titrated in the pH range of 7.98–7.07 at 37 °C. Near UV CD spectra were recorded after each pH adjustment. Log CD at 320 nm was plotted against pH and pK_a was determined using Eq 3.

$$\log(\text{CD}) = \log(\text{CD}_{\text{max}}) - \log(1 + 10^{(\text{pK}_1 - x)}) \quad (3)$$

where x is pH.

pH dependence of the rate of DXP synthase-catalyzed DXP formation. The reaction was measured in 50 mM KH_2PO_4 , 50 mM Tris containing 0.1 mM ThDP, 2 mM MgCl_2 , 1 mM DTT, 0.5 mM D, L-GAP and 1 mM pyruvate in the pH range of 6.65 – 8.08 at 37 °C. The reaction was started by addition of DXP synthase (20 μg) and monitored the slope at 290 nm for 200 s.

DXP synthase titration experiments with substrates and analogues.

CD titration of DXP synthase with pyruvate analogues MAP, BAP, AcPhi. These titrations were carried out in buffer B (see General methods) in the near-UV (280-450 nm) wavelength region at 37 °C. All the analogues revealed a positive band with λ_{max} at ~300 nm on DXP synthase. The concentration range for MAP was 1-100 μM , for BAP 1-40 μM . A similar titration with MAP was also carried out in the presence of D, L-GAP

(1.5 mM). Apparent dissociation constants (K_d^{app}) were calculated by fitting the data to a quadratic equation (Eq 4) using Sigmaplot v.10.0.

$$CD_{\lambda} = ((E + x + K_d) - \sqrt{((E + x + K_d)^2 - (4Ex))}) / ((2E) / (CD^{\max}_{\lambda})) \quad (4)$$

where CD_{λ} is the observed CD signal at the given wavelength, CD^{\max}_{λ} the maximum CD signal at saturation with MAP, E the concentration of enzyme, x the concentration of substrate analogue.

The titration with AcPhi was performed in the concentration range of 1-700 μ M and data were fitted to a Hill function (Eq 1),

Titration of DXP synthase (55.9 μ M active sites concentration) with pyruvate (0.05-1 mM) was carried out in buffer B (see General methods) at 4 $^{\circ}$ C. After apparent saturation with 1 mM pyruvate, 500 μ M D, L-GAP was added.

Titration of DXP synthase variants with pyruvate. R420A, R478A, Y392F DXP synthase variants (30 μ M active sites concentration) was titrated with pyruvate (10-200 μ M, 10-500 μ M, 30-500 μ M respectively) in buffer B (see General methods) at 5 $^{\circ}$ C. The apparent $K_d^{pyruvate}$ was calculated by using Eq 1.

2.2.5 Stopped-flow CD measurements

Kinetic traces were fit to the appropriate equations by using Sigma Plot v 10.0.

$$CD_{\lambda}^{(t)} = CD_1 \cdot e^{-k_1 t} + c \quad (5)$$

$$CD_{\lambda}^{(t)} = CD_1 \cdot e^{-k_1 t} + CD_2 \cdot e^{-k_2 t} + c \quad (6)$$

$$CD_{\lambda}^{(t)} = CD_1 \cdot e^{-k_1 t} + CD_2 \cdot e^{-k_2 t} - CD_3 \cdot e^{-k_3 t} + c \quad (7)$$

$$CD_{\lambda}^{(t)} = CD_1 \cdot e^{-k_1 t} - CD_2 \cdot e^{-k_2 t} + c \quad (8)$$

where k_1 , k_2 , and k_3 are the apparent rate constants, c is CD^{\max}_{λ} in the exponential rise to maximum model or CD^{\min}_{λ} in the exponential decay model.

Pre-steady state formation of 1',4'-iminoLThDP. A solution of DXP synthase (4.6 mg/ml, 68.1 μM active centers) in buffer A (see General methods) was placed in one syringe and an equal volume of pyruvate (2 mM) in the same buffer was placed in the second syringe. Spectra were recorded over a period of 7 s. Data were fit to a single-exponential model as in Eq (5).

Single turnover experiments of DXP synthase and variants with pyruvate in the absence of D-GAP. DXP synthase, R420A, R478A, Y392F (81.4 μM , 60 μM , 60 μM , 70 μM active centers respectively) in one syringe was mixed with equal volume of pyruvate (50 μM for wt and 30-35 μM for variants) in the second syringe, both in buffer A (see General methods) at 6 °C. The reaction was monitored at 313 nm for 50 s, and data were fit to a triple exponential model as in Eq (7) and Eq (6) for R420A.

Pre-steady state rate of decarboxylation of 1',4'-iminoLThDP in the presence of GAP. In one syringe LThDP was pre-formed at 6 °C using the above method, then was rapidly mixed with 200 μM D, L-GAP in the second syringe. Spectra was recorded over a period of 5 s. Data were fitted to Eq (5). Similar experiments were carried out using different concentrations of D-GAP for wt DXP synthase. For R420A (59.3 μM active sites concentration), 300 μM pyruvate and 2 mM D-GAP. For R478A (47.5 μM active sites concentration), 300 μM pyruvate, and 2 mM D-GAP was used. For Y392F (54.8 μM active sites concentration), 411 μM pyruvate and 200 μM D-GAP (or 500 μM D-GAP) was used.

Pre-steady state production of 1-deoxy- D-xylulose-5-phosphate. DXP synthase (0.070 mg/ml, 1.04 μM active centers) in buffer A was mixed with an equal volume of 4 mM pyruvate and 2 mM D-GAP in the same buffer placed in the second syringe. The R478A,

R420A or Y392F DXP synthase variant (1.04 μM active sites concentration) in buffer A placed in one syringe was mixed with an equal volume of 2 mM pyruvate (1 mM for R420A) and 2 mM D-GAP (1 mM for R420A) in the same buffer placed in the second syringe. Spectra were recorded over a period of 100 s and data were fit to a double-exponential model as in Eq (6).

2.2.6 NMR measurements

Detection of ThDP-bound intermediates by ^1H NMR spectroscopy. ^1H NMR spectra were recorded with suppression of the water resonance by pre-saturation and 16384 scans were collected with a recycle delay of 2.0 s. The reaction mixture containing wt DXP synthase (31 mg/ml, 459.3 μM active centers) in 20 mM Tris (pH 8.0), 100 mM NaCl, 0.1 mM ThDP and 0.5 mM MgCl_2 was mixed with 1 mM pyruvate in the same buffer. The reaction was incubated at 5 $^\circ\text{C}$ for 5 s (and an identical sample for 20 s) and quenched with 12.5% TCA in 1M DCl/D₂O. The mixture was centrifuged at 15,700 g for 20 min and the ^1H NMR spectrum of the supernatant was recorded.

The reaction mixture containing Y392F (28 mg/ml, 415 μM active centers) in 20 mM Tris (pH 8.0), 100 mM NaCl, 0.2 mM ThDP and 1 mM MgCl_2 (buffer prepared in D₂O to reduce the intensity of buffer peak in the region 7 – 8 ppm) was mixed with 1 mM pyruvate in the same buffer. The reaction was incubated on ice for 50 s and quenched with 12.5% TCA in 1M DCl/D₂O.

Similar reaction conditions were used to measure ^1H NMR of the variants R478A, R420A and Y392F in the presence of D-GAP where 250-300 μM enzyme was incubated with 500 μM pyruvate on ice for 30 second to form LThDP. The reaction mixture was

then incubated on ice for an additional 30 sec with D-GAP (2 mM for R478A and R420A, 5 sec with 500 μ M for Y392F), then quenched with acid.

Detection of DXP product by ^1H NMR spectroscopy. A reaction mixture containing 1.5 mg/ml (22.22 μ M active centers) DXP synthase in 20 mM KH_2PO_4 (pH 7.5) containing 100 mM NaCl, 0.1 mM ThDP, 0.5 mM MgCl_2 and 1 mM DTT was mixed with 15 mM D-GAP and 10 mM pyruvate in the same buffer. After overnight incubation at 4 $^\circ\text{C}$, the ^1H NMR spectrum of the supernatant was recorded.

Detection of [1- ^{13}C]-DXP by gradient ^{13}C Heteronuclear Single Quantum Coherence NMR spectroscopy. NMR spectra were acquired on a Varian 600 or 500 MHz instrument. A reaction mixture containing R478A (18 mg/ml) in 20 mM KH_2PO_4 (pH 7.5), 100 mM NaCl, 150 μ M ThDP, 0.5 mM MgCl_2 was mixed with 500 μ M [3- ^{13}C] pyruvate and incubated on ice for 30 s to pre-form [C2 β - ^{13}C]-LThDP (200 μ l reaction volume). The reaction mixture was then incubated on ice with 2 mM D-GAP for 5 s and then quenched with 12.5% TCA in 1M DCl/D $_2\text{O}$. The mixture was centrifuged at 15,700 g for 20 min, and the ^1H NMR spectrum of the supernatant was recorded. The water signal was suppressed by pre-saturation. A total of 4096 scans were collected with a recycle delay of 2.0 s. The data indicate that only LThDP is bound to the enzyme (Figure 2.13a). This same mixture was subjected to 1D gradient ^{13}C heteronuclear single quantum coherence (gCHSQC) NMR analysis to determine the extent of [1- ^{13}C]-DXP product formation during this time period. The $^{13}\text{CH}_3$ region was integrated (Figure 2.13b) to determine the extent of [1- ^{13}C]-DXP formation. The coupled spectra (not shown) indicate $J_{\text{CH}} = 127$ Hz for each of the species present.

2.3 RESULTS and DISCUSSION

2.3.1 CD spectroscopy gives evidence of an elevated pK_a of the APH^+ form of ThDP on DXP synthase. The CD spectrum of DXP synthase displays a negative signal at 320 nm on complexation with ThDP (Figure 2.1), which can be assigned to the AP tautomer of ThDP bound to the enzyme on the bases of numerous other examples from Rutgers. Next, the CD spectrum was recorded at different pH values to convert the AP form of ThDP to the APH^+ form (Scheme 2.1). On titration from pH 7.98 to 7.07 the amplitude of the CD signal at 320 nm gradually diminished (Figure 2.1), indicating that the AP form of ThDP is dominant at pH 7.98 and the APH^+ form is dominant at pH 7.07 (while the APH^+ form has no CD signature identified so far, its existence on three enzymes was recently demonstrated by solid state NMR). Plotting the CD amplitude at 320 nm against pH gave a pK_a of 7.5 (Figure 2.1, inset) for the protonic equilibrium $[(AP) + (IP)] / [APH^+]$.

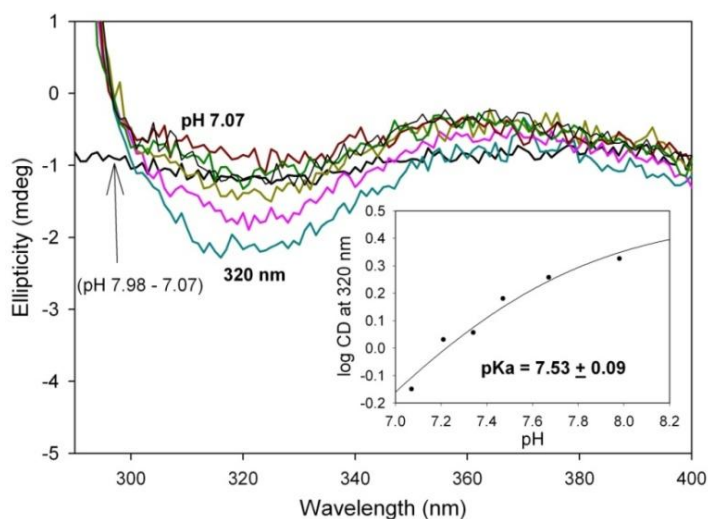


Figure 2.1 pH titration of the AP form of ThDP on DXP synthase at 320 nm. (Inset) Log CD at 320 nm was plotted against pH and pK_a was determined using Eq 3.

2.3.2 Pyruvate analogues on DXP synthase form stable ThDP-bound pre-decarboxylation intermediates. As reported earlier by the Johns Hopkins group⁽³¹⁾ pyruvate analogues act as inhibitors of DXP synthase, hence we carried out CD titration of DXP synthase with several pyruvate analogues (MAP, BAP, AcPhi) at 37 °C (Scheme 2.2). The CD titration results are summarized in Table 2.1.

Methyl acetylphosphonate (MAP) is an inhibitor of many ThDP enzymes, which utilize pyruvate as substrate.⁽²⁸⁾ It was reported that MAP and butyl acetylphosphonate (BAP) exhibit competitive inhibition with respect to pyruvate in DXP synthase.^(24, 32) The titration experiment shows formation of a positive CD band at 300 nm (Figure 2.2a) on addition of MAP (1-100 μM), which can be assigned to the 1',4'-iminophosphono-LThDP formed on DXP synthase.⁽³³⁾ After saturation with MAP, D, L-GAP was added incrementally (25-200 μM) showing no changes in the spectra. The sample was then dialyzed overnight against buffer B (see General methods), the CD spectrum was recorded for the dialyzed protein showing that the protein-bound MAP wasn't removed under both conditions. A plot of CD amplitude at 300 nm against $[\text{MAP}] / [\text{active centers}]$ shows saturation at 0.5 (Figure 2.2b, inset) suggesting that MAP is binding to half of the active sites with $K_d = 3.35 \mu\text{M}$ (Figure 2.2b). Similar results were obtained even in the presence of GAP with $K_d = 1.82 \mu\text{M}$ (not shown).

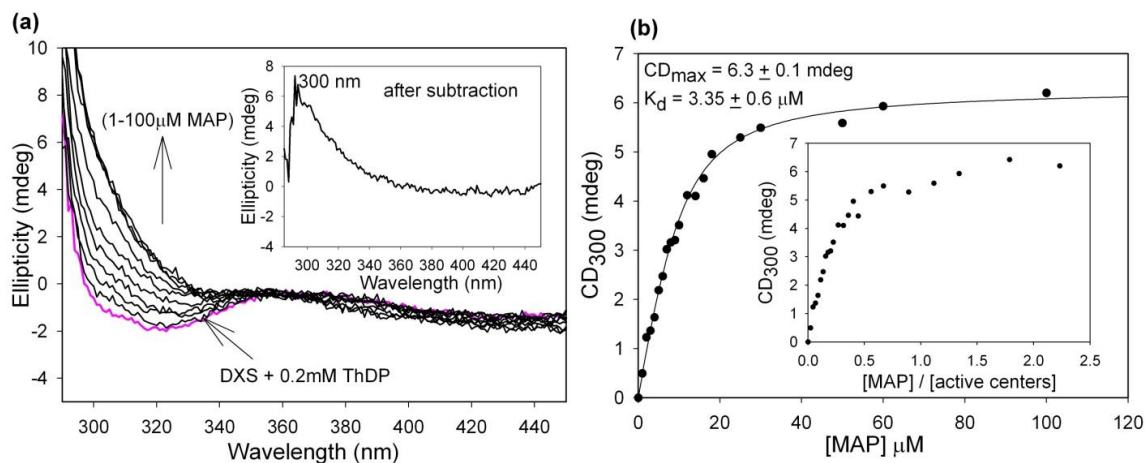


Figure 2.2 (a) CD titration of DXS + 0.2mM ThDP with MAP at 37⁰C. (Inset) The 1',4'-iminopyrimidinyl tautomer is seen at 300 nm after subtraction of the spectrum from that of the DXS + 0.2mM ThDP. (b) CD amplitude of IP form at 300 nm plotted against concentration of MAP using Eq 4. (Inset) CD amplitude at 300 nm plotted against ratio of [MAP] / [active centers].

A similar experiment with BAP (1-40 μM) led to the formation of CD signal at 300 nm (Figure 2.3a) with comparable K_d value of 4.6 μM (Figure 2.3b); however, apparently all sites could be filled, unlike with MAP (Figure 2.3b, inset). After dialysis the CD spectrum indicated that BAP had been removed.

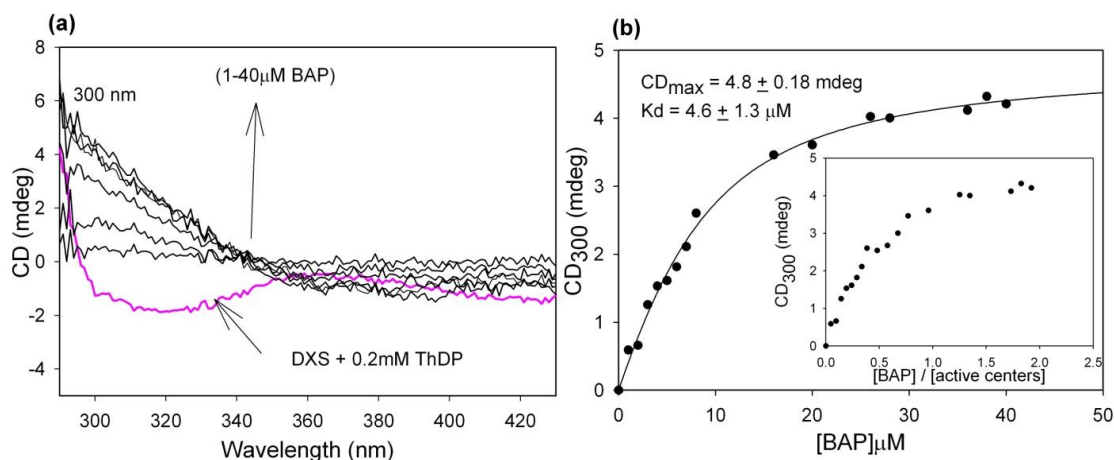


Figure 2.3 (a) CD titration of DXS synthase with BAP at 37 °C forms 1',4'-imino-pyrimidinylThDP tautomer seen at 300 nm. (b) CD amplitude of the IP form at 300 nm plotted against concentration of BAP using Eq 4. (Inset) CD amplitude at 300 nm plotted against ratio of $[BAP] / [active\ centers]$.

It was reported earlier from Rutgers that acetylphosphate AcPhi $[CH_3C(=O)P(H)(=O)O^-]$ is the most potent pyruvate mimic inhibitor of several ThDP-dependent enzymes.⁽³⁴⁾ It was found that increasing concentration of AcPhi developed a positive CD band at 305 nm, which was assigned to 1',4'-iminophosphinoLThDP, a stable analogue of the pre-decarboxylation intermediate C2 α -lactylThDP.⁽²⁵⁾ We carried out a CD titration of DXS synthase with AcPhi (1-700 μ M) and observed formation of a positive CD signal at 310 nm (Figure 2.4) which could be assigned to the 1',4'-iminophosphinoLThDP with K_d 16 μ M. The CD spectrum of a sample dialyzed for overnight indicated that AcPhi was also released from the enzyme.

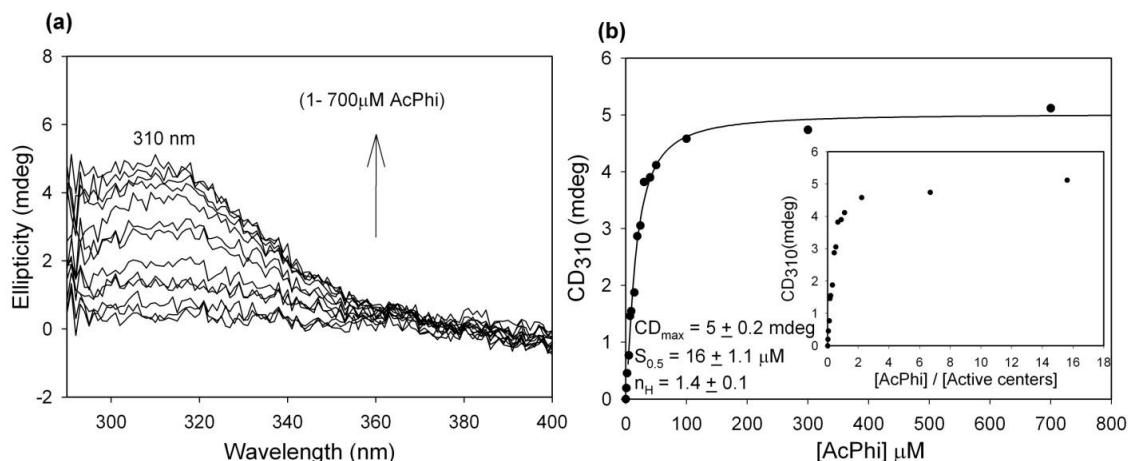


Figure 2.4 (a) CD titration of DXP synthase with AcPhi at 37 °C. The 1',4'-imino-pyrimidinylThDP tautomer is seen at 310 nm. (b) CD amplitude of IP form at 310 nm plotted against concentration of AcPhi using Eq 1. (Inset) CD amplitude at 310 nm plotted against ratio of [AcPhi] / [active centers].

2.3.3 Direct observation of the pre-decarboxylation LThDP intermediate formed from pyruvate on DXP synthase. According to the above results, DXP synthase stabilizes pre-decarboxylation intermediate analogues of pyruvate. These results suggested that an attempt be made to carry out such studies with pyruvate itself. Indeed, in a CD titration of DXP synthase with pyruvate at 4 °C, there developed a positive CD signal at 313 nm (Figure 2.5a), gradually replacing the original negative AP signal at 320 nm. The signal at 313 nm revealed apparent saturation (i.e., reached steady state concentration) with 1 mM pyruvate with $K_{d,app} \sim 90 \mu\text{M}$, and was assigned to the 1',4'-iminoLThDP. Addition of 500 μM D, L-GAP (250 μM D-GAP) to the same sample immediately quenched the CD band at 313 nm and formed a new positive CD band at 288 nm (Figure 2.5a, inset), assigned to the condensation product DXP. To confirm the identity of the compound

produced, protein was separated and the CD spectrum of the supernatant again displayed a positive signal at 288 nm, indicating that the signal corresponds to product and is no longer protein bound.

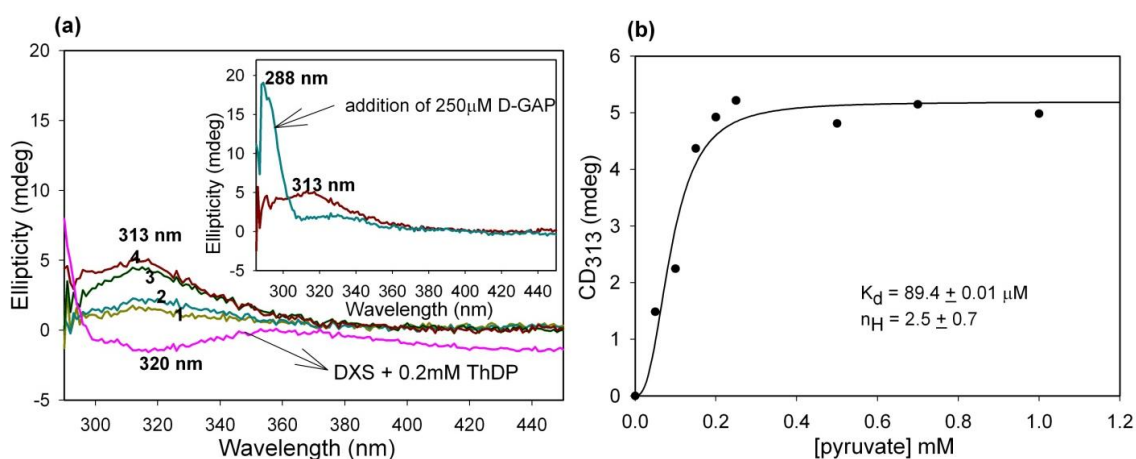


Figure 2.5 (a) CD titration of DXS + 0.2mM ThDP with pyruvate (1) 50 μM , (2) 100 μM , (3) 150 μM , (4) 1 mM in at 4 $^{\circ}\text{C}$. The formation of 1',4'-iminoLThDP is seen at 313 nm. (Inset) Addition of 250 μM D-GAP quenched the signal at 313 nm and formed DXS product according to the positive band centered at 288 nm. (b) Determination of $K_{d,\text{app}}$ for pyruvate on DXS + 0.2mM ThDP by monitoring formation of LThDP at 313 nm.

The formation of 1',4'-iminoLThDP was observed even with high concentration of pyruvate at 4 $^{\circ}\text{C}$, indicating that LThDP is stable at 4 $^{\circ}\text{C}$. Raising the temperature to 37 $^{\circ}\text{C}$ formed acetolactate product according to a negative CD band at 300 nm similar to that seen in Figure 2.6. Again, the protein was separated and the supernatant confirmed that the (*R*)-acetolactate was not protein bound. Acetolactate formation at different [pyruvate] led to $K_{m(\text{app})}^{\text{pyruvate}}$ 51 mM (Figure 2.6).

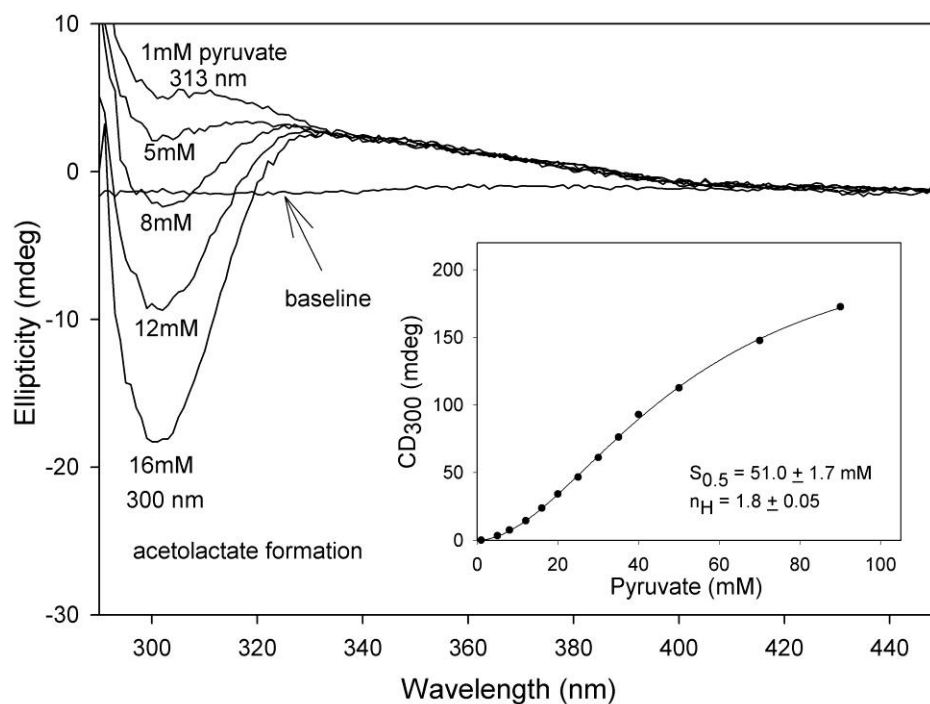


Figure 2.6 Dependence of (*R*)-acetolactate production on pyruvate concentration at 37 °C. (Inset) CD amplitude of (*R*)-acetolactate at 300 nm plotted against pyruvate concentration using Eq 1.

2.3.4 pH dependence of steady state formation of DXP by DXP synthase. The rate of formation of DXP product by DXP synthase at pH values of 6.65-8.08 was directly measured at 37 °C using CD₂₉₀. The data plotted for log (slope) vs pH revealed a pK_{app} of 7.6 (Figure 2.7) which correlates well with the pK_a of 7.5 for the protonic equilibrium $[(AP) + (IP)] / [APH^+]$ (Figure 2.1). That is, the pK_a of the enzyme-bound APH^+ form is very near the pH of optimal activity of the enzyme signaling the need for all forms APH^+ , AP and IP in the mechanism.

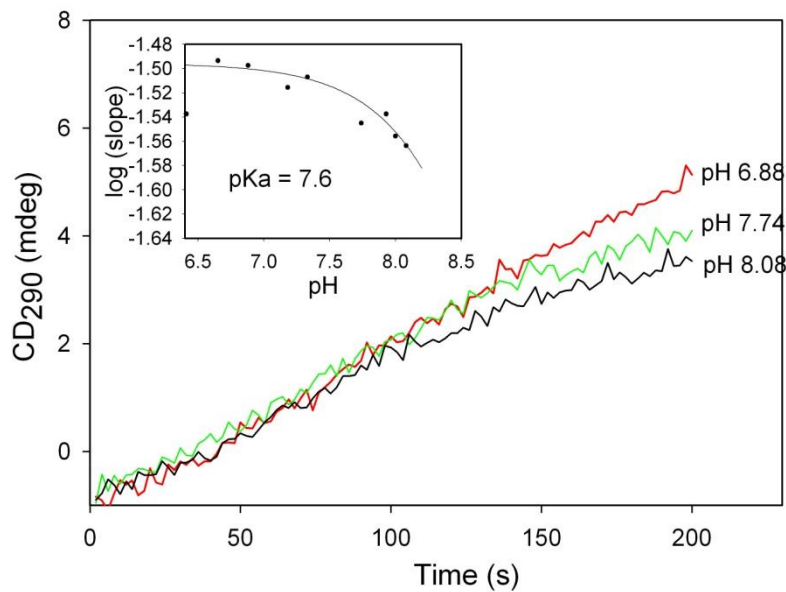


Figure 2.7 pH dependence of DXP product formation using CD spectroscopy.

2.3.5 Time-resolved spectroscopic studies leading to key microscopic rate constants for DXP synthase mechanism.

Pre-steady state rate of formation of the pre-decarboxylation intermediate 1',4'-imino-LThDP on DXP synthase. A stopped-flow CD experiment was carried out to determine the rate of interconversion of the ThDP-bound covalent intermediates on DXP synthase. The experimental condition selected was as used in the steady state experiment of DXP synthase with pyruvate, which enabled observation of an intermediate at 313 nm, assigned to the pre-decarboxylation intermediate. In the pre-steady state experiment DXP synthase in one syringe was rapidly mixed with saturating concentration of pyruvate in the second syringe, giving rise to an increase at 313 nm, and reaching a steady state in 2 s with a rate constant of 1.1 s^{-1} (Figure 2.8a).

Characterizations of 1',4'-iminoLThDP by NMR using a chemical quench method. The above study showed that addition of pyruvate to DXP synthase generates a positive CD band at 313 nm with a rate constant equal to 1.1 s^{-1} under pre-steady state conditions. According to several studies on the subject at Rutgers, this behavior signifies the presence of the rare IP tautomeric form of ThDP. However, this would be appropriate for both a pre-decarboxylation intermediate (LThDP) and a post-decarboxylation ThDP-bound DXP intermediate (Scheme 2.1), since both carry tetrahedral substitution at C2 α , a condition that demands the IP form at pH values $> \text{pK}_a$ of the APH⁺. To resolve the ambiguity, an NMR method developed by Tittmann⁽¹⁵⁾ was used, a method that recognized that the chemical shift of the C6'-H resonance is different for LThDP and HThDP, and indeed for carboligated product-ThDP adducts as well. Accordingly, an NMR sample of DXP synthase with pyruvate was prepared under pre-steady state conditions (quenched in 5 s and 20 s) confirming that the 313 nm intermediate corresponds to LThDP (Figure 2.8b).

Integration of the C2-H and C6'-H resonances showed that approximately the same % of ThDP was converted to LThDP in 5 s (~50%) and in 20 s (~55%). We conclude from these NMR experiments that: (1) The 313 nm species in the CD spectrum represents formation of LThDP and (2) The NMR sample prepared by quenching the DXP synthase and pyruvate reaction mixture in 20 s showed the presence of LThDP and ThDP, indicating the stability of LThDP.

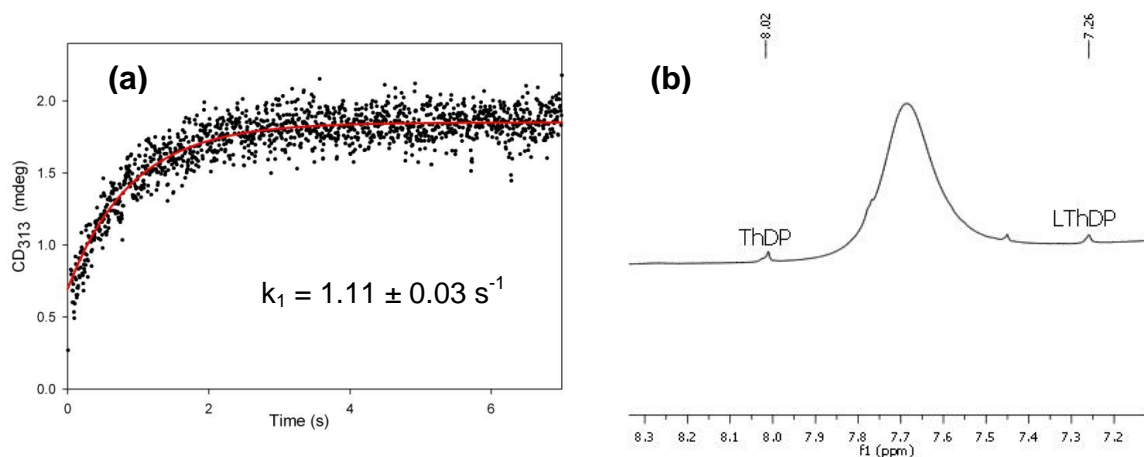


Figure 2.8 (a) Rates of 1',4'-iminoLThDP formation at 6 °C by DXP synthase with pyruvate under pre-steady state conditions at 6°C. The reaction was monitored at 313 nm for 7s. The data were fitted using a single exponential Eq 4 (see Material and Methods). (b) Detection of 1',4' –iminoLThDP by ¹H NMR at 7.26 ppm.

Detection of the rate constant for decarboxylation of LThDP in the presence of D,L-GAP.

As mentioned before, the CD signal at 313 nm formed from pyruvate was rapidly quenched by addition of D-GAP suggesting that the decarboxylation of LThDP is accelerated in the presence of D-GAP. To obtain quantitative support for this hypothesis, LThDP was pre-formed in one syringe by mixing DXP synthase and pyruvate at 6 °C then rapidly mixed with D-GAP placed in the second syringe on the stopped-flow CD instrument. Time dependent depletion of the 313 nm band (decarboxylation of LThDP, Figure 2.9a) was observed with a rate constant of 29.5 s^{-1} (Figure 2.9a, inset). An interpretation of the total behavior at 313 nm (Figure 2.9a) is that decarboxylation proceeds until all of the D-GAP is consumed (the drop in the curve; the concentration of D-GAP reacting is only 50 μM), after which time the remaining pyruvate forms more

LThDP (the rise in the curve). This experiment repeated with different D-GAP concentrations gave a value of 42 s^{-1} for DXP synthase saturated with D-GAP (Figure 2.9b).

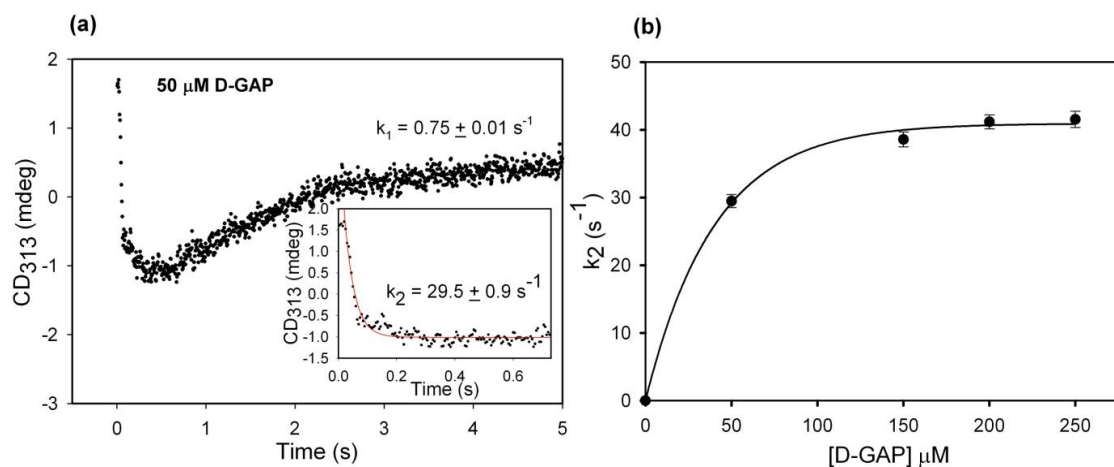


Figure 2.9 (a) Rate constant of 1',4'-iminoLThDP decarboxylation by DXP synthase with pyruvate in the presence of D-GAP at 6 °C. (Inset) The LThDP decomposition data from (a) were treated using Eq 5. (b) Dependence of the rates of 1',4'-iminoLThDP decarboxylation by DXP synthase on concentration of D-GAP.

Determination of the rate constant for DXP product release. Earlier it was shown that DXP, the product of pyruvate + D-GAP is characterized by a positive CD band centered at 288 nm (Figure 2.5a, inset). The stopped-flow CD instrument has optimum lamp sensitivity at specific wavelengths to form the signal, 297 nm being the one nearest to the 288 nm suggested for DXP detection. To determine the rate of product release by CD, much less DXP synthase (1.04 μM active centers) was mixed with high concentration of pyruvate (4 mM) and D-GAP (2 mM) in the second syringe, providing a rate constant of

1.2 s^{-1} at 297 nm (Figure 2.10). The small concentration of DXP synthase assured that the CD observations pertain to formation of free, rather than enzyme-bound DXP.

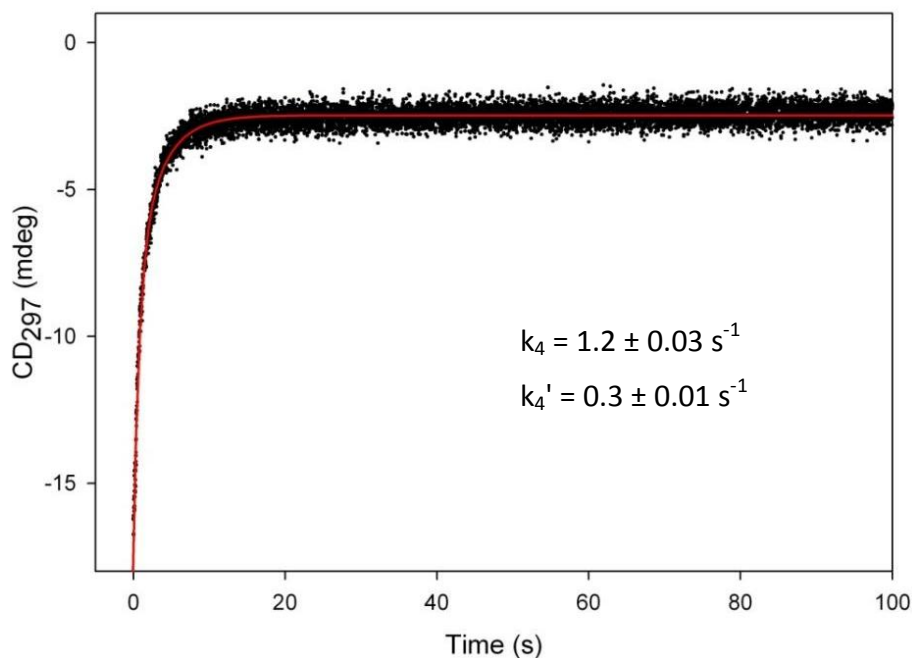


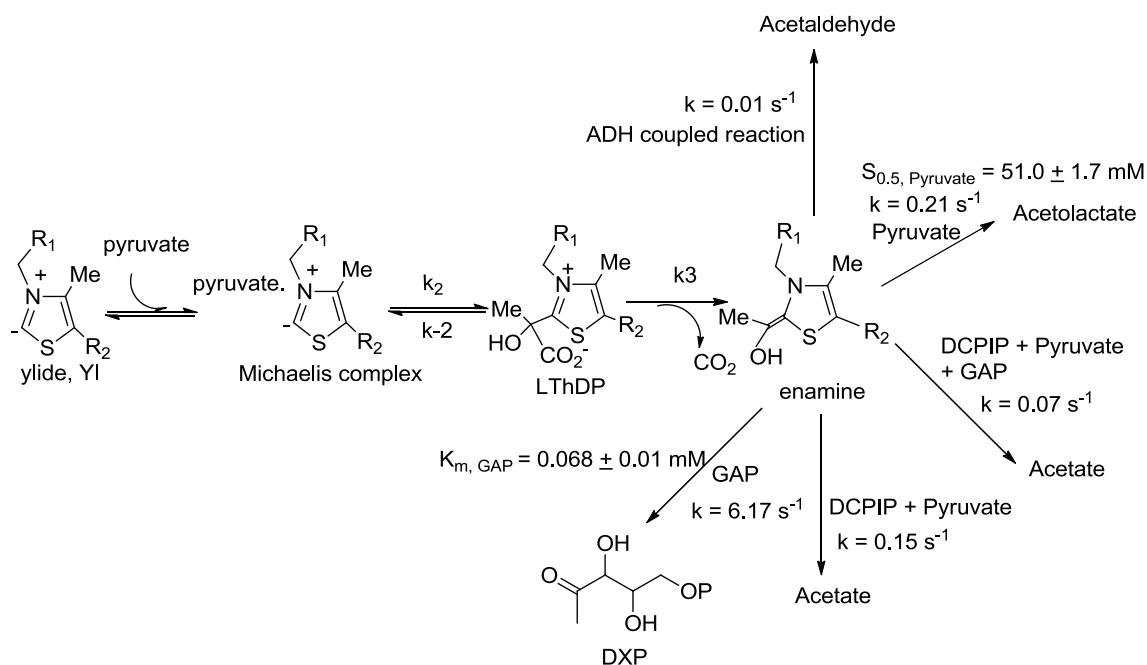
Figure 2.10 DXP product formation by DXP synthase at 6 °C and fitted using Eq 6.

2.3.6 NMR confirmation of DXP formation by DXP synthase from pyruvate and D-GAP. To confirm the identity of the product formed by DXP synthase from pyruvate and D-GAP with a positive CD band at 288 nm, an NMR sample was prepared using lower concentration of DXP synthase (22.22 μM active centers) and high concentration of pyruvate (10 mM) and D-GAP (15 mM). After removal of protein, the ^1H NMR spectrum identified the DXP product in the supernatant in comparison with the spectrum of an ‘authentic’, commercially available DXP sample.⁽¹⁸⁾

2.3.7 The rate of enzyme-bound enamine reacting with alternative acceptors.

As shown in Scheme 2.3, one could envision alternative trapping of the enamine resulting from LThDP decarboxylation and the rates of these reactions needed to be established under the reaction conditions. Protonation of the enamine would lead to HEThDP then release acetaldehyde whose rate of formation with the YADH/NADH coupled assay was 0.01 s^{-1} . The DCPIP reduction assay was carried out to obtain evidence of decarboxylation in the presence and in the absence of D,L-GAP, giving the rate constants of 0.07 s^{-1} and 0.15 s^{-1} , respectively. The rate of carbonylation of the enamine with a second pyruvate molecule leading to acetolactate (identified by the negative CD band at 300 nm) was estimated to be 0.21 s^{-1} using the molar ellipticity reported earlier.⁽³⁰⁾ The rate of DXP formation (4.21 s^{-1}) at $37 \text{ }^\circ\text{C}$ was calculated from the maximum slope of the change in CD with time at 290 nm. To calculate the rate constant, the molar ellipticity of DXP had to be established using CD and NMR spectroscopy. Eq (2) was used to calculate the molar ellipticity ($13,200 \text{ deg cm}^2 \text{ dmol}^{-1}$) of DXP. A summary of the rate of enamine reaction with the alternative acceptors is given in Scheme 2.3. Clearly, reaction with D-GAP (4.21 s^{-1}) is the preferred outcome by a significant factor, but DXP synthase could produce significant acetolactate at very high pyruvate, or low GAP concentrations.

Scheme 2.3 Alternative acceptors for the enamine reactions under steady state conditions at 37 °C.



2.3.8 Arg-478 is essential for D-GAP binding. Previous molecular docking and structural analysis^(24, 27) suggested the phosphoryl group of D-GAP is anchored in the active site through interactions with two arginine residues, Arg-420 and Arg-478 (Figure 2.11) and may be important for D-GAP binding. Thus, R478A DXP synthase was created from JHU group and kinetically characterized. In agreement with values obtained from JHU, a higher $K_m^{\text{D-GAP}}$ for the R478A variant was measured by CD analysis ($K_m^{\text{D-GAP}} = 0.53 \pm 0.10 \text{ mM}$, Figure 2.12a) where DXP formation is monitored at 290 nm.⁽¹⁷⁾ These data suggest Arg-478 is involved in D-GAP binding and recognition.⁽²⁷⁾ The importance of Arg-478 to D-GAP affinity was also confirmed by using protein fluorescence at JHU.

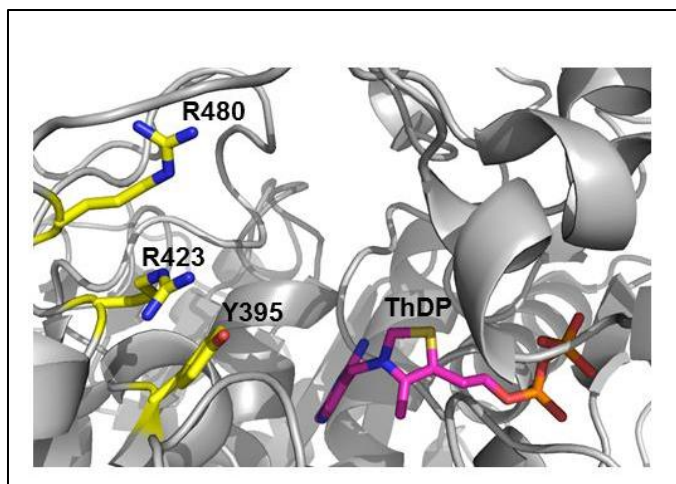


Figure 2.11 Active site residues of interest highlighted on *D. radiodurans* DXP synthase.⁽²⁷⁾ R480, R423 and Y395 correspond to R478, R420 and Y392, respectively, on *E. coli* DXP synthase.

The critical role of D-GAP to promote decarboxylation on DXP synthase⁽¹⁷⁾ raises questions about contributions of D-GAP-binding residues in this event. Thus, the individual steps of LThDP formation and decarboxylation were investigated on R478A DXP synthase using stopped-flow CD under pre-steady state conditions at 6 °C, using enzyme in excess of pyruvate (single turnover conditions). Upon titration with pyruvate LThDP forms on R478A DXP synthase (positive CD band centered at 315 nm, Figure 2.12b). The rates of LThDP formation ($k_1 = 0.85 \pm 0.03 \text{ s}^{-1}$) and decarboxylation in the absence of D-GAP ($k_2 = 0.04 \pm 0.004 \text{ s}^{-1}$) on R478A DXP synthase (Figure 2.12c), determined by measuring the accumulation and disappearance of LThDP at 315 nm, are within two-fold of the rates observed on wild type DXP synthase.⁽¹⁷⁾ In an experiment to measure D-GAP promoted decarboxylation of LThDP, LThDP was pre-formed in one syringe by mixing R478A DXP synthase and pyruvate at 6 °C and was then rapidly

mixed with D-GAP under saturating concentrations for this variant as determined by CD analysis placed in the second syringe. The rate of D-GAP promoted LThDP decarboxylation on R478A DXP synthase is comparable to wild type (Figure 2.12d).

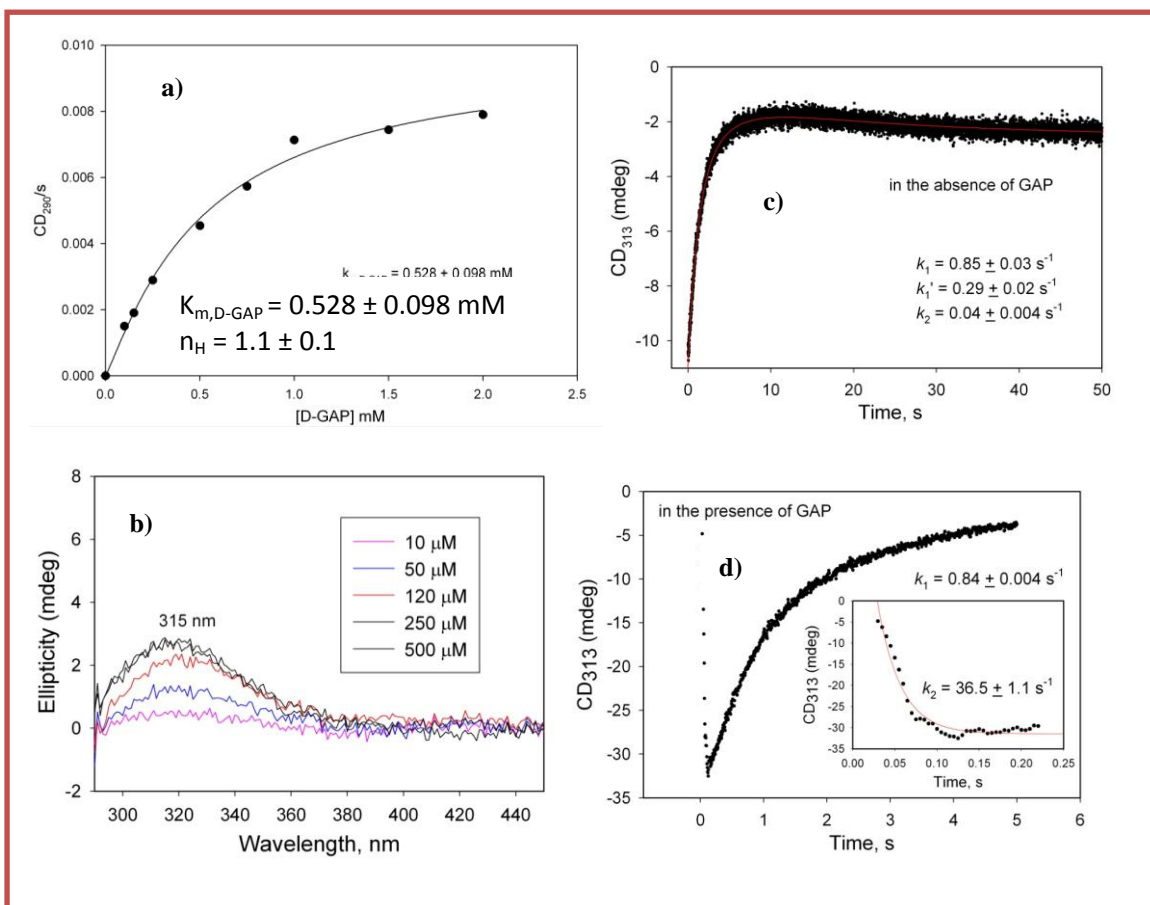


Figure 2.12 a) Determination of $K_{m, D-GAP}$ by monitoring DXP formation by variant R478A at 290 nm by CD; b) Formation of 1',4'-iminopyrimidylLThDP (315 nm) from pyruvate by R478A DXP synthase; c) Pre-steady state analysis of LThDP formation and decarboxylation on R478A, in the absence of D-GAP; d) Pre-steady state analysis of LThDP decarboxylation and re-synthesis on R478A in the presence of D-GAP (inset) fitting the expansion of early behavior, see Section 2.3.14.

Although product formation is likely occurring during this time, as determined by gCHSQC NMR spectroscopy (Figure 2.13), there is negligible contribution of the DXP signal (288 nm) at 313 nm (< 0.1 mdeg), and the rate of LThDP depletion can be confidently determined. Overall, the results indicate that while Arg-478 is important for D-GAP binding, the enzyme can still achieve a comparable rate of D-GAP-promoted LThDP decarboxylation in its absence, at high D-GAP concentration.

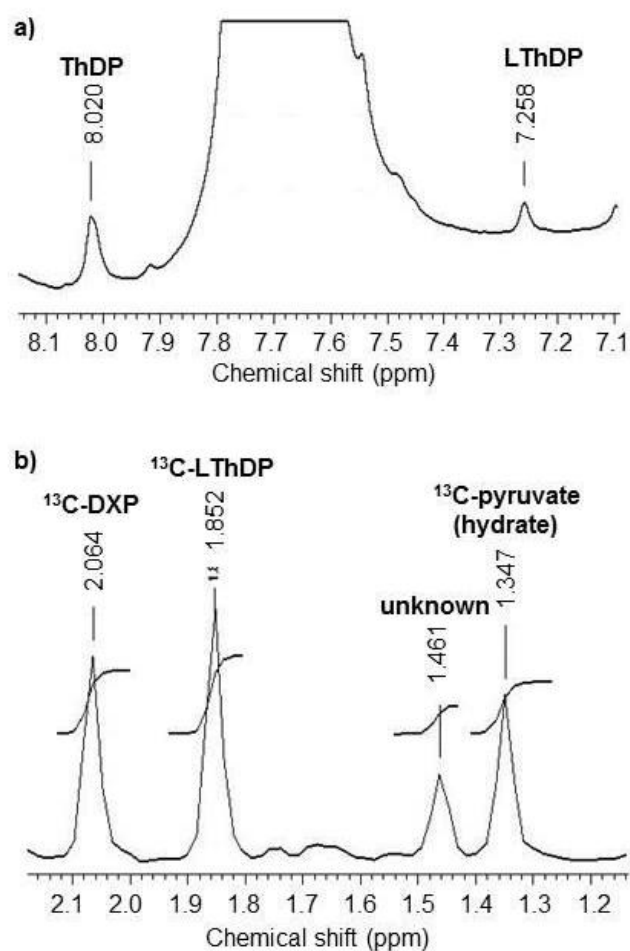


Figure 2.13 NMR detection of $[1-^{13}\text{C}]$ -DXP formation by R478A DXP synthase during pre-steady state, D-GAP promoted decarboxylation of pre-formed $[\text{C}2\beta-^{13}\text{C}]$ -LThDP. a)

Only LThDP is present on R478A DXP synthase 5 s after addition of D-GAP; b) Detection of $^{13}\text{CH}_3$ labeled groups: $[1-^{13}\text{C}]\text{-DXP}$ (28.5 %), $[\text{C}2\beta-^{13}\text{C}]\text{-LThDP}$ (35.5 %) and $[3-^{13}\text{C}]\text{-pyruvate}$ (23.3 %) by 1D gCHSQC spectroscopy (decoupled) of the same sample as in a).

2.3.9 The R420A substitution reduces affinity for D-GAP and stabilizes LThDP in the absence of D-GAP. Molecular docking analysis ⁽²⁴⁾ and crystallography studies have suggested Arg-420 as a possible anchoring point for the phosphoryl group of D-GAP (Figure 2.11). Thus, R420A DXP synthase was created by JHU group. The enzyme assay with and without coupled assay suggested that saturation with D-GAP could not be achieved which was further confirmed by CD (Figure 2.14a). Further, quenching of fluorescence was not observed upon titration of D-GAP to R420A DXP synthase up to concentrations of 15 mM, supporting a role of R420 in D-GAP binding.

2.3.10 The R420A substitution stabilizes LThDP in the absence of D-GAP but does not reduce the rate of D-GAP promoted decarboxylation. The rate of LThDP formation ($k_1 = 1.24 \pm 0.01 \text{ s}^{-1}$) on R420A, determined by monitoring LThDP formation at 313 nm as described above (Figure 2.14b,c), is also comparable to wild type DXP synthase (Table 2.2), suggesting Arg-420 is not critical for catalysis in LThDP formation. However, decarboxylation of LThDP in the absence of D-GAP on this variant is not measurable over 50 s, demonstrating a remarkable stabilizing effect of R420A on LThDP compared to wild type DXP synthase (Figure 2.14c). The rate of D-GAP promoted decarboxylation of LThDP on R420A DXP synthase was measured as described above for the R478A

variant and is comparable to wild type DXP synthase (Table 2.2, Figure 2.14d), indicating it is not essential for catalysis in D-GAP promoted decarboxylation of LThDP. The observation that R420A DXP synthase catalyzes the rate limiting step at a comparable rate to wild type DXP synthase under pre-steady state conditions suggests the near 4000-fold decrease in turnover efficiency measured for this variant under steady-state conditions is likely caused by a substantial increase in $K_m^{\text{D-GAP}}$.

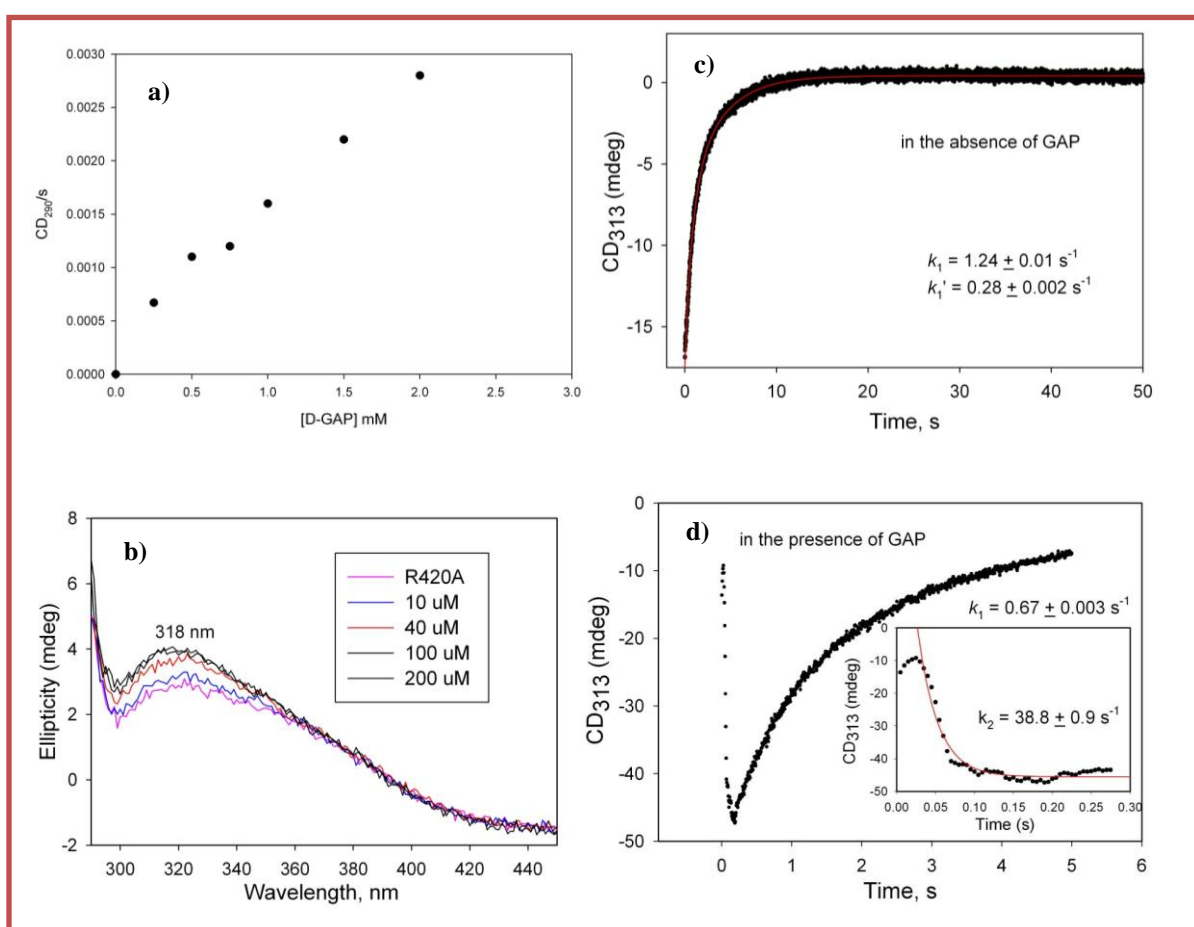


Figure 2.14 a) Determination of $K_m^{\text{D-GAP}}$ by monitoring DXP formation by variant R420A at 290 nm by CD; b) Formation of $1',4'$ -iminopyrimidylLThDP (318 nm) from pyruvate by R420A DXP synthase; c) Pre-steady state analysis of LThDP formation and

decarboxylation on R420A, in the absence of D-GAP; d) Pre-steady state analysis of LThDP decarboxylation and re-synthesis on R420A in the presence of D-GAP (inset) fitting the expansion of early behavior, see Section 2.3.14.

2.3.11 Tyr-392 contributes to D-GAP affinity. The observation that $K_d^{\text{pyruvate}} > K_m^{\text{pyruvate}}$ suggests the E-LThDP complex exhibits lower affinity compared to the E-LThDP-GAP ternary complex and prompted an investigation of residues that might be involved in binding pyruvate and stabilization of ThDP-bound intermediates along the reaction coordinate. The crystal structure of PDHc E1 component in complex with phosphono-LThDP indicates Tyr-599 stabilizes phosphono-LThDP via hydrogen bonding with one of the phosphonyl oxygen atoms.⁽²⁸⁾ On the basis of this observation, it was reasoned that Tyr-599 plays a similar role to stabilize the carbonyl oxygen of LThDP and position this intermediate for decarboxylation.⁽²⁸⁾ Sequence homology predicts Tyr-599 in PDHc E1 to be analogous to Tyr-392 in *E. coli* DXP synthase (Figure 2.11). Xiang *et al.* hypothesized on the basis of structure that Tyr-392 may interact with D-GAP⁽²⁷⁾ but reported a Y392F variant to exhibit turnover efficiency similar to wild type DXP synthase. We hypothesized that in a manner similar to Tyr-599 of PDHc E1, Tyr-392 may move into position to stabilize LThDP either upon binding of pyruvate in a manner that does not promote decarboxylation, or upon binding of D-GAP to facilitate decarboxylation. To investigate the role of Tyr-392 in DXP synthase substrate binding and catalysis, Y392F DXP synthase was constructed at JHU. The variant Y392F DXP synthase exhibits a change in affinity for D-GAP ($K_m^{\text{D-GAP}} = 210 \pm 20 \mu\text{M}$) which is supported by steady-state kinetic analysis using CD ($K_m^{\text{D-GAP}} = 280 \pm 30 \mu\text{M}$, Figure 2.15a). Contrary to our

expectations, nearly a 1.5-fold increase in K_m^{pyruvate} is observed for Y392F suggesting the hydroxyl group of Tyr-392 may contribute to, but is not essential for, binding of pyruvate or ThDP-bound intermediates along the reaction coordinate.

Interestingly, consistent with fluorescence binding experiments carried out on Y392F DXP synthase at JHU, CD analysis at 5 °C confirms the formation of 1',4'-iminopyrimidinyl LThDP, characterized by the appearance of a CD signal at 313 nm (Figure 2.15b), upon titration of Y392F DXP synthase with pyruvate. An apparent K_d^{pyruvate} on Y392F of 113 μM is comparable to that measured on wild type DXP synthase 90 μM using CD spectroscopy.⁽¹⁷⁾

2.3.12 Y392F stabilizes LThDP in the absence of D-GAP but does not affect D-GAP promoted decarboxylation. To determine the rate of formation and subsequent decarboxylation of LThDP (313 nm) on Y392F in the absence of D-GAP, stopped-flow CD experiments were performed under pre-steady state conditions at 6 °C, using Y392F DXP synthase in excess of pyruvate as described above. While the rate constant for formation of LThDP on Y392F is comparable to wild type ($k_1 = 1.06 \pm 0.03 \text{ s}^{-1}$, Figure 2.15c), LThDP appears to undergo decarboxylation in the absence of D-GAP at a lower rate ($k_2 = 0.01 \pm 0.003 \text{ s}^{-1}$), indicating that this substitution stabilizes LThDP on DXP synthase (Figure 2.15c). Further evidence for LThDP stability on Y392F was obtained by NMR analysis⁽¹⁵⁾ of a mixture of Y392F DXP synthase and pyruvate which was incubated on ice for 50 s and then quenched with TCA. The proton NMR spectrum shows the presence solely of LThDP with a C6'-proton chemical shift of 7.26 ppm,⁽¹⁷⁾ confirming its stability on Y392F.

The rate constant for D-GAP-dependent decarboxylation of LThDP on Y392F was measured using stopped-flow CD spectroscopy. In this experiment, LThDP was pre-formed in one syringe by mixing Y392F and pyruvate at 6 °C and was then rapidly mixed with D-GAP placed in the second syringe. The rate constant for decarboxylation of LThDP on Y392F ($k_2 = 39.5 \pm 1.4 \text{ s}^{-1}$, Figure 2.15d) was measured by monitoring depletion of the CD band at 313 nm. A similar experiment carried out using 500 μM D-GAP in the second syringe afforded the same rate of LThDP decarboxylation, confirming saturation with D-GAP.

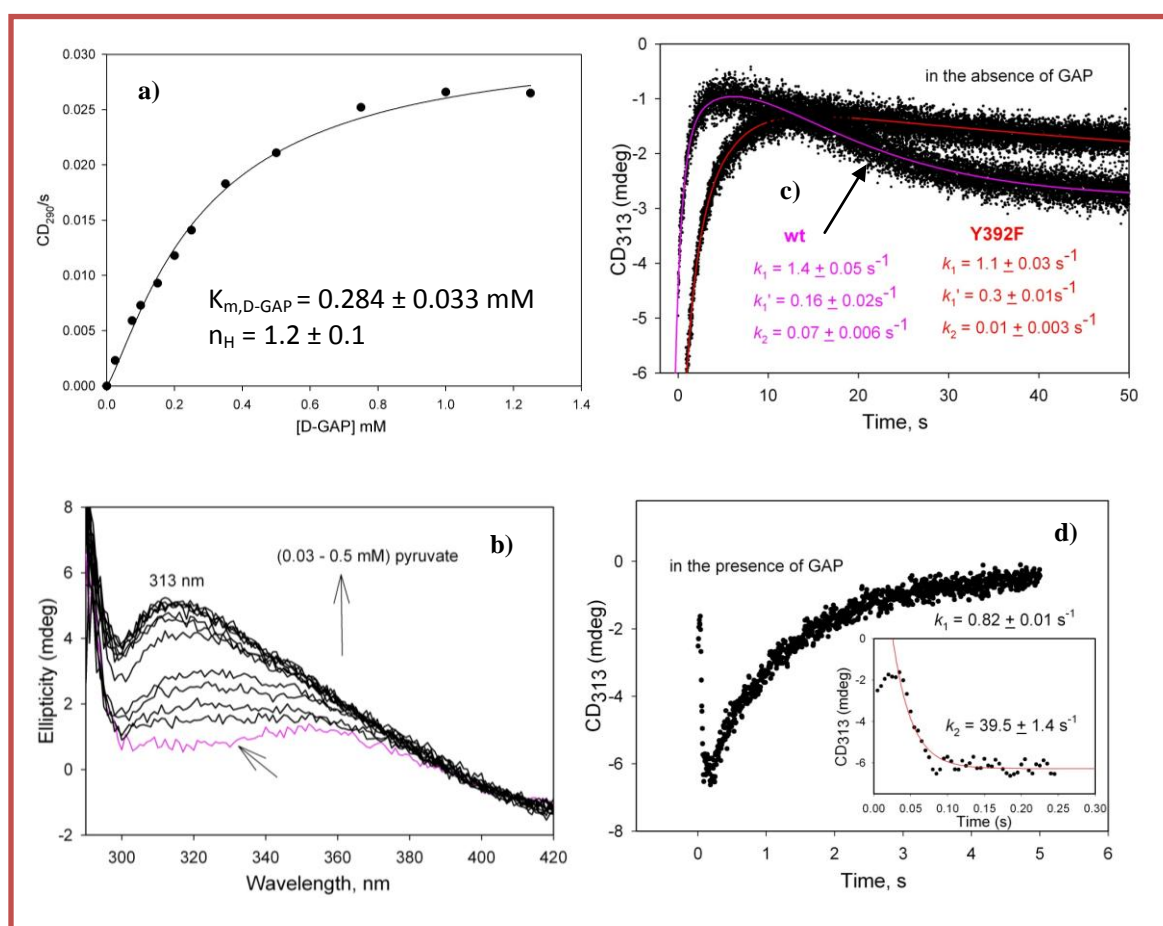


Figure 2.15 a) Determination of $K_{m, \text{D-GAP}}$ by monitoring DXP formation by variant Y392F at 290 nm by CD; b) Formation of 1',4'-iminopyrimidylLThDP (313 nm) from

pyruvate by Y392F DXP synthase; c) Pre-steady state analysis of LThDP formation and decarboxylation on Y392F (superimposable of wt and Y392F), in the absence of D-GAP; d) Pre-steady state analysis of LThDP decarboxylation and re-synthesis on Y392F in the presence of D-GAP (inset) fitting the expansion of early behavior, see Section 2.3.14.

2.3.13 DXP product formation by R420A, R478A and Y392F DXP synthase. Time-resolved CD spectroscopy was used to determine the rates for the formation of DXP at 290 nm⁽¹⁷⁾ from pyruvate and D-GAP on R420A, R478A and Y392F (Figure 2.16, Table 2.2). In each case, the DXP synthase variant (1.04 μ M active centers) in one syringe was mixed with pyruvate and D-GAP placed in the second syringe at 6 °C. Despite significant increases in $K_m^{\text{D-GAP}}$ for these variants, the rates of DXP formation are within two-fold of wild type DXP synthase in each case (Table 2.2)

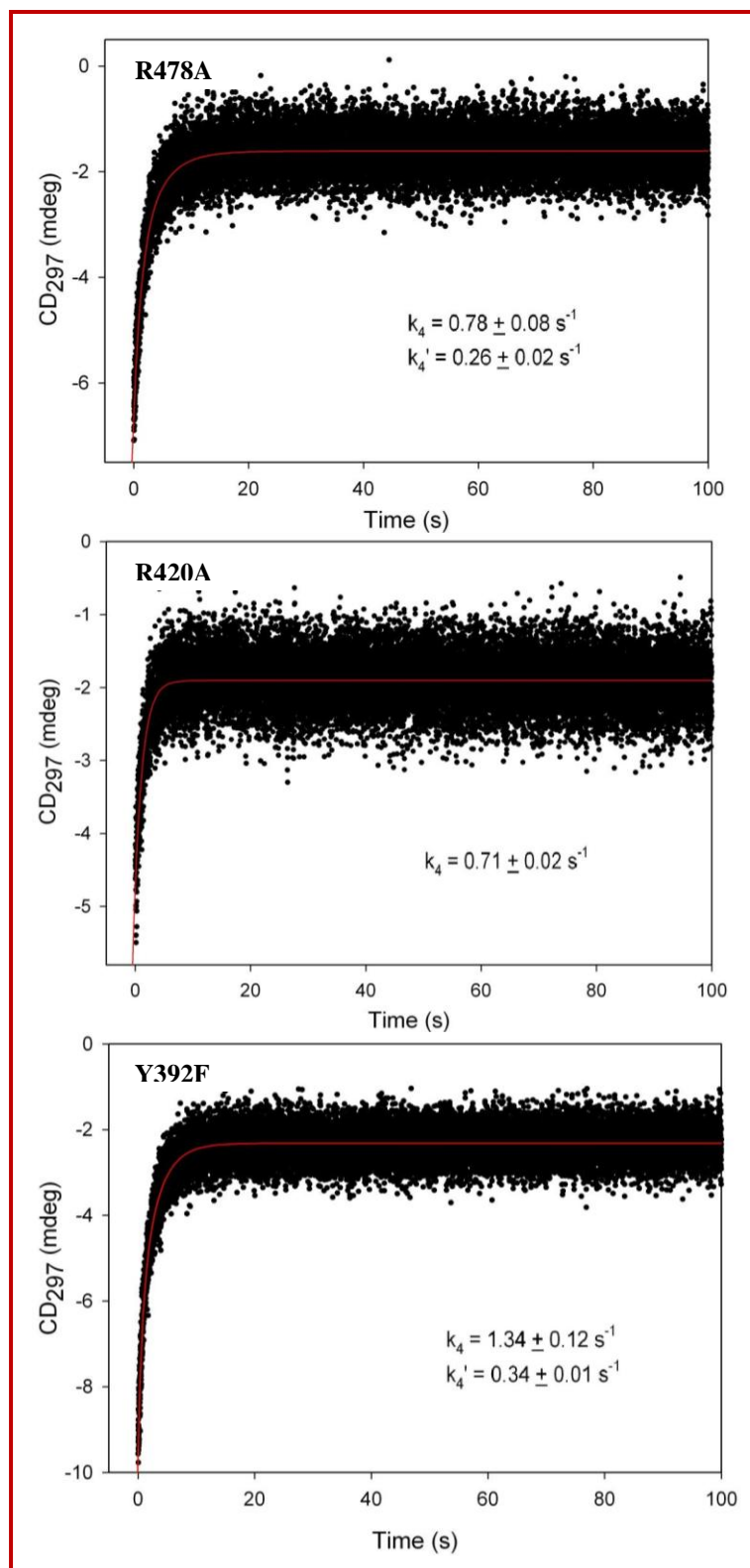


Figure 2.16 Pre-steady state rate of DXP formation by the DXP synthase variants R478A, R420A and Y392F at 6 °C.

2.3.14 Behavior of CD_{313} in stopped-flow CD experiments of LThDP decarboxylation in the presence of GAP. Based on our CD analysis of D-GAP-promoted decarboxylation of LThDP, we reported that re-synthesis of LThDP in the presence of excess pyruvate could account for the subsequent increase in the signal at 313 nm upon LThDP decarboxylation and depletion of D-GAP. Similarly, apparent LThDP re-synthesis following a rapid LThDP decarboxylation phase is observed here with all three variants. Despite having D-GAP in excess for R478A and R420A, the signal at 313 nm is shown to increase, albeit at a lower rate than LThDP formation in the absence of D-GAP (Table 2.2). Further, LThDP is observed by proton NMR after 30 s for R variants and 5 s for Y392F in the presence of pyruvate and excess D-GAP, suggesting LThDP can accumulate even in the presence of D-GAP which is known to promote decarboxylation at a higher rate than LThDP formation. In addition, closer inspection of the behavior of the signal at 313 nm on wild type DXP synthase and all three variants reveals two distinct “pauses”, time periods during which the signal at 313 nm does not change. The first pause (20-30 ms) occurs immediately upon addition of D-GAP, prior to the rapid decrease in signal at 313 nm, and a second, longer pause occurs for a period of ~200 ms immediately following LThDP depletion and prior to apparent LThDP re-synthesis (Figures 2.12d, 2.14d, 2.15d). The cause of this peculiar behavior is unknown and raises questions about the conformational dynamics and reactivity of active sites on DXP synthase as reported on ThDP enzymes BFDC and YPDC. ^(35, 36)

2.4 CONCLUSIONS

The CD assignments of the 1',4'-iminopyrimidine form of ThDP-bound pre-decarboxylation intermediates formed upon binding of pyruvate and analogues are summarized in Table 2.1. A combination of steady state and time-resolved CD spectroscopy was used to study the individual rate constants with wt and R478A, R420A and Y392F variants in the DXP synthase-catalyzed reaction (Table 2.2). On the basis of this information, LThDP formation appears to be the rate limiting step and LThDP has remarkable stability on DXP synthase, particularly on the Y392F and R420A variants. Apparently, the acceptor substrate D-GAP accelerates decarboxylation of LThDP significantly, while in the absence of D-GAP, decarboxylation is very slow on wt DXP synthase and variants, making DXP synthase unique among ThDP enzymes. These studies suggest a new approach for inhibitor design to develop new anti-infective agents targeting early stage isoprenoid biosynthesis.

Table 2.1 Assignment of the 1',4'-iminopyrimidine tautomeric form of ThDP- bound pre-decarboxylation intermediates from substrate and analogues on DXP synthase using CD spectroscopy.

DXP synthase wt & variants	Substrate analogues	&	IP positive CD band (nm)	K_d (μM)
wt	MAP		300	3.35 ± 0.6
wt	AcPhi		310	16 ± 1.1
wt	BAP		300	4.6 ± 1.3
wt	MAP + GAP		299	1.82 ± 0.5
E370A	MAP		300	6.2 ± 0.18^a
Y392F	ACPi		310	90.5 ± 25
wt	pyruvate		313	89.4 ± 0.01
Y392F	pyruvate		313	113 ± 1
R478A	pyruvate		315	80 ± 28
R420A	pyruvate		318	37 ± 8
E370A	Pyruvate		299	not saturated

^{a)} K_d is in mM.

Table 2.2 Microscopic rate constants for LThDP formation and decarboxylation and DXP formation on R478A, R420A and Y392F at 6°C.

Enzymes	k_1 (s ⁻¹)		k_2 (s ⁻¹)		k_4 (s ⁻¹)
	- D-GAP	+ D-GAP	- D-GAP	+ D-GAP	
Wild-type^a	1.39 ± 0.05 (0.16 ± 0.02) ^b	0.68 ± 0.01	0.07 ± 0.006	42.0 ± 1.0	1.24 ± 0.03 (0.29 ± 0.01) ^b
R478A	0.85 ± 0.03 (0.29 ± 0.02) ^b	0.84 ± 0.004	0.04 ± 0.004	36.5 ± 1.1	0.78 ± 0.08 (0.26 ± 0.02) ^b
R420A	1.24 ± 0.01 (0.28 ± 0.01) ^b	0.67 ± 0.003	No decomposition	38.8 ± 0.9	0.71 ± 0.02
Y392F	1.06 ± 0.03 (0.28 ± 0.01) ^b	0.82 ± 0.01	0.01 ± 0.003	39.5 ± 1.4	1.34 ± 0.12 (0.34 ± 0.01) ^b

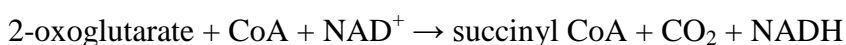
^aAnalysis reported in Patel *et al.*⁽¹⁷⁾ k_1 is the forward rate constants for LThDP formation, k_2 is the rate of decarboxylation of LThDP, k_4 is the rate of DXP product formation.
^bfitting to a biphasic equation producing two rate constants, the slower in parentheses. (two consecutive exponentials).

CHAPTER 3

Detection of an enamine intermediate and C2 α -hydroxy-carboxypropylidene-ThDP radical on E1 component of 2-oxoglutarate dehydrogenase complex from *Escherichia coli*

3.1 INTRODUCTION

The 2-oxo glutarate dehydrogenase multienzyme complex (OGDHc) is known for its role in the citric acid cycle. It catalyzes the formation of succinyl-Coenzyme A (succinyl-CoA), the rate-limiting step in the citric acid cycle.



The OGDHc is composed of multiple copies of three enzyme components:

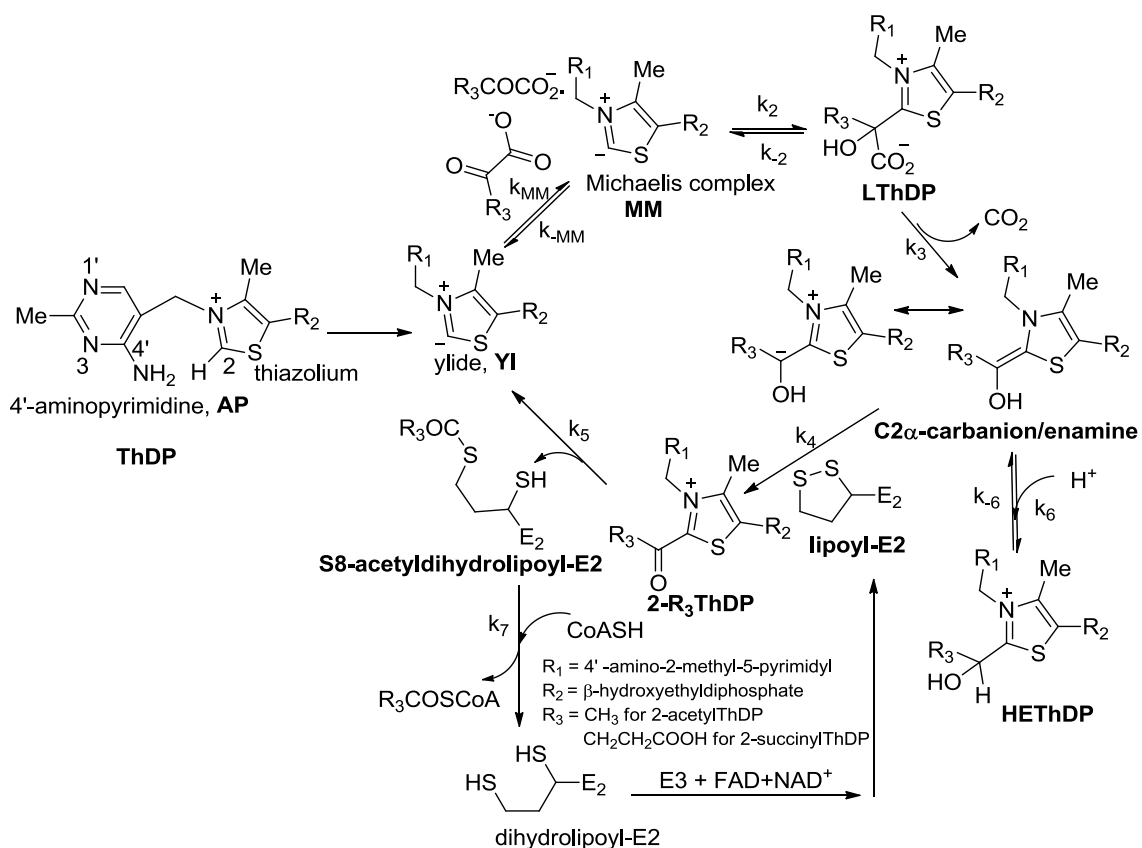
1. A thiamin diphosphate (ThDP) dependent 2-oxoglutarate dehydrogenase (E1o, 105 kDa, EC 1.2.4.2).
2. A dihydrolipoylsuccinyl transferase (E2o, 45 kDa, EC 2.3.1.6)
3. A dihydrolipoyl dehydrogenase (E3, 55 kDa, EC 1.8.1.4).

The three components act sequentially in the catalytic cycle of OGDHc (Scheme 3.1A)

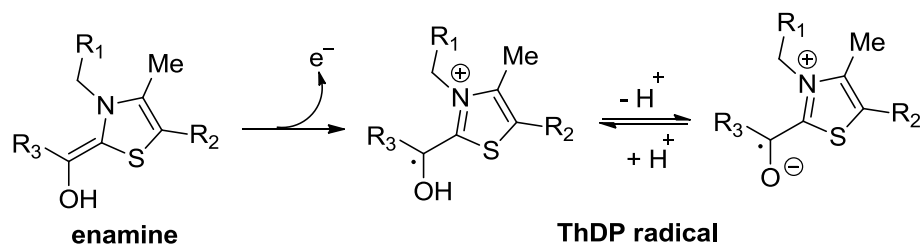
The first two components carry out the formation of succinyl CoA while the third one reoxidizes dihydrolipoylE2o to lipoylE2o. The mechanism is similar to other 2-oxo acid dehydrogenase complexes, such as pyruvate dehydrogenases (PDHc) and branched-chain dehydrogenases (BCDHc). The E1o catalyzes the decarboxylation of the substrate 2-oxoglutarate (2-OG) using ThDP as a cofactor, then reductively succinylates a lipoyl group bound to a lysine residue in E2o. The E2o is known as a succinyl transferase responsible for transferring the succinyl group from the succinyldihydrolipoyl group of

E2o to CoA, and the dihydrolipoyl group so generated on E2o is finally reoxidized to the dithiolane ring by the flavoprotein E3, with NAD^+ as the ultimate electron acceptor. Our group reported that *E. coli* E1o has a broad substrate specificity making it an excellent candidate for protein engineering.^(37, 38) Taking this into consideration, we focused on the reaction mechanism catalyzed by *E. coli* E1o.

Scheme 3.1 A. Mechanism of pyruvate and 2-oxoglutarate dehydrogenase complexes.



B. Formation of one electron oxidation product ThDP radical.



Circular dichroism of E1o with its substrates 2-OG and 2-oxoadipate (2-OA) revealed two positive CD bands, ~300 nm and 350 nm. The 300 nm signal was found to be the post-decarboxylation product based on TH method⁽¹⁵⁾ where multiple reaction samples were prepared by mixing E1o with substrate 2-OG and acid quenched within millisecond to minute time points. The gradient carbon HSQC NMR confirmed the HETHDP-like intermediate with C6'-H chemical shift at 7.37 ppm. While in the presence of the alternate enamine acceptor DCPIP, we observed HETHDP as well as succinylThDP at 7.45 ppm.^(15, 39) Evidence from stopped-flow CD and continuous wave electron paramagnetic resonance (cw-EPR) spectroscopy with 2-OG and 2-OA suggests that the CD signal at 350 nm could be the enamine and/or one electron oxidation product hydroxy-carboxypropylidene-ThDP radical (Scheme 3.1B) as seen with E1o-ec and some other ThDP enzymes.⁽⁴⁰⁻⁴³⁾ The significant stability of an enamine and/or radical allowed us to characterize the intermediate by EPR spectroscopy and to determine the pre-steady state rates of its formation and depletion with both the substrates 2-OG and 2-OA. Also, with 2-OG, we may be able to observe the effect of various enamine acceptors on the CD signal at 350 nm. A combination of CD, stopped-flow CD, NMR and EPR spectroscopic tools were used to provide spectroscopic assignments of the ThDP-bound intermediates on E1o-ec and formation of hydroxy-carboxypropylidene-ThDP radical with its real substrate 2-OG as well as with the longer analogue 2-OA. This study helps to understand the mechanism of this enzyme catalyzing the rate-limiting step in the citric acid cycle.

3.2 MATERIALS and METHODS

3.2.1 Materials

Thiamin diphosphate (ThDP), dithiothreitol, and isopropyl- β -D-thiogalactopyranoside (IPTG) were from U.S. Biochemical Corp. 2-oxo glutaric acid, 2-oxo adipic acid, glyoxylic acid, NAD⁺, coenzyme A (CoA), and 2,6-dichlorophenolindophenol (DCPIP) were from Sigma-Aldrich.

Purification of E1o-ec and E2o-ec¹⁻¹⁷⁶ didomain is described under Appendix Chapter 3.

Methods

3.2.2 Activity Measurements

DCPIP activity measurement

The E1-specific activity of wild type E1o was measured by monitoring the reduction of DCPIP at 600 nm using a Varian DMS 300 spectrophotometer. The assay medium (1 ml) contained in 20 mM KH₂PO₄ (pH 7.0), 2 mM MgCl₂, 0.2 mM ThDP, 0.1 mM DCPIP and 2 mM 2-OG at 30 °C. The reaction was initiated by adding the enzyme (10 μ g). One unit of activity is defined as the amount of DCPIP reduced (μ mol/min/mg of E1o). For K_m measurement, similar conditions were used in the presence of substrates [2-OG (0.001-4 mM) or 2-OA (0.005-3.5 mM)]. The observed slope was plotted against [substrate] and K_m values were calculated by using Eq 9 in Chapter 2 (Table 3.1A).

$$v = (V_m * x^n) / (x^n + (S_{0.5}^n * (1+x/K_i))) \quad (9)$$

Where V_m is the maximum slope observed, x is the ligand concentration, n is the Hill coefficient ($S_{0.5} = K_m$ if $n=1$) and K_i is the inhibition constant.

Overall activity measurement

The overall activity of E1o was determined from the substrate-dependent reduction of NAD⁺ at 340 nm after reconstitution of E1o:E2o: E3 at a mass ratio of 1:1:1 (mg/mg/mg) for 20 min at 25 °C in 20 mM KH₂PO₄ (pH 7.2) containing 150 mM NaCl. The assay medium (1 ml) contained 0.1 M Tris-HCl (pH 8.0), 0.2 mM ThDP, 1 mM MgCl₂, 2.6 mM dithiothreitol, 2.5 mM NAD⁺ and substrates [2-OG (0.01-2 mM) or 2-OA (0.08-3 mM)]. The reaction was initiated by addition of CoA (0.13 mM) and E1o (5 µg) at 30 °C. The initial steady state velocities were determined from the progress curves recorded at 340 nm. One unit of activity is defined as the amount of NADH produced (µmol/min/mg of E1o). The slope was plotted against [substrate] and K_m was calculated by using Hill Eq 1 in Chapter 2 (Table 3.1B).

Table 3.1 A. DCPIP activity measurement of E1o with substrates at 30°C.

substrates	DCPIP (µmol min ⁻¹ mg ⁻¹)	<i>k</i> _{cat} (s ⁻¹)	<i>K</i> _m (mM)	<i>k</i> _{cat} / <i>K</i> _m (s ⁻¹ mM ⁻¹)
2-oxoglutarate	0.64	2.24	0.0010 ± 0.0001	2240
2-oxoadipate	0.58	2.03	0.0075 ± 0.001	270.7

B. Overall NADH activity measurement of E1o with substrates at 30°C.

substrates	Activity (µmol min ⁻¹ mg ⁻¹)	<i>k</i> _{cat} (s ⁻¹)	<i>K</i> _m (mM)	<i>k</i> _{cat} / <i>K</i> _m (s ⁻¹ mM ⁻¹)
2-oxoglutarate	10.9 (0.1) ^a	38.17 (0.35)	0.066 ± 0.007 (0.139 ± 0.05)	578.3 (2.52)
2-oxoadipate	0.2	0.7	0.132 ± 0.028	5.30

^a HLADH activity with 2-OG

Formation of succinic semialdehyde by E1o with 2-OG. The activity was measured using a horse liver alcohol dehydrogenase (HLADH) coupled assay by monitoring the depletion of NADH at 340 nm on a Varian DMS 300 spectrophotometer. The assay medium (1 ml) contained in 20 mM KH_2PO_4 (pH 7.0), 0.2 mM ThDP, 2 mM MgCl_2 , HLADH (0.25 unit/ml), NADH (0.35 mM) and 2-OG (0.1-6 mM) at 30 °C. The reaction was initiated by adding the enzyme (10 μg). One unit of activity is defined as the amount of NADH depleted ($\mu\text{mol}/\text{min}/\text{mg}$ of E1o). K_m was determined using Eq 1 in Chapter 2.

3.2.3 Circular dichroism experiments with substrates

CD spectra were recorded on an Applied Photophysics Chirascan CD Spectrometer (Leatherhead, U.K.) in 2.4 ml volume with 1 cm path length cell.

The titrations were carried out in 20 mM KH_2PO_4 (pH 7.0) containing 150 mM NaCl, 0.2 mM ThDP and 1 mM MgCl_2 at 20 °C. CD spectra were recorded in the near-UV (290-450 nm) wavelength region. The concentration used for E1o was 20 μM (active sites concentration) and substrates 2-OG (0.05-5 mM) or 2-OA (0.2-5 mM).

3.2.4 Stopped-flow CD

Kinetic traces were recorded on a Pi*-180 stopped-flow CD spectrometer (Applied Photophysics, U.K.) using 10 mm path length. The intermediates seen on CD at ~298 and ~352 nm were detected at 297 nm and 365 nm respectively, as dictated by the high sensitivity of the lamp at those wavelengths. Data from six to seven repetitive shots were averaged and fit to the appropriate Eq 5-7 (see Chapter 2). All stopped-flow CD

experiments were performed in 20 mM KH_2PO_4 (pH 7.0) containing 0.5 mM ThDP and 2 mM MgCl_2 at 20 °C.

Pre-steady state rate determination of ThDP-bound intermediates on E1o. E1o (38 μM active centers) was placed in one syringe and substrates 2-OG (4 mM) or 2-OA (2 mM) in the second syringe. The reactions were monitored for 50 s at 297 nm and 365 nm.

Pre-steady state behavior of CD at 365 nm on 2-OG concentration. E1o (38 μM active centers) from one syringe was mixed with 2-OG (120, 200, 240, 600 μM) placed in the second syringe and the reaction was monitored for 50 s at 20 °C. Similar experiments were carried out in the presence of alternative enamine acceptors lipoyl domain (LDo, 310 μM) and E2o-¹⁻¹⁷⁶didomain (DDo, 60 μM) from E2o-ec, DCPIP (50 μM) and glyoxylate (GA, 2 mM) combined with 2-OG in the second syringe.

3.2.5 Rapid chemical quench and NMR experiments

The rapid reaction mixing was performed using a Kintek RQF-3 model (Kintek Corp) and NMR spectra were acquired on a Varian INOVA 600 MHz instrument. The water signal was suppressed by pre-saturation.

Reconstitution of apo enzyme with $[\text{C}_2, \text{C}_6'-^{13}\text{C}_2]$ ThDP. A solution of purified apo E1o (0.12 mM) was incubated in ice with 1 equivalent of $[\text{C}_2, \text{C}_6'-^{13}\text{C}_2]$ ThDP (0.12 mM) and 5 mM MgCl_2 for 30 min.

Sample preparation. The individual reactions were done at different time points in 20 mM KH_2PO_4 (pH 7.4). Syringe A contained in $[\text{C}_2, \text{C}_6'-^{13}\text{C}_2]$ ThDP labeled E1o (120 μM active centers), syringe B contained in substrate 2-OG (20 mM) or 2-OA (20 mM) and DCPIP (8 mM) or succinic semi aldehyde (20 mM) and syringe C contained in acid

quench solution of 12.5% TCA in 1M DCl/D₂O. The reaction with substrate 2-OG was performed at time period of 10 to 2000 ms and the same reaction in the presence of DCPIP for 10 to 200 ms. For longer time scales the reactions with 2-OG (30 s, 3 min), in the presence of DCPIP (20 s) and with succinic semi aldehyde (30 s) were mixed manually by following the same protocol. First, 200 μ l of labeled E1o was mixed with 200 μ l of substrates and quenched with 200 μ l of acid solution. The quenched reaction was centrifuged at 15700g for 20 min and the supernatant was separated and filtered through Gelman 0.45 μ M discs. The filtrate was analyzed by gCHSQC NMR spectroscopy at 25 °C.

3.2.6 Sample preparation for EPR spectroscopy

The reaction mixture (200 μ l) containing 50 mM Tris-HCl (pH 7.4), 2 mM ThDP, 2 mM MgCl₂, 150 μ M E1o-ec, 10% glycerol was mixed with 10 mM substrates 2-OG or 2-OA at room temperature in an Eppendorf tube and transferred into an EPR tube. After ~30 s, the samples with 2-OG or 2-OA were frozen in liquid nitrogen and the sample was inserted into the ESR probe.

3.3 RESULTS and DISCUSSION

3.3.1 *ThDP on E1o*. It was reported from CD studies at Rutgers that ThDP enzymes can exist in the AP or the IP tautomeric forms.⁽²⁵⁾ Increasing the concentration of E1o, led to the appearance of a positive CD band at 304 nm and a negative one at 328 nm, attributed to the IP and AP tautomeric forms of ThDP, respectively (Figure 3.1).

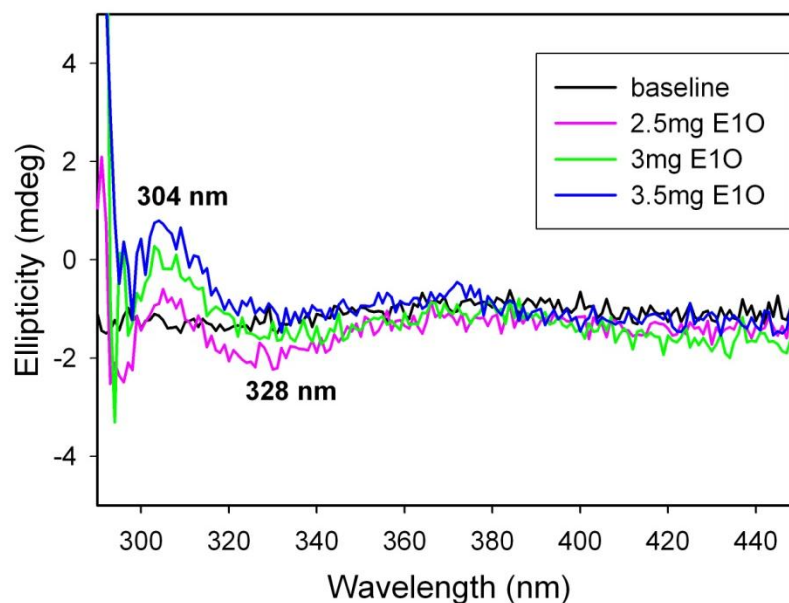


Figure 3.1 Observation of IP and AP form of ThDP on E1o without substrate. E1o (23.80 μm , 28.57 μm , 33.33 μm active centers) in 20 mM KH_2PO_4 (pH 7.0) containing 0.2 mM ThDP and 2 mM MgCl_2 and CD spectra were recorded in range of 290-450 nm.

3.3.2 Formation of post decarboxylation intermediate on E1o with substrates 2-OG and 2-OA.

The enzyme E1o-ec with its natural substrate 2-OG and also with 2-OA formed two positive CD signal ~ 300 nm and ~ 350 nm (Figure 3.2) upon titration. Based on information available for CD assignments, the positive band at 300 nm could pertain to either pre- or post-decarboxylation intermediates. To solve this ambiguity gradient carbon HSQC NMR experiment was performed by using $[\text{C}_2, \text{C}_6\text{'-}^{13}\text{C}_2]\text{ThDP}$ labeled E1o, prepared by incubation of apo E1o with $[\text{C}_2, \text{C}_6\text{'-}^{13}\text{C}_2]\text{ThDP}$ which was then mixed with substrate 2-OG and quenched in acid at different time points to precipitate the enzyme and the supernatant was used for NMR measurement.

The NMR spectrum revealed chemical shift of C6'H at 7.36 ppm (Figure 3.3A, left) corresponding to a HETHDP-like compound (hydroxy-carboxypropylidene-ThDP) according to the TH method. This in the presence of the alternate enamine acceptor DCPIP undergoes oxidation to AcThDP which has chemical shift of 7.37 next to the HETHDP at 7.33 ppm (chemical shift reported with pyruvate).^(15, 39) Indeed the NMR spectrum in the presence of DCPIP resulted in two NMR peaks 7.37 ppm and 7.47 ppm (Figure 3.3A, right). Since the chemical shift difference for HETHDP and AcThDP is very little, 7.37 ppm was assigned to hydroxy-carboxypropylidene-ThDP (HETHDP-like) and 7.47 the succinylThDP (AcThDP-like). At later times, there is a depletion of both resonances corresponding to hydroxy-carboxypropylidene-ThDP (HETHDP-like) and succinylThDP (Figure 3.3B). Depletion of the 7.47 ppm resonance could be due to hydrolysis of succinylThDP as reported for hydrolysis of acetylThDP.⁽³⁹⁾

The chemical shift of C6'-H for hydroxy-carboxypropylidene-ThDP was further confirmed by an acid quench NMR experiment of E1o-ec with succinic semialdehyde (7.37 ppm, Figure 3.3C). The presence of hydroxy-carboxypropylidene-ThDP in the NMR spectrum even after a 3 min incubation of E1o with 2-OG suggests the stability of post-decarboxylation intermediate correlates well with our CD results (stability of 300 nm CD band), the band which is even stronger with the 2-OA substrate.

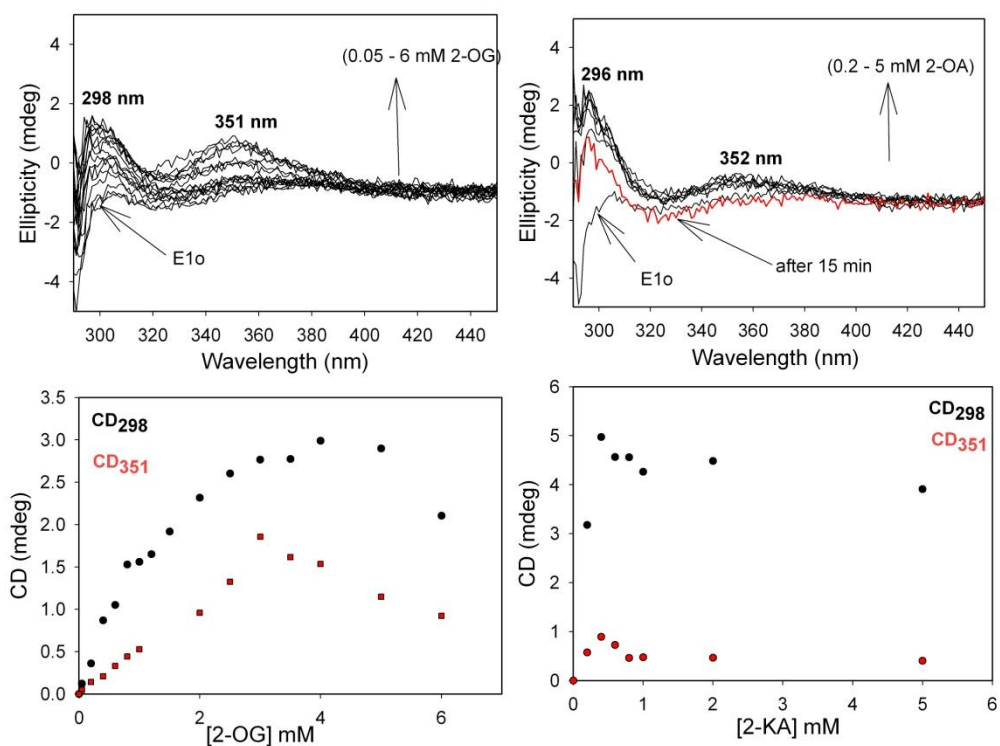
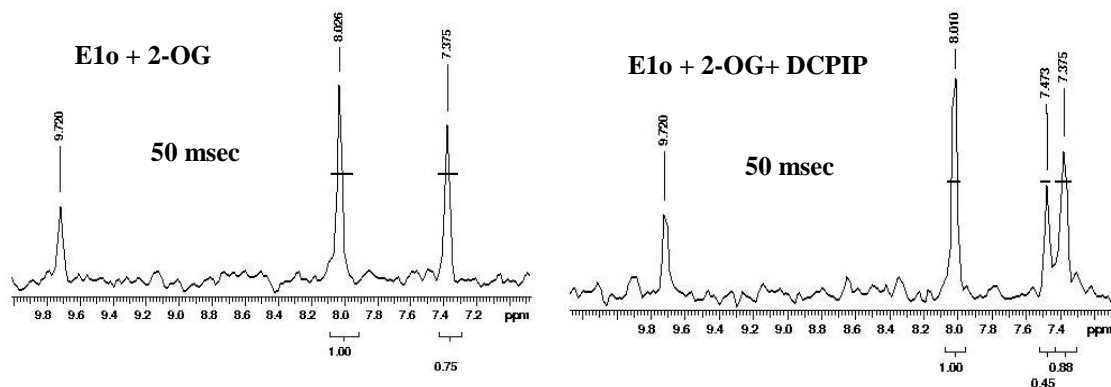


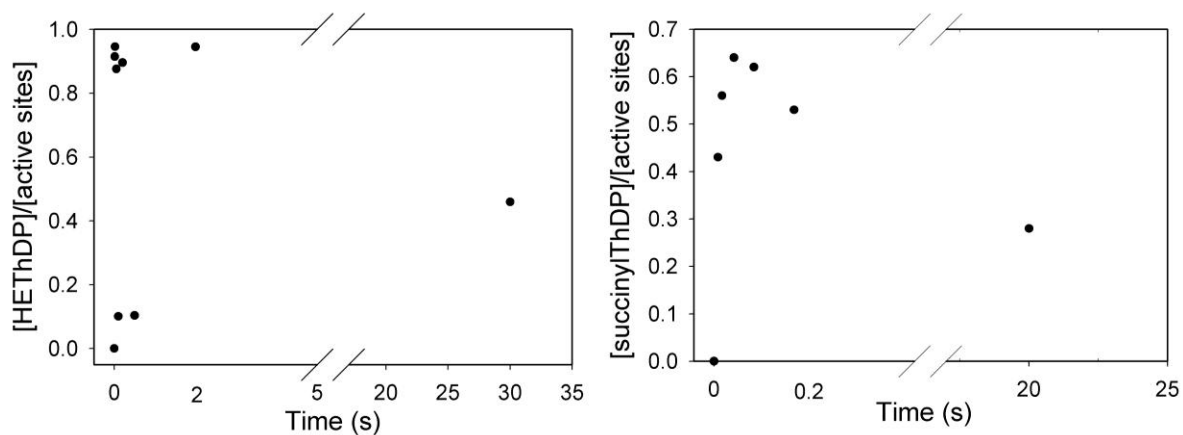
Figure 3.2 (Top) Formation of post-decarboxylation intermediate on E1o-ec with 2-OG (left) and 2-OA (right) ~298 nm and an enamine and/or hydroxy-carboxypropylidene-ThDP radical ~ 351 nm (left). (Bottom) CD changes at 298 and 351 nm were plotted against concentration of substrate.

Figure 3.3 A. NMR spectrum of acid quench reaction after 50 msec incubation of $[C_2, C_6\text{'-}^{13}C_2]$ ThDP labeled E1o with 2-OG in the absence (left) and presence (right) of DCPIP. The C6'H chemical shift of 8.01, 7.36 and 7.46 corresponds to ThDP, hydroxy-carboxypropylidene-ThDP and succinylThDP, respectively.

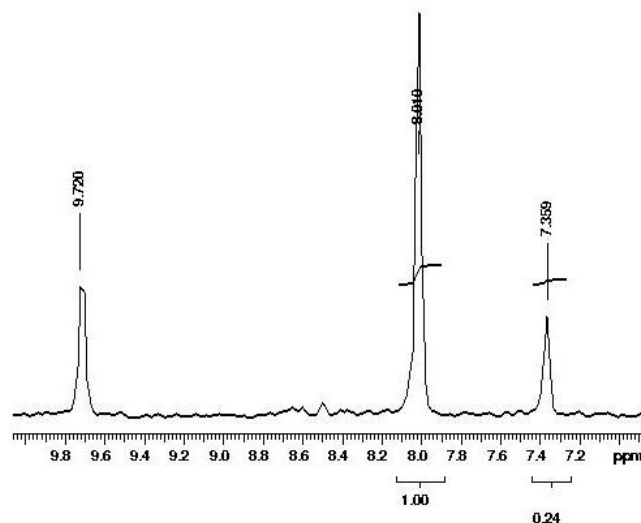
A.



B. Time-dependent behavior of hydroxy-carboxypropylidene-ThDP (HEThDP-like) at 7.36 and succinylThDP at 7.46 ppm in A.



C. Formation of hydroxy-carboxypropylidene-ThDP by reacting E1o with succinic semialdehyde.



3.3.3 Pre-steady state rates of formation of ThDP-bound intermediates on E1o with substrates 2-OG and 2-OA.

To determine the pre-steady state rates of formation of the CD species seen at 300 nm and 350 nm, E1o (38 μM active centers) placed in one syringe was mixed with substrates 2-OG (4 mM) or 2-OA (2 mM) placed in the second syringe and the reaction was monitored for 50 s at 297 nm and at 365 nm (two different experiments). The observed rates of the formation of post-decarboxylation intermediate at 297 nm are: $0.78 \pm 0.02 \text{ s}^{-1}$ (with 2-OG) and $0.55 \pm 0.02 \text{ s}^{-1}$ (with 2-OA) (Figure 3.4 A), while at 365 nm the rates are: $k_1 = 2.8 \pm 0.1 \text{ s}^{-1}$, $k_1' = 0.3 \pm 0.01 \text{ s}^{-1}$, $k_2 = 0.011 \pm 0.008 \text{ s}^{-1}$ (with 2-OG) and with 2-OA, $k_1 = 1.5 \pm 0.1 \text{ s}^{-1}$, $k_2 = 0.02 \pm 0.004 \text{ s}^{-1}$ (Figure 3.4 B). The rates of formation of post-decarboxylation intermediate with 2-OG and 2-OA are comparable.

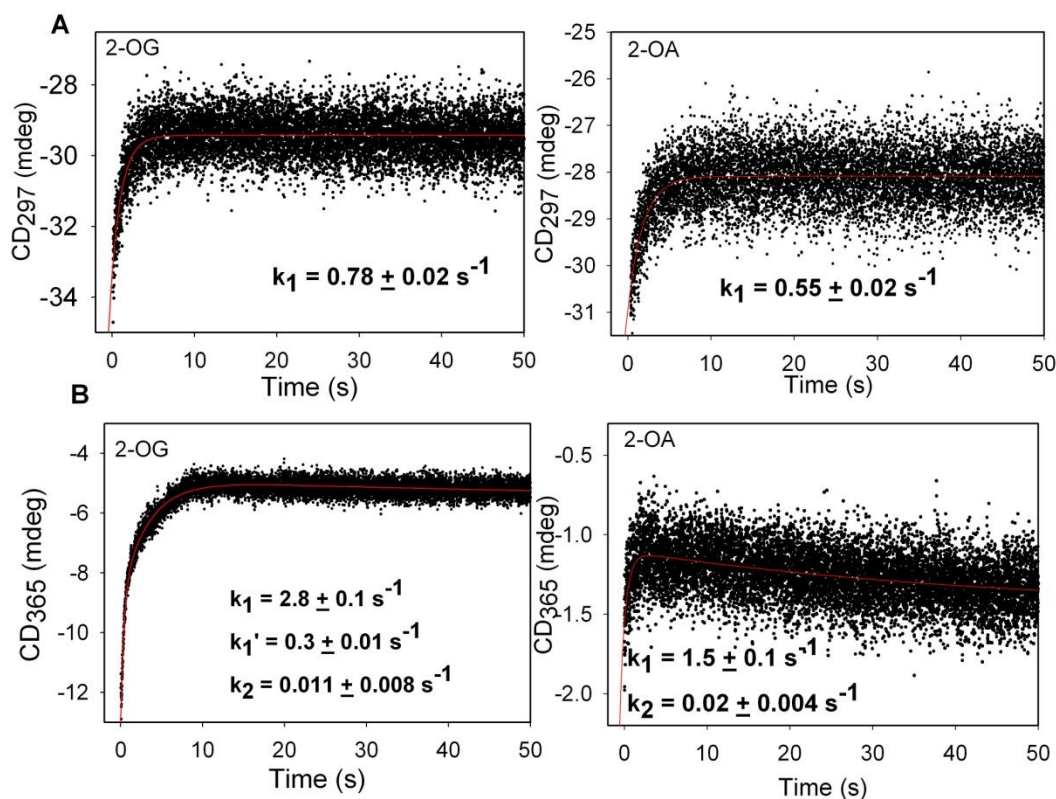


Figure 3.4 Pre-steady state rate determination of **A.** post-decarboxylation intermediate, data were fitted to Eq 5 in Chapter 2; **B.** an enamine and/or radical, on E1o with substrates 2-OG and 2-OA, data were fitted using Eq 7 & 8 (Chapter 2), respectively.

The stopped-flow CD results suggests that the formation of the 350 nm species is faster than that of the post-decarboxylation intermediate at 300 nm; this suggest that the species at 350 nm precedes formation of the post-decarboxylation intermediate, consistent with the assignment of the newly-observed band at 350 nm (never observed before with either E1o or any other ThDP enzyme) to the enamine.

3.3.4 What is the origin of the positive CD signal ~350 nm?

As mentioned above that E1o component upon addition of substrates 2-OG and 2-OA generates a new CD band at 350 nm which we have not seen before.

There are three possible assignments for this transient species:

1. The enamine product of decarboxylation
2. The one-electron oxidation product of the enamine, hydroxy-carboxypropylidene-ThDP radical or
3. The two-electron oxidation product 2-succinylThDP.

Very recently, we have ruled out the 3rd possibility of 2-succinylThDP as a product since it could be generated from the reaction of fluoropyruvate with E1p, which gives rise to a new CD band at 40-45 nm longer wavelength i.e., around 390-395 nm (performed by Dr. Natalia Nemeria). Also, the Cambridge group has observed hydroxy-carboxypropylidene-ThDP radical on the *E. coli* E1o with 2-OG and elucidated the radical formation mechanism.⁽⁴⁰⁾ On the other hand, the evidence from the NMR experiment with 2-OG suggests that enamine is being formed, which after protonation forms hydroxy-carboxypropylidene-ThDP at 7.36 ppm.

We tried to obtain additional evidence to be able to discern between the enamine and the radical, by trying different potential acceptors for the enamine at 365 nm. As control, we carried out stopped-flow CD experiments mixing E1o with increasing concentrations of 2-OG, and could observe relatively good stability of the 365 nm signal with high concentration of substrate (Figure 3.5). At low concentration of substrate we could see formation and depletion of the signal, which was thought to be an ideal condition for comparing the CD behavior at 365 nm in the presence of possible enamine

acceptors/interceptor. This behavior was also observed in steady state CD experiments where the 350 nm band was depleted after a certain amount of time (Figure 3.2, Right).

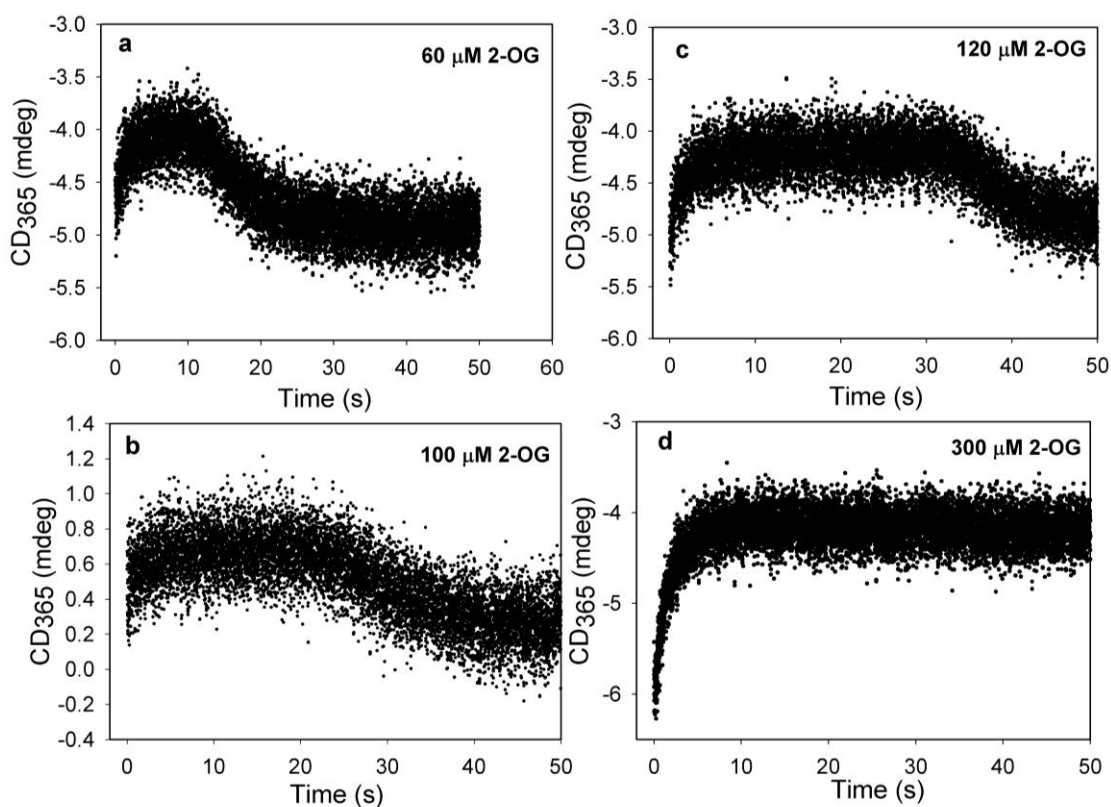


Figure 3.5 Stopped-flow CD behavior at 365 nm with different concentrations of 2-OG mixed with E1o-ec **a.** 60 μM , **b.** 100 μM , **c.** 120 μM , **d.** 300 μM after mixing (in the syringe was placed double the concentration of the amount mentioned here).

Indeed, stopped-flow CD experiments were carried out with enamine acceptors E2o-lipoyldomain and E2o¹⁻¹⁷⁶didomain, DCPIP and glyoxylate (Figure 3.6). According to the stopped-flow results, DCPIP and glyoxylate act similarly as acceptors, while the E2o¹⁻¹⁷⁶ didomain appears to be the best acceptor compared to others. The presence of these three acceptors (DCPIP, glyoxylate, E2o¹⁻¹⁷⁶didomain) shortened the lifetime of the 365 nm CD band supporting the possibility of an enamine (Figure 3.6 b-d). In contrast

and surprisingly, the lipoyl domain in fact stabilizes the CD signal at 365 nm which is consistent with the radical, 2nd possibility. It is also possible that the CD signal seen at 350 nm represents an overlap of two species, an enamine and hydroxycarboxypropylidene-ThDP radical. To obtain evidence for radical formation, we performed EPR spectroscopy with the help of Prof. Gary Gerfen at Albert Einstein College of Medicine where E1o-ec was incubated with 2-OG or 2-OA for ~30 s and reactions were stopped by freezing in liquid nitrogen.

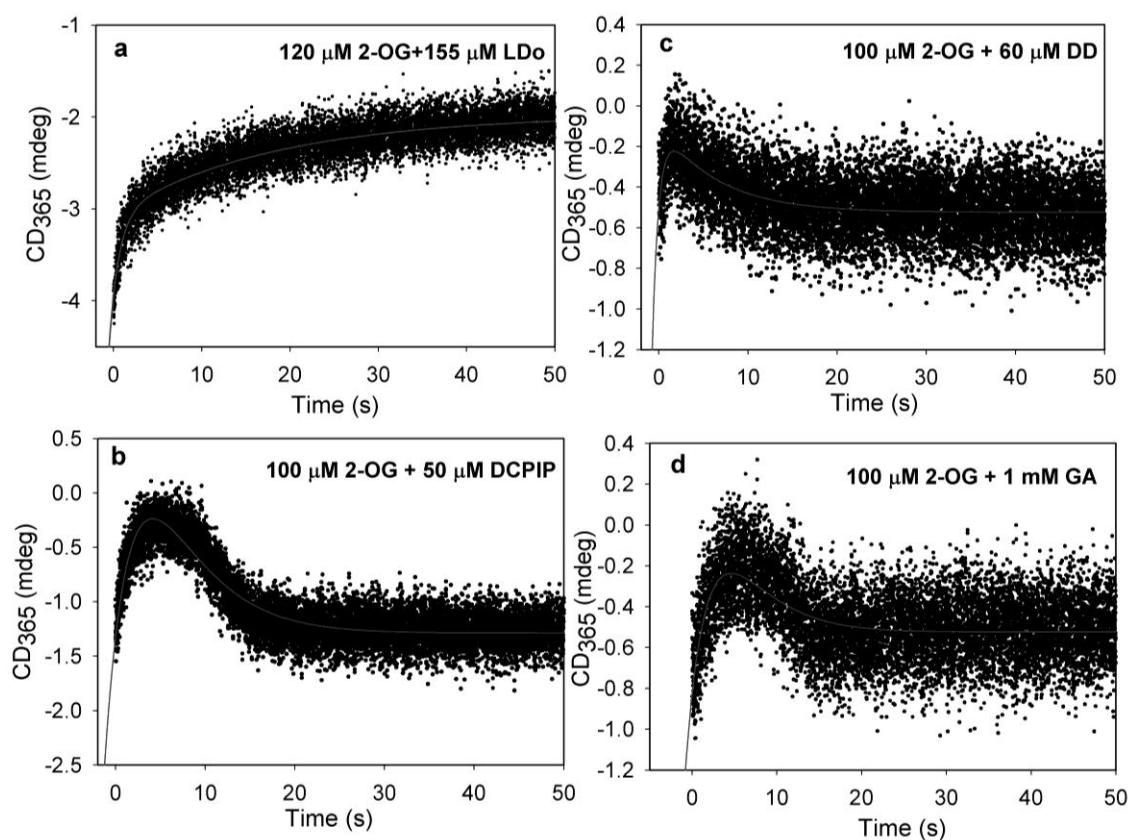


Figure 3.6 Effect of different enamine acceptors on the CD at 365 nm. Typically, E1o (38 μM active sites concentration) from one syringe was mixed with the acceptors

(concentration mentioned in figure) premixed with 2-OG in the second syringe a. E2o-ec lipoyl domain (LDo), b. DCPIP, c. E20-ec¹⁻¹⁷⁶ didomain (DDo), d. glyoxylate.

The sample prepared with excess substrates (10 mM) revealed a cw-EPR spectrum attesting to radical formation with both the substrates 2-OG and 2-OA (Figure 3.7). Not only could we reproduce the radical on E1o-ec with 2-OG⁽⁴⁰⁾ but also produced the same radical with the longer substrate 2-OA. This result further supports our second possibility of radical formation from an enamine, but does not rule out the idea that the positive CD band at 350 nm pertains to the enamine.

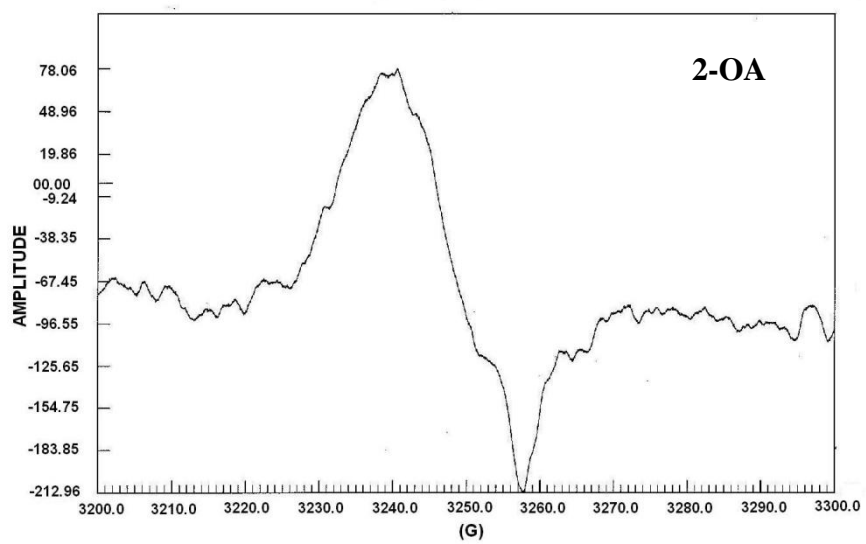
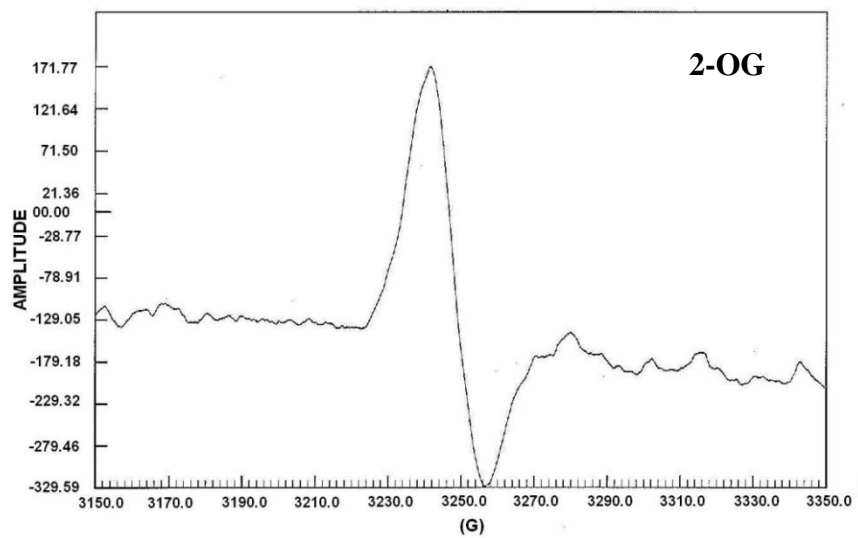


Figure 3.7 Radical detection on E1o-ec with 2-OG and 2-OA by EPR spectroscopy.

3.3.5 Identification of hydroxy-carboxypropylideneThDP radical with 2-OG and 2-OA

The experimental and simulated X-band EPR spectrum with 2-OG and 2-OA showed an identical pattern to that reported by the Cambridge group,⁽⁴⁰⁾ but not exactly identical to that reported for pyruvate: ferredoxin oxidoreductase (PFOR). Also, in PFOR a single electron from ThDP-bound intermediate is transferred to an Fe-S cluster which does not exist in E1o as confirmed by the X-ray structure,⁽⁴⁴⁾ suggesting that in the case of E1o the single electron from the enamine is transferred to molecular oxygen.

Table 3.2 Pre-steady state CD rate determination on E1o with 2-OG in the presence of enamine acceptors.

19 μM E1o, 100 μM 2-OG together with acceptors	Formation (k, s^{-1})	Depletion (k, s^{-1})
only 2-OG (no acceptor)	Very little	0.049 ± 0.001
155 μ M lipoyl domain ^a	0.9 ± 0.05 ; 0.06 ± 0.002	No depletion
60 μ M E2o ¹⁻¹⁷⁶ didomain	1.38 ± 0.2	0.15 ± 0.01
50 μ M DCPIP	0.27 ± 0.03	0.21 ± 0.02
1 mM glyoxylate	0.3 ± 0.1	0.26 ± 0.1

^a120 μ M 2-OG was used

3.4 CONCLUSIONS

Evidence from stopped-flow CD and NMR experiments suggests the formation of the enamine intermediate on E1o-ec with its true substrate 2-OG, and the longer 2-OA substrate with a positive CD band at 350 nm. EPR spectroscopy provides strong evidence for the formation of an enamine derived radical, as observed by others, which allowed us to assign the CD at 350 nm to either the enamine and/or hydroxy-carboxypropylidene-ThDP radical. The pre-steady state rates in the presence of various acceptors are summarized in Table 3.2 and lead to the following conclusions from the stopped-flow CD results: 1. The lifetime of the enamine and/or radical at 350 nm is shorter with 2-OA than with 2-OG (Figure 3.4B) 2. Formation of the enamine and/or ThDP radical is faster than the formation of post-decarboxylation intermediate (Figure 3.4) 3. The 350 nm CD signal is stable if high concentrations of substrates are used (Figure 3.5) 4. The known enamine acceptors DCPIP, glyoxylate and more surprisingly the E2o-ec¹⁻¹⁷⁶ didomain, reduced the lifetime of 350 nm, unlike the lipoyl domain from E2o-ec (Figure 3.6). This study provides experimental observation of a ThDP-bound intermediate, almost certainly of the enamine, followed by thiamin-derived radical on E1o-ec with its true substrate 2-OG and also with the longer substrate 2-OA, further confirming the substrate specificity of this enzyme, making it valuable for protein engineering.

CHAPTER 4

Investigation of the donor and acceptor range for chiral carboligation catalyzed by the E1 component of the 2-oxoglutarate dehydrogenase complex

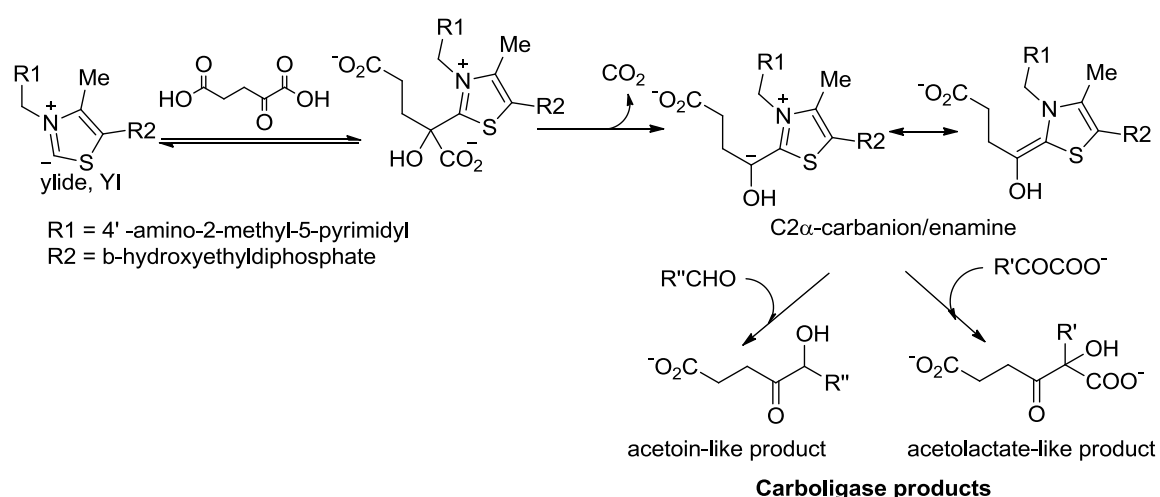
4.1 INTRODUCTION

A number of important ThDP enzymes including transketolases, glyoxylate carboligase, 1-deoxy- D-xylulose-5-phosphate synthase, benzaldehyde lyase (benzoin condensation) catalyze the carboligation (C-C bond formation); it is a side reaction for nearly all ThDP-dependent 2-oxoacid decarboxylases.^(1, 31, 45-47) This property of ThDP-dependent enzymes has been exploited for purposes of chiral synthesis for a number of years.^(45, 48) We have explored for such purposes the E1 component (E1o) of the *Escherichia coli* 2-oxoglutarate dehydrogenase multienzyme complex (OGDHc): the 2-oxoglutarate undergoes E1o-catalyzed decarboxylation to the nucleophilic enamine, which then adds to an aldehyde acceptor, analogously to the pathway of a number of ThDP enzymes. Our synthetic program was initiated by making substitutions of the enzyme at the putative binding site of the γ -carboxyl group of the substrate so that the enzyme would accept substrate analogues lacking the charged γ -carboxyl group.⁽³⁷⁾ The Rutgers group has previously constructed several active site variants in yeast pyruvate decarboxylase (YPDC) from *Saccharomyces cerevisiae* and in the E1 component of the *Escherichia coli* pyruvate dehydrogenase complex (E1p) which were capable of catalyzing such reactions.⁽⁴⁹⁾ The E477Q YPDC variant was an effective acetoin synthase, while the D28A or D28N YPDC variants catalyze acetolactate formation.⁽⁵⁰⁾ The E636Q and

E636A E1p active site variants also became acetolactate synthases.⁽⁵¹⁾ Note, YPDC and E1p produced the opposite enantiomers of acetoin in excess.

The E1o component of OGDHc also catalyzes carboligation reactions. The central ThDP-bound enamine intermediate reacts with the electrophilic acceptor substrate, typically an aldehyde, which results in the formation of acetoin-like or acetolactate-like ligated products (Scheme 4.1).

Scheme 4.1 E1o catalyzed reaction mechanism of carboligase product formation.



In our initial report on this topic, we observed that E1o has a broad substrate range, making it an excellent candidate for protein engineering. This allowed us to investigate extensions of the carboligation studies with E1o, where both the 2-oxoacid and the acceptor aldehyde could be varied over a wide range of reactivity, greatly adding to the versatility of E1o for carboligase reactions (Figure 4.1). The products and enantiomeric excess (*ee*) were confirmed by circular dichroism (CD), ¹H nuclear magnetic resonance (NMR) and chiral gas chromatography (GC). This work adds to the power of E1o as a chiral synthetic tool by demonstrating that (a) this enzyme can also accept 2-oxoalverate

(2-OV) and 2-oxoisovalerate (2-OiV) as substrates, in addition to its natural substrate 2-OG, and (b) that ethyl glyoxylate and surprisingly methylglyoxal can also serve as aldehyde acceptors, in addition to glyoxylate and other straight chain aldehydes.

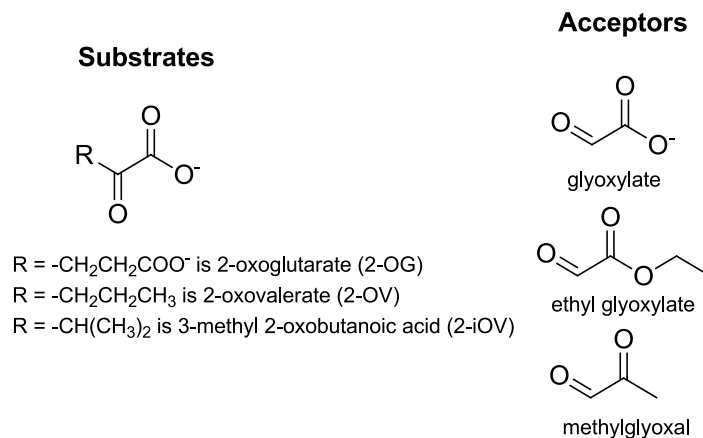


Figure 4.1 Substrates and acceptors for carbonylase reaction by E1o.

4.2 MATERIALS and METHODS

4.2.1 Materials

2-Oxoglutarate, 2-oxovalerate, 2-oxoisovalerate, glyoxylate, ethyl glyoxylate, and methylglyoxal were from Sigma-Aldrich. *E. coli* strain JW0715 containing the plasmid pCA24N encoding the OGDHc-E1 (E1o) component [ASKA clone (-)] was obtained from National Bio Resource Project (NIG, Japan). Amicon® Ultra-4 Centrifugal Filter Units are purchased from EMD Millipore.

Protein purification and activity measurements of *E. coli* E1o are described in Appendix Chapter 3.

4.2.2 CD spectroscopy to monitor the carboligase product formation

CD spectra were recorded on Applied Photophysics Chirascan CD Spectrometer (Leatherhead, U.K.) in 2.4 ml volume with 1 cm path length cell.

Carboligase reaction. E1o (2 mg/ml, 19 μ M active centers) in 20 mM KH_2PO_4 (pH 7.0) containing 0.2 mM ThDP and 2 mM MgCl_2 was incubated overnight with 2-OG (2 mM) in the presence of the acceptors [glyoxylate (1 mM), ethyl glyoxylate (1 mM), or methyl glyoxal (1 mM)] and CD spectra were recorded in the wavelength range of 260-400 nm at 30 $^\circ\text{C}$. Similar reactions were performed using the other substrates 2-OV (5 mM) or 2-OiV (5 mM) with the above acceptors (10 mM). This was necessitated by the K_m for 2-OV and 2-OiV being greater than for 2-OG. The protein was separated from the carboligase product using an Amicon® Ultra-4 Centrifugal Filter Unit. The filtrate was collected and the CD spectra were recorded between 260 and 400 nm.

4.2.3 NMR spectroscopy to characterize the carboligase product

The ^1H NMR was recorded on a Varian 500 MHz INOVA spectrometer at 25 $^\circ\text{C}$. The reactions were carried out at room temperature in 1 ml of 20 mM KH_2PO_4 (pH 7.0) buffer containing 0.5 mM ThDP and 2 mM MgCl_2 , reacting for overnight 2 mg/ml E1o (19 μ M active centers), 10 mM donor substrates and 15 mM acceptors. After separation of protein from reaction mixture by using a centrifugal unit (Millipore), the pH of the supernatant was adjusted to ~ 3 and the product(s) was extracted into CDCl_3 to record the ^1H NMR spectrum.

4.2.4 Chiral GC analysis for *ee* measurement

GC analysis was carried out on a Varian CP-3800 gas chromatograph equipped with a Chiraldex B-DM chiral column (Astec, Advanced Separation Technologies, Inc.) and a flame ionization detector at a flow rate of 1.5 ml/min. Acetoin was extracted from the reaction mixture (after adjustment of pH to ~4) with chloroform and injected onto the Chiraldex B-DM chiral column. The enantiomers were assigned according to their relative retention time. It is known that the (*S*)-enantiomer interacts more favorably with the matrix than the (*R*)-enantiomer. Hence, the (*S*)-enantiomer has a longer retention time.⁽⁴⁹⁾ By using the same method racemic benzoin and (*R*)-benzoin were used as standards.

4.3 RESULTS and DISCUSSION

As with all ThDP-dependent decarboxylations, E1o catalyzes the initial formation of a pre-decarboxylation covalent ThDP-bound intermediate by reaction at the C2 thiazolium atom of the enzyme-bound ThDP with the substrate's keto carbon. Decarboxylation of this intermediate leads to a strongly nucleophilic enamine, which, in the absence of the other components of the complex (the E2o-E3 sub-complex), may react with electrophilic compounds leading to the so-called carboligase products (Scheme 4.1). The carboligase products with a chiral α -hydroxyketone are valuable building blocks for organic synthesis. Since the plasmid for the *Escherichia coli* E1o is available from Japan, the methods are ideal for design and synthesis of such chiral products even on an industrial scale.

4.3.1 The ThDP-dependent enzyme E1o can catalyze carboligase reactions not only with acid but also with ester as acceptor substrate.

The first studies of the carboligase activity of the E1o using as substrate 2-OV and the acceptors acetaldehyde and glyoxylate using rat and beef heart particulate fractions were already published in 1970 by the Westerfeld group; however, no *ee* was reported for the products.⁽⁵²⁾ Just recently, Müller et al. reported the use of E1o from the same source in carboligase reactions with 2-OG and several aliphatic and aromatic aldehyde acceptors with no additional functional groups.⁽⁵³⁾

We have carried out carboligase reactions with E1o from *Ecoli* using three different 2-oxoacids with three aldehyde acceptors, with very different chemical properties [two of which had not been reported before to lead to carboligase products], which lead to products in good yield with up to 60-95% *ee* (Figures 4.1 & 4.2). While the natural substrate 2-OG has a negatively charged carboxylate group, the E1o was found to also catalyze the decarboxylation of 2-OV and 2-OiV with no second charge in the 2-oxoacid, one with a straight chain, the other a branched one (Figure 4.1).

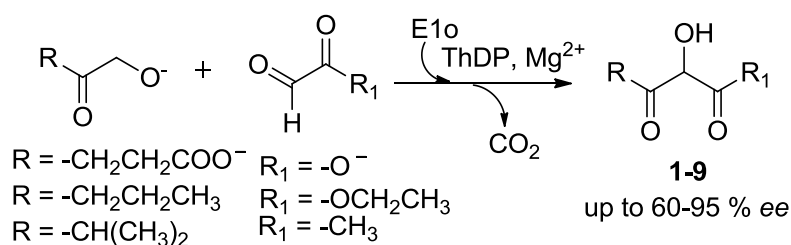


Figure 4.2 E1o catalyzed formation of acetoin-like chiral product using different substrates and acceptors.

Remarkably, all three substrates 2-OG, 2-OV and 2-OiV could utilize glyoxylate as acceptor for carboligation, and could also utilize its ethyl ester and methylglyoxal as acceptors, producing compounds with good enantioselectivity. The novel products formed by the carboligase reaction include chiral 2-hydroxy-1,3-diketones and 2-hydroxy- β -ketoesters. The 2-OV and 2-OiV when reacted with the acceptors glyoxylate and ethyl glyoxylate produce the (*S*)-enantiomer; whereas, 2-OG forms the (*R*)-enantiomer. This may be the result of 2-OV and 2-OiV having hydrophobic tails, while that of 2-OG is hydrophilic. There is no clear enantiomeric preference observed with the methylglyoxal acceptor reacting with the three 2-oxoacids.

4.3.2 Characterization of chiral product and ee calculation by using CD spectroscopy and chiral GC.

The *ee* of the product was determined using chiral GC and circular dichroism (CD) spectroscopy and ^1H NMR was used to confirm the product (Figure 4.3, 4.4 and 4.5). After recording the CD spectrum of the product, protein was separated and the supernatant pH was adjusted to ~ 3 , conditions under which the product could be extracted into chloroform. This enabled us to record the product's NMR spectrum, and to perform chiral GC separations. Since all products have in common the CH-OH functional group, they all exhibit a ^1H NMR resonance with a proton chemical shift near 5 ppm. CD spectroscopy enabled assessment of the enantiomer being formed: the (*R*)-enantiomer displays a negative CD band, and the (*S*)-enantiomer a positive one, very near 278 nm, reminiscent of the CD spectrum of acetoin enantiomers. All of the products here discussed with incorporation of the C(=O)CH-OH functional group have a very useful

spectral property: all exhibit the same CD band, a band that is also very useful for kinetic measurements.⁽¹⁷⁾ It was earlier shown at Rutgers that the chiral column used for GC analysis interacts more favorably with (*S*)-enantiomers, increasing their retention time. This observation was used to identify the enantiomers and to calculate their *ee* value (Figure 4.3, Table 4.1). Before carrying out *ee* measurements of the new compounds, racemic benzoin and (*R*)-benzoin were used as standards for the chiral GC column, further confirming the (*R*) or (*S*) enantioselectivity, while also providing an approximate retention time expected of the new products on the chiral column.

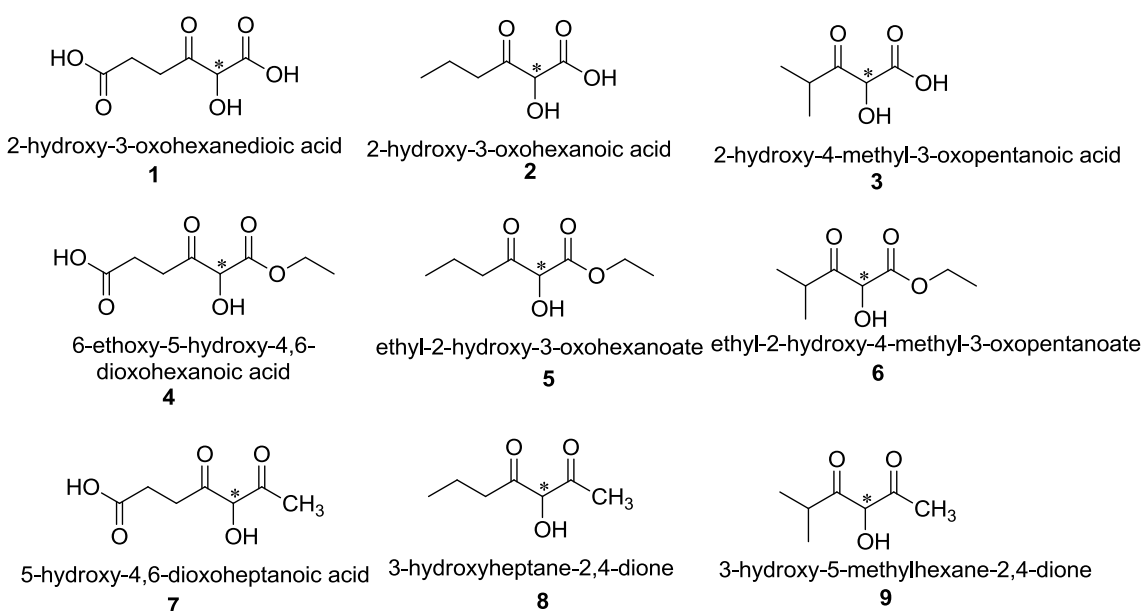
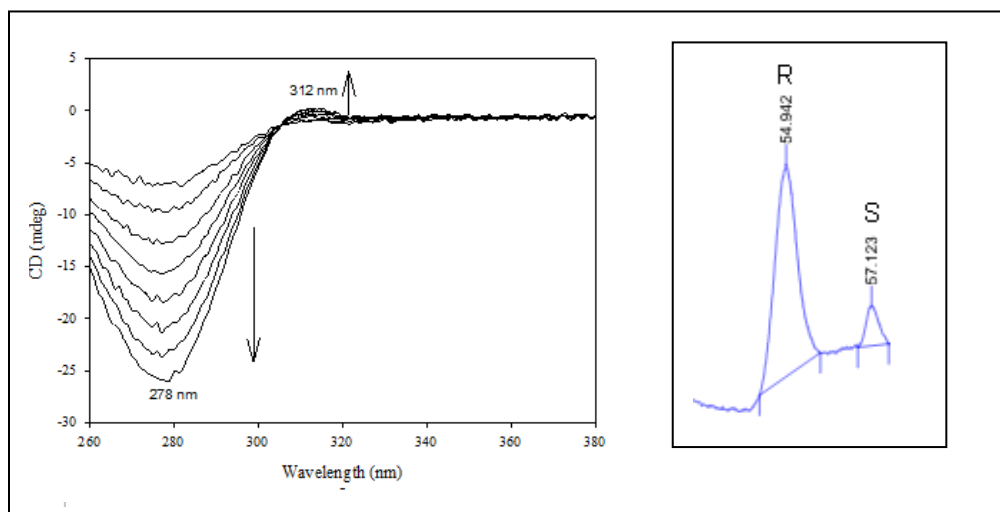


Figure 4.3 Structure and nomenclature of the chiral products produced from the E1o catalyzed reaction by using variety of acceptors and substrates.

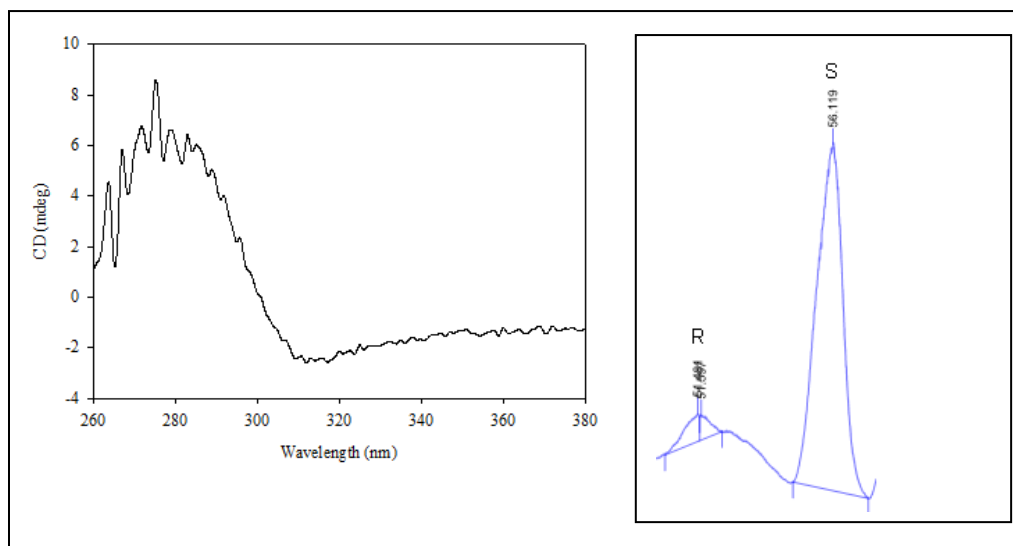
This is the first example of the use of an ester and 2-oxoaldehyde as acceptors in a ThDP enzyme catalyzed carbonylase reaction. This is important since some of the carbonylase reactions produce β -ketoacids, which are prone to thermal decarboxylation.

Figures 4.4 (Left) CD spectra of compounds **1-9** where negative CD signal corresponds to (*R*) and positive one to (*S*)-enantiomers. (Right) Chiral GC analysis of compounds **1-9**.

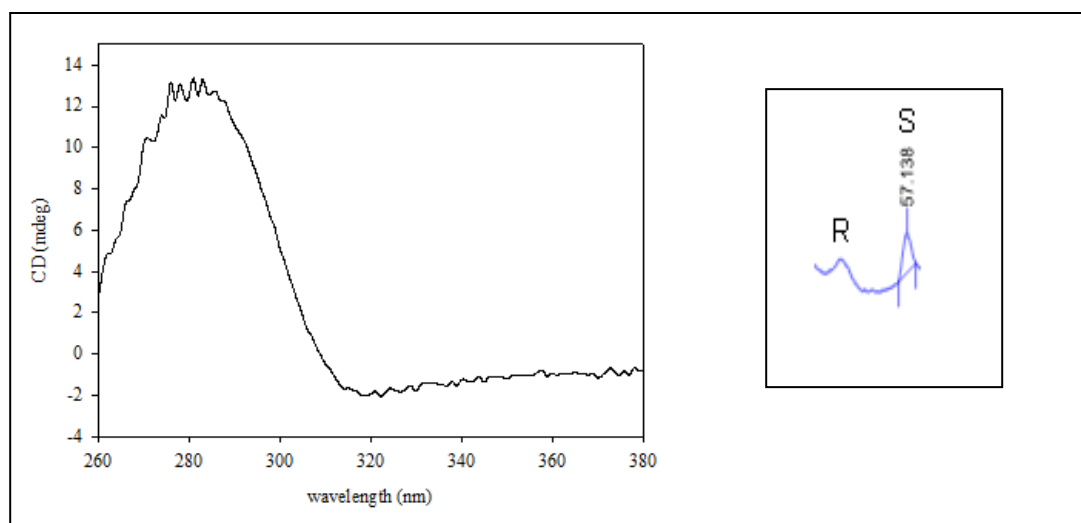
Compound 1



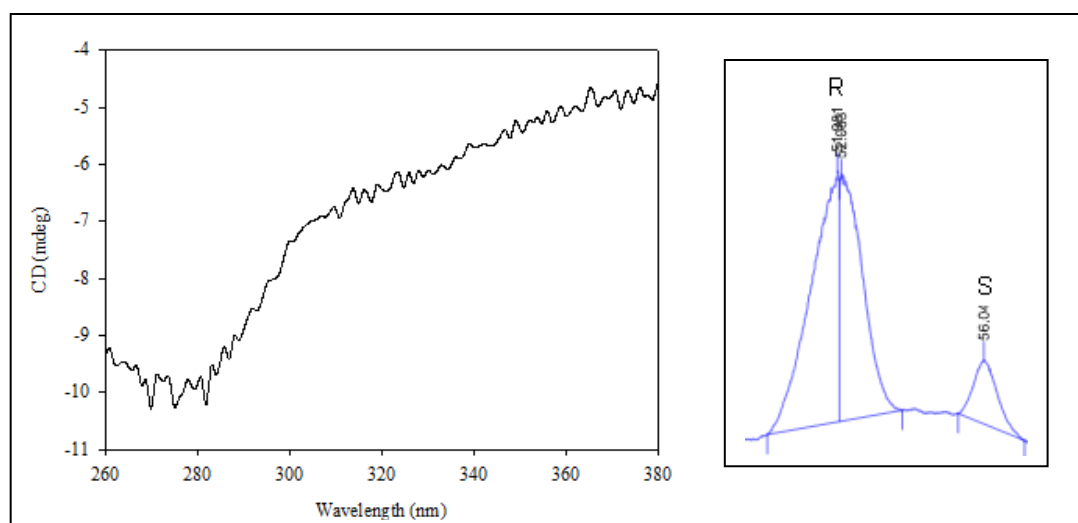
Compound 2

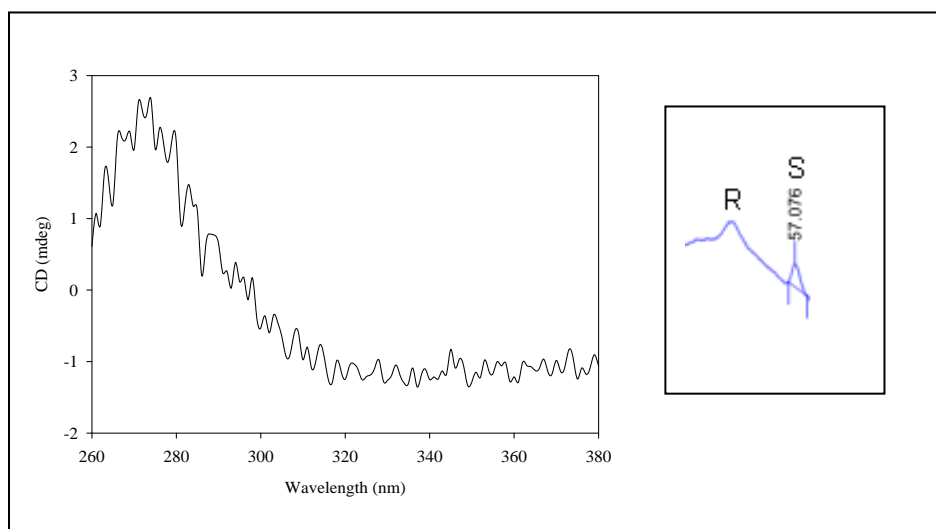
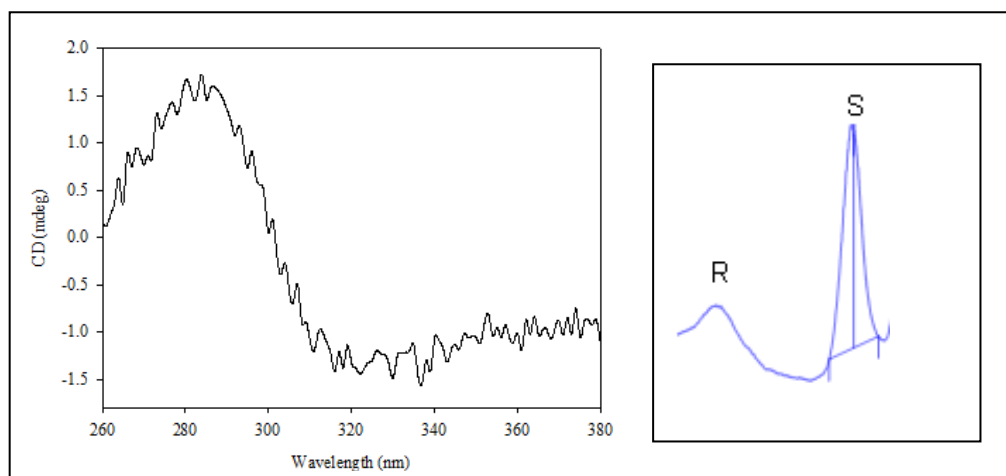


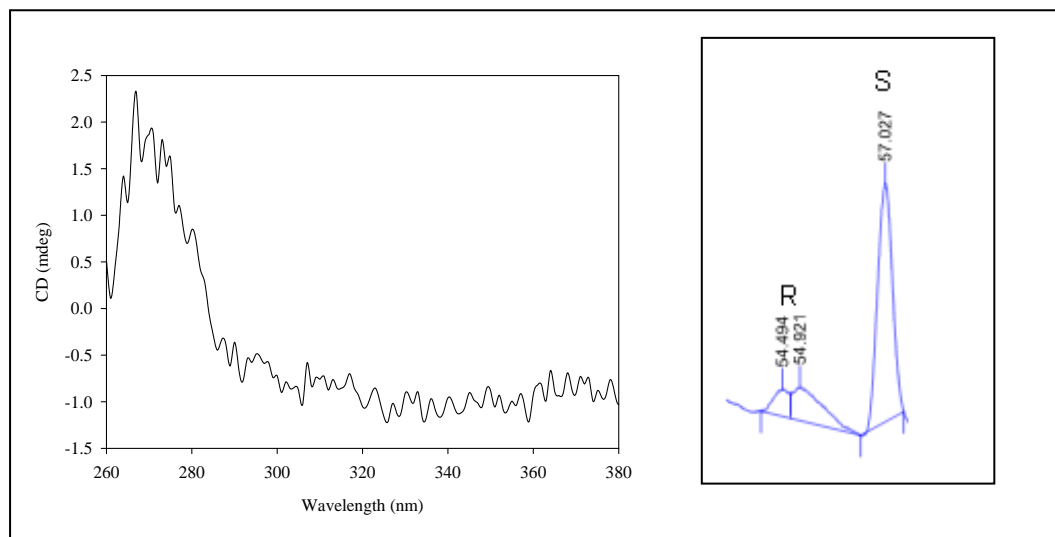
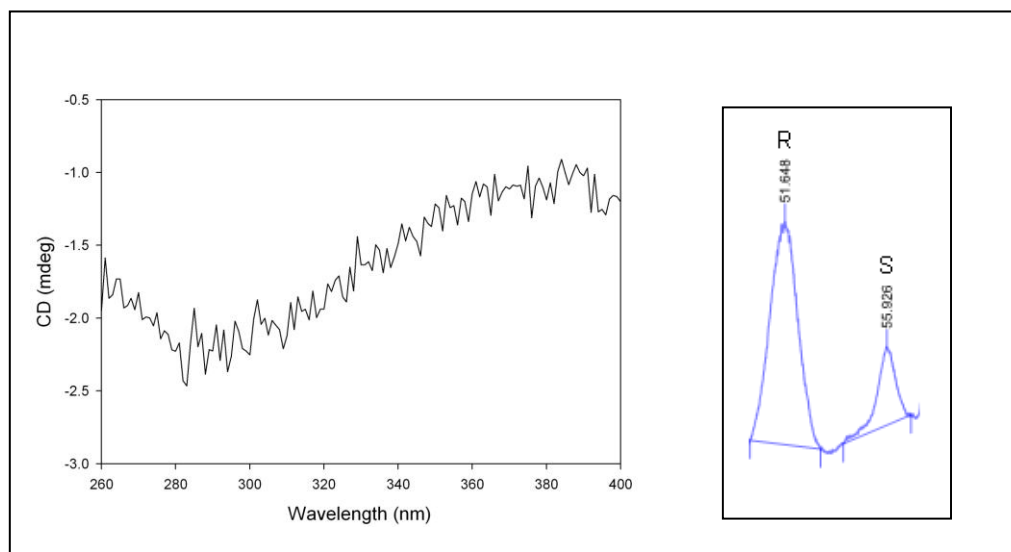
Compound 3



Compound 4



Compound 5**Compound 6**

Compound 7**Compound 8**

Compound 9

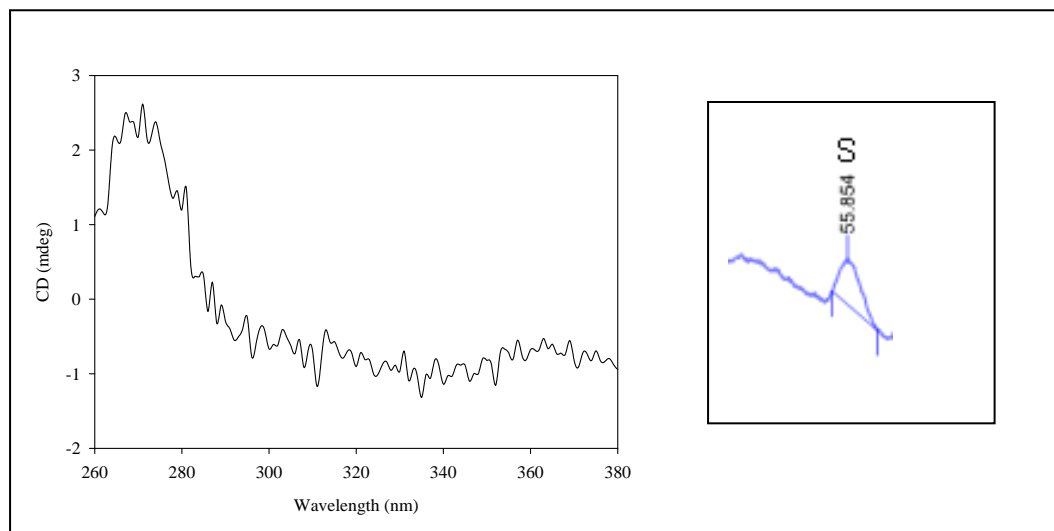


Figure 4.5 Characterization of compounds **1-9** by ^1H NMR.

Compound **1**: δ 2.77 (s, 1H), 3.49 (q, 2H, $J = 7$ Hz), 3.74 (q, 2H, $J = 7$ Hz), 5.01 (s, 1H).

Compound **2**: δ 0.80 (t, 3H, $J = 7$ Hz), 1.51 (m, 2H, $J = 7$ Hz), 2.65 (t, 2H, $J = 7$ Hz), 5.0 (s, 1H).

Compound **3**: δ 1.2 (dd, 6H, $J = 7$ Hz), 2.65, 3.50 (m, 0.5H, $J = 7$ Hz), 3.14 (s, 1H), 4.33 (s, 1H).

Compound **4**: δ 1.40 (t, 3H, $J = 7$ Hz), 3.00 (s, 1H), 3.74 (q, 2H, $J = 7$ Hz), 4.14 (q, 2H, $J = 7$ Hz), 4.40 (q, 2H, $J = 7$ Hz) and 5.01 (s, 1H).

Compound **5**: δ 0.96 (t, 3H, $J = 7.3$ Hz), 1.24 (t, 3H, $J = 7$ Hz), 1.69 (m, 2H, $J = 7.3$ Hz), 2.84 (t, 2H, $J = 7.3$ Hz), 3.0 (s, 1H), 3.73 (q, 2H, $J = 7$ Hz), 5.0 (s, 1H).

Compound **6**: δ 1.19 (d, 6H, $J = 7$ Hz), 1.25 (t, 3H, $J = 7$ Hz), 3.36 (m, 1H, $J = 7$ Hz), 3.73 (q, 2H, $J = 7$ Hz), 4.33 (s, 1H).

Compound **7**: δ 2.03 (s, 3H), 2.33 (dd, 2H, $J = 6.4$ Hz), 2.57 (s, 1H), 2.67 (s, 1H), 5.01 (s, 1H).

Compound **8**: δ 0.93 (t, 3H, $J = 7.5$ Hz), 1.65 (m, 2H, $J = 7.5$ Hz), 1.99 (s, 3H), 2.78 (t, 2H, $J = 7.5$ Hz), 5.13 (s, 1H).

Compound **9**: δ 1.19 (d, 6H, $J = 7$ Hz), 2.1 (s, 3H), 3.34 (m, 1H, $J = 7$ Hz), 4.81 (s, 1H).

4.4 CONCLUSIONS

The E1o component of OGDHc catalyzes the formation of acetoin-like products for all the reactions tested, in high enantiomeric excess, as determined with chiral GC (Table 4.1). In addition, E1o displays different enantioselectivities in product formation, depending on both substrate and acceptor being used. For example, E1o yields the (*R*)-enantiomer with 2-OG as the substrate and glyoxylate acceptor. On the other hand, the (*S*)-enantiomer is produced with 2-OV as the substrate and glyoxylate as acceptor.

Table 4.1 Enantiomeric excess of acetoin-like product formation by E1o using chiral GC.

Substrates	Acceptors	Product	<i>ee</i> % ^a
2-OG	Glyoxylate	1	90 % (<i>R</i>)
2-OV		2	96 % (<i>S</i>)
2-OiV		3	67 % (<i>S</i>)
2-OG	Ethyl-glyoxylate	4	81 % (<i>R</i>)
2-OV		5	52 % (<i>S</i>)
2-OiV		6	81 % (<i>S</i>)
2-OG	Methyl-glyoxal	7	83 % (<i>S</i>)
2-OV		8	81 % (<i>R</i>)
2-OiV		9	>90 % (<i>S</i>)
^a A yield of ~ 95-100% for all the acetoin products was determined by ¹ H NMR as no starting material (substrate) was detected at the end of overnight incubation.			

Two other issues impact the significance of the work: (1) The E1o plasmid from *E. coli* is available to all from the source mentioned in the Experimental Section and can provide active enzyme in good yield, and (2) the work is readily extended to the synthesis of longer chain 2-oxoacids, since preliminary results suggest that 2-oxoadipic acid and glyoxylate form the corresponding carbonylase product (*S*)-2-hydroxy-3-oxoheptanedioic acid. The results suggest that E1o from *E. coli* offers a good starting point for protein engineering and optimization to synthesize stable chiral intermediates for fine chemical synthesis. This contribution expands the scope of both the 2-oxo acid donor and the aldehyde acceptor significantly for their use in carbonylase condensation reactions by this enzyme.

CHAPTER 5

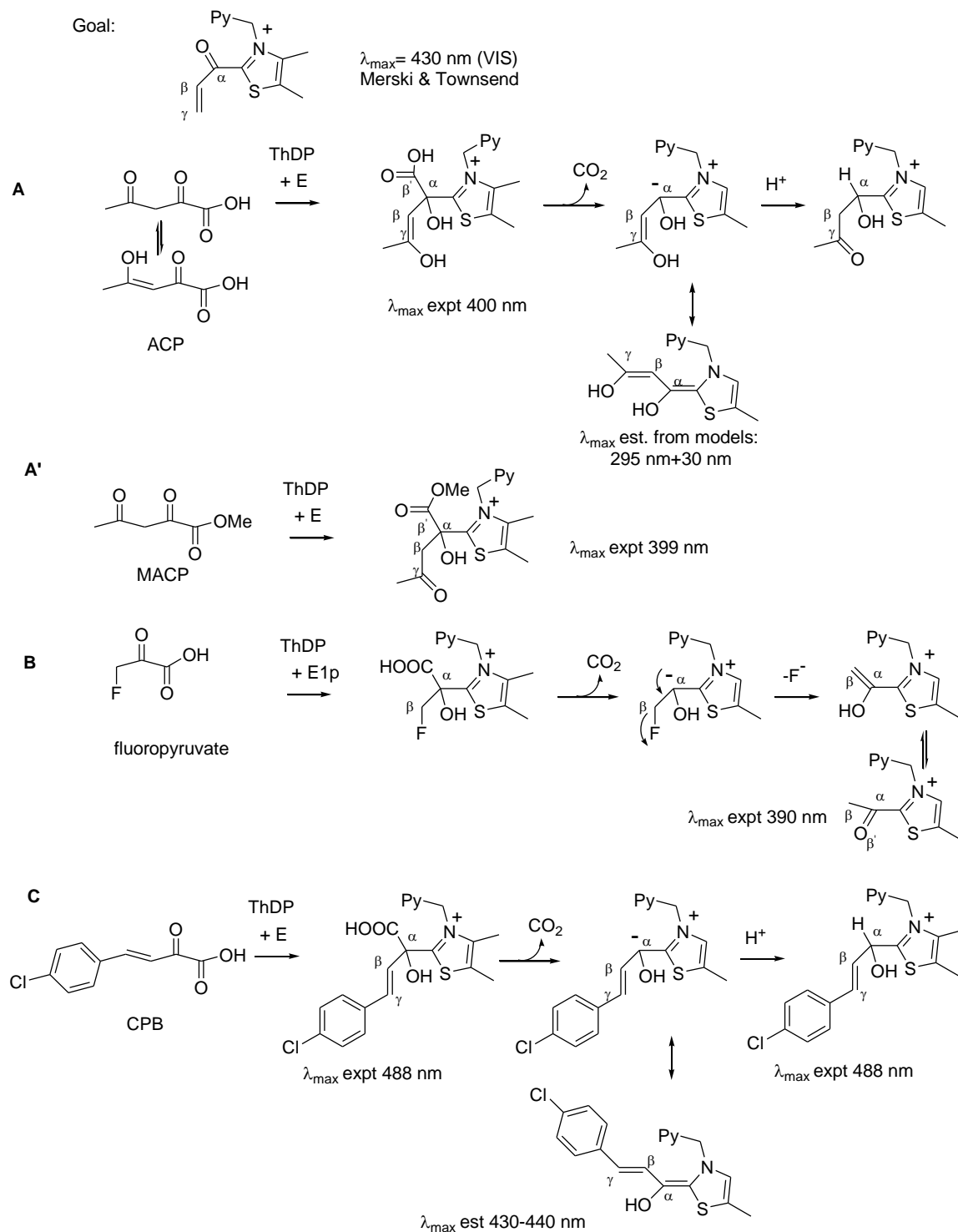
Identification of charge transfer transitions related to thiamin-bound intermediates on enzymes provides a plethora of signatures useful in mechanistic studies

5.1 INTRODUCTION

Thiamin diphosphate (ThDP, the vitamin B1 coenzyme) is a cofactor used for biological decarboxylations of 2-oxoacids, as well as in C-C bond formations resembling a benzoin condensation. A common theme of these reactions is formation of a covalent adduct between the C2 atom of the thiazolium ring of ThDP with the carbonyl group of the substrate. A typical example is the decarboxylation (Scheme 1.1, Chapter 1) carried out by yeast pyruvate decarboxylase (YPDC, EC 4.1.1.1).⁽⁵⁴⁾ Such reactions proceed by a series of ThDP-bound covalent complexes, including the pre-decarboxylation tetrahedral intermediate C2 α -lactylThDP (LThDP), the enamine, a C2 α -trigonal post-decarboxylation intermediate, followed by the tetrahedral (second) post-decarboxylation intermediate C2 α -hydroxyethylThDP (HEThDP). The spectral signatures are best seen in circular dichroism (CD) spectra, where proximal bands are often fortuitously resolvable due to having opposite phases (a property absent in absorption spectra). So far the following assignments have been made on more than 10 ThDP enzymes: (1) A positive CD band centered near 300-315 nm pertaining to the 1',4'-iminopyrimidineThDP tautomer (IP form) in either enzyme-bound ThDP⁽²⁵⁾ or in intermediates related to the tetrahedral adducts LThDP and HEThDP at pH values near or above the pK_a of the 4'-aminopyrimidinium (APH⁺) conjugate acid;^(55, 56) (2) A negative CD band centered at 320

nm pertaining to the canonical 4'-aminopyrimidine form (AP form)^(26, 55, 56) (3) electronic transitions corresponding to the enamine, the only obvious conjugated ThDP-bound intermediate where λ_{max} depends on the group attached to the C2 α atom (ranging from 295 nm for CH₃^(33, 54, 57) to ~ 380 nm⁽⁵⁸⁻⁶¹⁾ for a phenyl ring, to 430-440 nm for a cinnamyl substituent,^(62, 63) and (4) the Michaelis complex reported by a negative CD band centered around 330-340 nm.^(16, 25) While the λ_{max} of the IP form in ref⁽⁵⁴⁾ and the enamines in ref⁽⁵⁵⁾ could be well reproduced in chemical models, those of the AP form⁽²⁵⁾ and the Michaelis complex⁽⁵⁶⁾ could not, and the band pertinent to the AP form almost certainly originates from a charge transfer (CT) transition between the 4'-aminopyrimidine as donor and the thiazolium ring as acceptor.^(55, 56) In view of the accumulated information at Rutgers, we were intrigued by Merski and Townsend's report of an intermediate with λ_{max} of 430 nm on the first enzyme in clavulanic acid biosynthesis. This was attributed to 2-acryloylthiamin diphosphate, a λ_{max} that could not be achieved by any of the conjugated synthetic models created.⁽⁶⁴⁾ Having available a battery of ThDP enzymes, we undertook a study of four alternate 2-oxoacid substrates, acetyl pyruvate (ACP), its methyl ester (MACP), fluoropyruvate and (*E*)-4-(4-chlorophenyl)-2-oxo-3-butenic acid (CPB) (Scheme 5.1) in a search for CT bands that could serve as reporters of ThDP-bound covalent intermediates on enzymes, while also attempting to understand the origin of the Merski-Townsend observation. The compound MACP could form only an LThDP-like pre-decarboxylation complex, a model for the pre-and post-decarboxylation tetrahedral intermediates produced by ACP. On decarboxylation of fluoropyruvate to the enamine, subsequent fluoride ion elimination is a source of 2-acetylThDP.^(65, 66)

Scheme 5.1 Mechanism of CT band formation on ThDP enzymes using **A. ACP**, **A'**. MACP, **B. fluoropyruvate**, **C. CPB**.



5.2 MATERIALS and METHODS

5.2.1 Materials. Alcohol dehydrogenase from yeast (ADH), horse liver alcohol dehydrogenase (HLADH), reduced nicotinamide adenosine dinucleotide (NADH), methyl 4-hydroxy-2-oxopent-3-enoate (MACP) and morpholinoethanesulfonic acid (MES) were purchased from Sigma Aldrich (St. Louis, MO). The potassium salt of (*E*)-4(4-chlorophenyl)-2-oxo-3-butenic acid (CPB) was synthesized as previously reported.⁽⁶²⁾ ThDP was purchased from USB (Cleveland, Ohio).

5.2.2 Synthesis of 4-hydroxy-2-oxopent-3-enoic acid.⁽⁶⁷⁾ Methyl 4-hydroxy-2-oxopent-3-enoate (MACP, 0.500g, 0.0034mole) was dissolved in a mixture of acetonitrile (20 ml) and 6N HCl (7.5 ml) and stirred at room temperature overnight. Acetonitrile was then removed by rotary evaporation while keeping the temperature of the water bath below 30 °C. An orange solid of 4-hydroxy-2-oxopent-3-enoic acid was formed and filtered out. ¹H NMR (500 MHz, CDCl₃) δ 6.47 (s, 1H), δ 2.29 (s, 3H).

5.2.3 Enzyme purification and activity assays

YPDC and E477Q variant were over expressed in *E.coli* BL21 (DE3) strain. Both have a C-terminal His₆-tag and were purified using a Ni-NTA column.^(68, 69)

For long-term storage, glycerol was added to the preparation to a final concentration of 50% (v/v), and the enzyme was stored at -20 °C. Protein concentration was determined with the Bio-Rad protein assay dye reagent (Bradford method). The purity was checked using SDS-PAGE.

Activity Measurements. The activity of wild type YPDC and its variants was measured using the ADH coupled assay by monitoring the depletion of NADH at 340 nm using a Varian DMS 300 spectrophotometer. The assay medium (1 ml) contained in 50 mM MES (pH 6.0), 2 mM MgCl₂, 1 mM ThDP, ADH (0.08 mg/ml), NADH (0.2 mg/ml) and 20 mM pyruvate at 25 °C. The reaction was initiated by adding the enzyme (3 µg). One unit of activity is defined as the amount of NADH depleted (µmol/min.mg of YPDC). By using the same reaction conditions enzyme E477Q (50 µg) was incubated for 5 min with ACP or MACP with all the component present except NADH. The reaction was initiated by addition of NADH at 30 °C. The aldehyde product formation (activity) was observed only with ACP not with its ester MACP.

Purification and activity measurement of E1o is described under Appendix Chapter 2.

BAL enzyme was obtained from Prof. McLiesh at IUPUI.^(60, 70, 71)

Activity measurement of BAL with CPB using HLADH. The reaction (1 ml) of 50 mM Tris (pH 8.0) containing 0.2 mM ThDP, 1 mM MgCl₂, 1 mg/ml BSA, 0.25 units HLADH, 0.35 mM NADH and 0.5 mM CPB. The reaction was initiated by addition of BAL (2.5 µg) at 30 °C.

5.2.4 Circular Dichroism Experiments

CD spectra were recorded on Applied Photophysics Chirascan CD Spectrometer (Leatherhead, U.K.) in 2.4 ml volume with 1 cm path length cell

pH titration experiment of variant E477Q with pyruvate. E477Q (33.33 µM active centers) in triple pH buffer system containing 50 mM acetic acid, 50 mM MES, 100 mM Tris, 0.5 mM ThDP, 5 mM MgCl₂ and 10 mM pyruvate was titrated in the pH range of

6.2–5.3 at 5 °C. To adjust the pH a symphony pH electrode (VWR), was used and CD spectra were recorded after each adjustment. Log CD at 305 nm was plotted against pH and pK_a was determined using Eq 3 in Chapter 2.

E477Q with ACP. Variant E477Q YPDC (83.33 μ M active centers) was titrated with ACP (0.05-10 mM) in 50 mM MES (pH 6.0) containing 0.5 mM ThDP and 2 mM $MgCl_2$ at 5 °C.

E477Q with MACP. Variant E477Q YPDC (33.33 μ M active centers) was titrated with ACP (0.05-10 mM) in 50 mM MES (pH 6.0) containing 0.5 mM ThDP and 2 mM $MgCl_2$ at 5 °C.

E1o with ACP: E1o (33.33 μ M active centers) was titrated with ACP (0.05-2 mM) in 20 mM KH_2PO_4 (pH 7.0) containing 0.2 mM ThDP and 2 mM $MgCl_2$ at 5 °C.

YPDC with CPB. YPDC (33.33 μ M active centers) was titrated with CPB (0.03-4 mM) in 50 mM MES (pH 6.0) containing 0.5 mM ThDP and 2 mM $MgCl_2$ at 5 °C.

BAL with CPB. BAL (25.45 μ M active centers) was titrated with CPB (0.08-10 mM) in 50 mM Tris (pH 8.0) containing 0.2 mM ThDP and 1 mM $MgCl_2$ at 30 °C. The K_d value was calculated by fitting the data to a Hill function (Eq 1 in Chapter 2).

5.2.5 Rapid-Scan Stopped-Flow Photodiode Array (PDA) Experiments of BAL with CPB. Experiments were carried out on an SX.18MV stopped-flow spectrophotometer from Applied Photophysics (Leatherhead, United Kingdom). Experiments were performed by mixing an equal volume of BAL (33.95 μ M) and CPB (10 mM). A slit width of 2 mm and a path length of 2 mm were used. Sigma plot 10.0 was used to fit the data using exponential model as in Eq 5 & 8 in Chapter 2.

5.3 RESULTS and DISCUSSION

5.3.1 ThDP on YPDC. Earlier it was shown that titrating slow E477Q YPDC variant with increasing concentrations of pyruvate forms LThDP, the pre-decarboxylation intermediate, present in its 1',4'-iminolThDP form (positive CD band ~300 nm), and as a Michaelis complex (negative band at 330 nm).⁽⁷²⁾ Raising the pH from 5.3-6.2 and recording the positive CD band at 305 nm formed from pyruvate with E477Q YPDC (1',4'-iminolThDP), showed an increase in amplitude (Figure 5.1), suggesting formation of the IP form from the N1-protonated 4'-aminopyridinium (APH⁺), and implying a pK_a near 6.1 for the APH⁺ form.⁽⁷³⁾

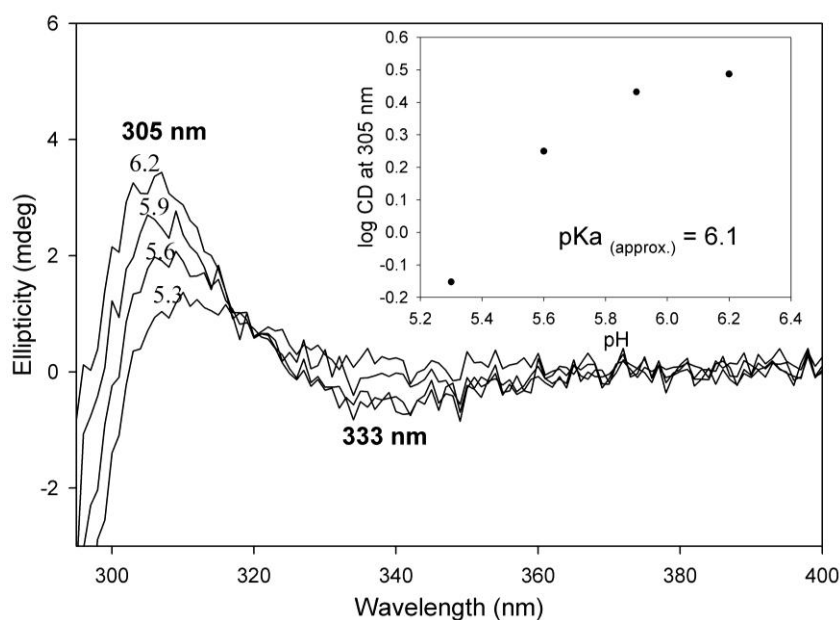


Figure 5.1 pH dependence of IP form of ThDP at 305 nm formed by titration of the E477Q YPDC variant with 10mM pyruvate at 5°C

5.3.2 Studies with ACP and MACP

In contrast to result with pyruvate, CD titration of E477Q YPDC with ACP did not give evidence for formation of either the IP form or of the Michaelis complex, instead, it revealed formation of a negative band at 400 nm that exhibited saturation, a band that increased in amplitude after overnight incubation at 4 °C, thus suggesting a slow reaction. The CD spectrum of the protein after separation of the supernatant confirmed that the species represented by the 400 nm CD band is protein bound. The negative CD band at 400 nm was assigned to a CT transition based on the following: The 400 nm could not be the enamine since the enamine derived from pyruvic acid has λ_{\max} 295 nm⁽⁵⁷⁾, and even an additional double bond could not shift the λ_{\max} beyond 330 nm. The CT band (Scheme 5.1A) is believed to correspond to the pre-decarboxylation intermediate on ThDP with $K_d = 1.64$ mM (Figure 5.2). A similar experiment carried out with E1o also revealed formation of CD band at 408 nm, but in this case with a positive phase (Figure 5.2). Next, a CD titration of E477Q YPDC was also carried out at 5 °C with MACP, the methyl ester of the acetopyruvate, which after overnight incubation also formed a negative CD band at 399 nm (Figure 5.2), at the same wavelength as with ACP. The weak signal at 399 nm was confirmed to be protein bound, as it persisted in a spectrum after the protein was separated from supernatant, and re-dissolved in fresh buffer.

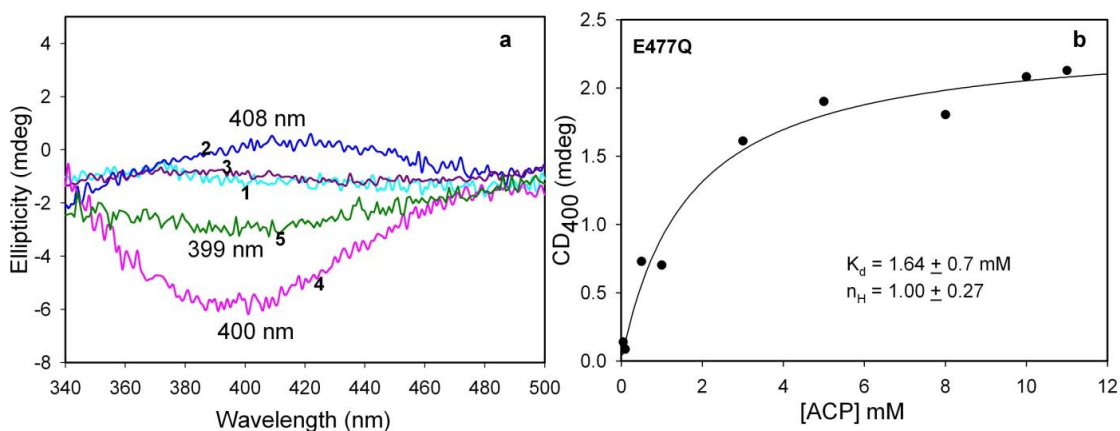


Figure 5.2 a) Formation of charge transfer band on the enzyme observed by CD at 5 °C. **1.** E1o enzyme, **2.** E1o with ACP, **3.** E477Q YPDC enzyme, **4.** E477Q with ACP, **5.** E477Q YPDC with MACP. **b)** Data from the experiment of E477Q YPDC with ACP were fitted using Eq 1 in Chapter 2.

Formation of the intermediate appears to be very slow with MACP (ester), while ACP undergoes slow turnover forming a steady state level of intermediate and saturating the available active centers. The results suggest that the similar CD band observed with both ACP and MACP pertains to the same pre-decarboxylation intermediate since the ThDP-MACP adduct could not be decarboxylated (Scheme 5.1A'). Irrespective of whether the CD band with ACP pertains to the pre- or post-decarboxylation tetrahedral intermediate (these could be differentiated according to their C6'-H ^1H chemical shifts),⁽¹⁵⁾ its wavelength excludes the enamine and clearly demonstrates the possibility of forming ThDP intermediates with λ_{max} at 400 nm even in the absence of significant conjugation, likely CT transitions in origin.

5.3.3 Reaction of fluoropyruvate with E1p (performed by Dr. Natalia Nemeria). It had been reported by Frey and coworkers that fluoropyruvate is a good source of 2-acetylThDP on E1p (Scheme 5.1C), where on decarboxylation to the enamine, subsequent fluoride ion elimination leads to the enol form of 2-acetylThDP, which then tautomerizes to the keto form.^(65, 66) CD spectra of E1p and some of its low activity active center variants revealed formation of a very broad new positive band near 390-395 nm, assigned to the enzyme-bound 2-acetylThDP. It is amply demonstrated in the literature that this intermediate can undergo rapid hydrolysis to acetate ion in model reactions, hence its short lifetime is not surprising. In fact the rate of decomposition appears similar in E1p and slow variants H407A and E571A. This acetyl group is the shortest side chain at the ThDP C2 position in our list in Table 5.1, again with a long λ_{\max} (390 nm) CT transition. This is our closest model for the Merski-Townsend observation attributed to 2-acryloyl-ThDP, and replacement of the methyl group by a vinyl group (extension of the π system by a C=C double bond according to the Woodward-Fieser rules),^(74, 75) would in essence account for the observed 430 nm λ_{\max} (390+30 nm).

5.3.4 Studies with a longer conjugated system CPB. CPB was the first conjugated 2-oxoacid giving evidence for an YPDC-bound enamine intermediate (λ_{\max} at 440 nm)⁽⁶²⁾ and is also a suicide substrate with YPDC.⁽⁷⁶⁾ We here observed formation of the enamine by CD on YPDC from CPB as a negative band at 440 nm (Figure 5.3, a), confirming that the ThDP-bound enamine is chiral.

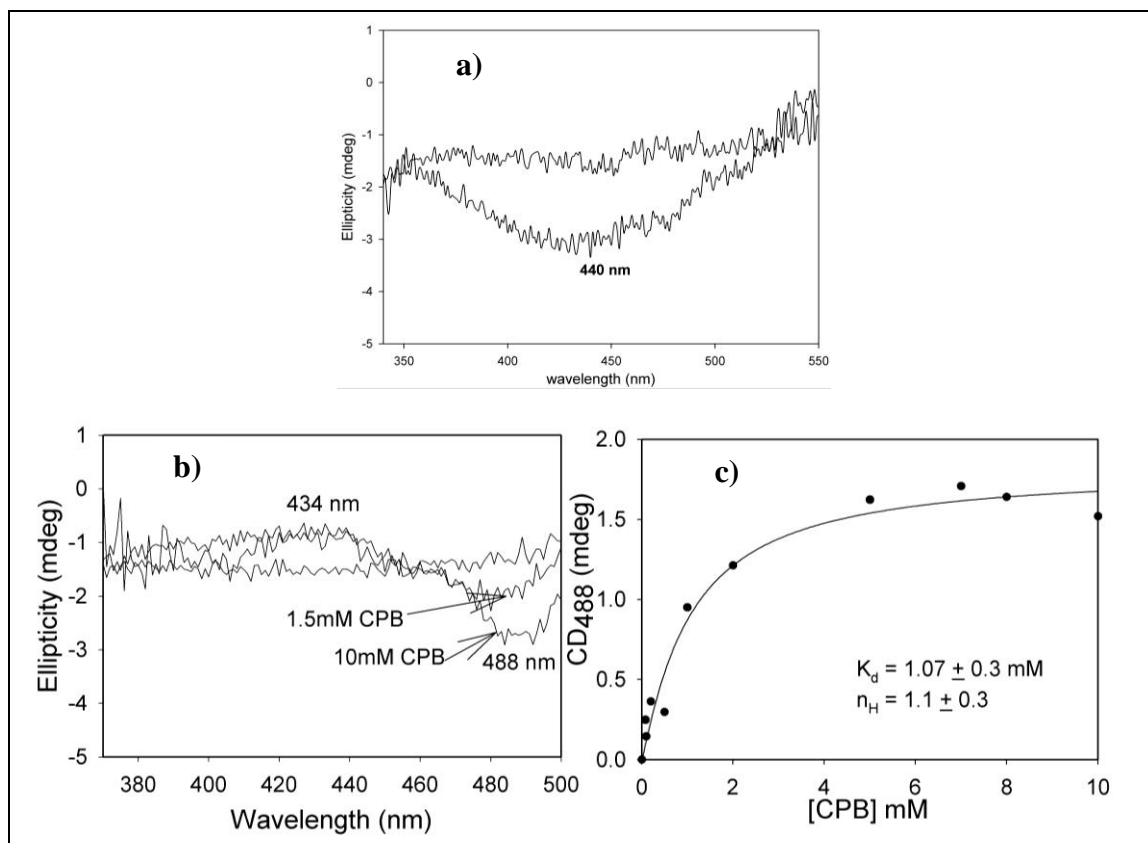


Figure 5.3 a) Formation of enamine by reacting YPDC with CPB at 5 °C. b) Formation of CT band by CD titration of BAL with CPB at 30 °C. c) Data were fitted to the Hill function (Eq 1 in Chapter 2).

Both VIS spectroscopy and CD confirm that the enamine derived from ThDP-CPB on YPDC has a λ_{\max} 440 nm. Unlike with YPDC, reaction of CPB with BAL at 30 °C formed a negative CT band at 488 nm and a positive one at 434 nm ($k_d = 1.1$ mM, Figure 5.3 b,c). These results are similar to those obtained by our group with (E)-2-oxo-4(pyridin-3-yl)-3-butenic acid (3-PKB) and the band near 480 nm was assigned to the LThDP-type pre-decarboxylation intermediate (Scheme 5.1C).⁽⁶¹⁾

A stopped-flow photodiode array (PDA) experiment was carried out by mixing BAL (33.95 μM active centers) in one syringe with an equal volume of 10 mM CPB placed in the second syringe at 30 $^{\circ}\text{C}$. Time dependent changes were observed at 480 nm and 430 nm (same as with CD) with rate constants of $0.0098 \pm 0.0007 \text{ s}^{-1}$ (formation of LThDP-like intermediate), $0.0031 \pm 0.0007 \text{ s}^{-1}$ (formation of an HETHDP-like intermediate from the enamine) and $0.0090 \pm 0.0002 \text{ s}^{-1}$ (formation of the enamine), respectively (Figure 5.4).

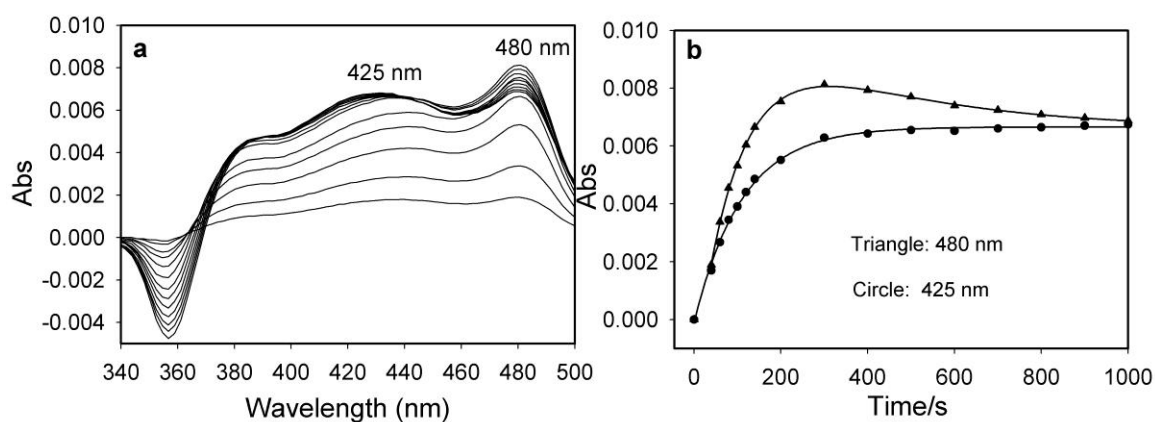


Figure 5.4 a. Time-dependent formation of a CT band on BAL with CPB detected by stopped-flow PDA at 30 $^{\circ}\text{C}$. **b.** Data were fitted using Eq 5 & 8 in Chapter 2.

The rates indicate that conversion of the LThDP-like intermediate (488 nm) to the enamine (434 nm) is very fast compared to depletion of the enamine to the HETHDP-like intermediate. Both the CD and stopped-flow PDA analysis confirmed that CPB on BAL forms a tetrahedral covalent adduct with ThDP leading to the appearance of a CT band. An X-ray structure of 3-PKB with benzoylformate decarboxylase revealed stability of the post-decarboxylation HETHDP-like intermediate, also confirming fast decarboxylation.⁽⁶¹⁾ Quantitative analysis of the kinetic data in Figure 5.4 is made

difficult since the LThDP- and HEThDP-like tetrahedral intermediates derived from 3-PKB or CPB have very similar λ_{max} values (477 and 473 nm in PDA spectra, respectively).⁽⁶¹⁾

5.4 CONCLUSIONS

A summary of the steady state formation of ThDP related intermediates reflected by formation of CT bands is given in Table 5.1 and Scheme 5.1. CD spectroscopy was used to identify the CT signal corresponding to substrates covalently bound to ThDP on four different enzymes. Moreover, it was shown that the pre-decarboxylation intermediate on addition of pyruvate to E477Q YPDC is preferentially in its IP tautomeric form and the pK_a for the APH^+ form is 6.1, very near the pH of optimum activity of 6.2⁽⁷¹⁾ (a finding that makes this the 8th example of the suggestion that at the optimal pH for activity, all forms APH^+ , IP and AP may be needed in the mechanism),⁽⁷⁷⁾ ensuring that all ionization states of ThDP are available for catalysis.

Table 5.1 Steady state detection of CT band related to ThDP on enzymes by CD spectroscopy.

Enzyme	Substrates	CT band (nm)
E477Q YPDC	ACP	-400
E1o	ACP	+408
E477Q YPDC	MACP	-399
E1p ^a	fluoropyruvate	+390
BAL	CPB	-480 & +434

^aperformed by Dr. Natalia Nemeria.

In conclusion, CT bands were characterized at long wavelength for both pre- and post-decarboxylation tetrahedral ThDP-bound covalent intermediates and for 2-acetylThDP for the first time. This offers a useful method, since the NMR method invented by Tittmann and Hübner enables differentiation between the pre- and post-decarboxylation intermediates. With this report, we now have identified spectroscopic signatures for all ThDP species in Scheme 1.1 in Chapter 1 with the exception of the ylide and the APH⁺ form. The presence of the APH⁺ form was established by solid state NMR on three ThDP enzymes.⁽⁷³⁾ Recently, Tittmann's group reported X-ray evidence for the existence of the ylide on pyruvate oxidase.⁽¹⁰⁾ Given these assignments, stopped-flow CD could be exploited to provide microscopic rate constants for individual steps on the reaction pathways, as demonstrated recently on the ThDP enzymes E1p,⁽⁷⁸⁾ glyoxylate carboligase⁽⁷⁹⁾ and 1-deoxy- D-xylulose-5-phosphate synthase.⁽³⁹⁾

We provide evidence that the Merski-Townsend observation can indeed be explained by a CT transition corresponding the interaction of a double bond of the C2 substituent with the positive charge on the thiazolium ring.

REFERENCES

1. Lindqvist, Y., Schneider, G., Ermler, U., and Sundstrom, M. (1992) Three-dimensional structure of transketolase, a thiamine diphosphate dependent enzyme, at 2.5 Å resolution, *EMBO J.* 11, 2373-2379.
2. Muller, Y. A., and Schulz, G. E. (1993) Structure of the thiamine- and flavin-dependent enzyme pyruvate oxidase, *Science* 259, 965-967.
3. Dyda, F., Furey, W., Swaminathan, S., Sax, M., Farrenkopf, B., and Jordan, F. (1993) Catalytic centers in the thiamin diphosphate dependent enzyme pyruvate decarboxylase at 2.4-Å resolution, *Biochemistry* 32, 6165-6170.
4. Arjunan, P., Umland, T., Dyda, F., Swaminathan, S., Furey, W., Sax, M., Farrenkopf, B., Gao, Y., Zhang, D., and Jordan, F. (1996) Crystal structure of the thiamin diphosphate-dependent enzyme pyruvate decarboxylase from the yeast *Saccharomyces cerevisiae* at 2.3 Å resolution, *J. Mol. Biol.* 256, 590-600.
5. Breslow, R. (1957) Rapid deuterium exchange in thiazolium salts, *J. AM. Chem. Soc* 79, 1762-1763.
6. Muller, Y. A., Lindqvist, Y., Furey, W., Schulz, G. E., Jordan, F., and Schneider, G. (1993) A thiamin diphosphate binding fold revealed by comparison of the crystal structures of transketolase, pyruvate oxidase and pyruvate decarboxylase, *Structure* 1, 95-103.
7. Jordan, F., Mariam, Y. H. (1978) N1'-Methylthiaminium diiodide. Model study on the effect of a coenzyme bound positive charge on reaction mechanisms requiring thiamin pyrophosphate, *J. AM. Chem. Soc* 100, 2534-2541.
8. Baykal, A. T., Kakalis, L., and Jordan, F. (2006) Electronic and nuclear magnetic resonance spectroscopic features of the 1',4'-iminopyrimidine tautomeric form of thiamin diphosphate, a novel intermediate on enzymes requiring this coenzyme, *Biochemistry* 45, 7522-7528.
9. Jordan, F. (1982) Role of the aminopyridine ring in thiamin-catalyzed reactions. II. Proton NMR evidence for high barriers to amino group rotation in 4-aminopyrimidines, including thiamin, at low pH in water, *J. Org. Chem* 47, 2748-2753.
10. Balakrishnan, A., Paramasivam, S., Chakraborty, S., Polenova, T., and Jordan, F. (2012) Solid-state nuclear magnetic resonance studies delineate the role of the protein in activation of both aromatic rings of thiamin, *J. Am. Chem. Soc.* 134, 665-672.

11. Cain, A. H., Sullivan, G. R., and Roberts, J. D. (1977) The protonation site of vitamin B1 as determined from natural-abundance ^{15}N nuclear magnetic resonance spectra, *J. Am. Chem. Soc.* *99*, 6423-6425.
12. Jordan, F., and Patel, H. (2013) Catalysis in Enzymatic Decarboxylations: Comparison of Selected Cofactor-dependent and Cofactor-independent Examples, *ACS Catal* *3*, 1601-1617.
13. Kern, D., Kern, G., Neef, H., Tittmann, K., Killenberg-Jabs, M., Wikner, C., Schneider, G., and Hubner, G. (1997) How thiamine diphosphate is activated in enzymes, *Science* *275*, 67-70.
14. Arduengo, A. J., Goerlich, J. R., and Marshall, W. J. (1997) A stable thiazol-2-ylidene and its dimer, *Liebigs Annalen-Recueil*, 365-374.
15. Tittmann, K., Golbik, R., Uhlemann, K., Khailova, L., Schneider, G., Patel, M., Jordan, F., Chipman, D. M., Duggleby, R. G., and Hubner, G. (2003) NMR analysis of covalent intermediates in thiamin diphosphate enzymes, *Biochemistry* *42*, 7885-7891.
16. Kale, S., Ulas, G., Song, J., Brudvig, G. W., Furey, W., and Jordan, F. (2008) Efficient coupling of catalysis and dynamics in the E1 component of Escherichia coli pyruvate dehydrogenase multienzyme complex, *Proc Natl Acad Sci U S A* *105*, 1158-1163.
17. Patel, H., Nemeria, N. S., Brammer, L. A., Freel Meyers, C. L., and Jordan, F. (2012) Observation of thiamin-bound intermediates and microscopic rate constants for their interconversion on 1-deoxy-D-xylulose 5-phosphate synthase: 600-fold rate acceleration of pyruvate decarboxylation by D-glyceraldehyde-3-phosphate, *J. Am. Chem. Soc.* *134*, 18374-18379.
18. Sprenger, G. A., Schorken, U., Wiegert, T., Grolle, S., de Graaf, A. A., Taylor, S. V., Begley, T. P., Bringer-Meyer, S., and Sahm, H. (1997) Identification of a thiamin-dependent synthase in Escherichia coli required for the formation of the 1-deoxy-D-xylulose 5-phosphate precursor to isoprenoids, thiamin, and pyridoxol, *Proc Natl Acad Sci U S A* *94*, 12857-12862.
19. Lois, L. M., Campos, N., Putra, S. R., Danielsen, K., Rohmer, M., and Boronat, A. (1998) Cloning and characterization of a gene from Escherichia coli encoding a transketolase-like enzyme that catalyzes the synthesis of D-1-deoxyxylulose 5-phosphate, a common precursor for isoprenoid, thiamin, and pyridoxol biosynthesis, *Proc Natl Acad Sci U S A* *95*, 2105-2110.
20. Hill, R. E., Himmeldirk, K., Kennedy, I. A., Pauloski, R. M., Sayer, B. G., Wolf, E., and Spenser, I. D. (1996) The biogenetic anatomy of vitamin B6. A ^{13}C NMR investigation of the biosynthesis of pyridoxol in Escherichia coli, *J. Biol. Chem.* *271*, 30426-30435.

21. Eubanks, L. M., and Poulter, C. D. (2003) Rhodobacter capsulatus 1-deoxy-D-xylulose 5-phosphate synthase: steady-state kinetics and substrate binding, *Biochemistry* 42, 1140-1149.
22. Sisquella, X., de Pourcq, K., Alguacil, J., Robles, J., Sanz, F., Anselmetti, D., Imperial, S., and Fernandez-Busquets, X. (2010) A single-molecule force spectroscopy nanosensor for the identification of new antibiotics and antimalarials, *FASEB J.* 24, 4203-4217.
23. Matsue, Y., Mizuno, H., Tomita, T., Asami, T., Nishiyama, M., and Kuzuyama, T. (2010) The herbicide ketoclozazole inhibits 1-deoxy-D-xylulose 5-phosphate synthase in the 2-C-methyl-D-erythritol 4-phosphate pathway and shows antibacterial activity against Haemophilus influenzae, *J Antibiot (Tokyo)* 63, 583-588.
24. Brammer, L. A., Smith, J. M., Wade, H., and Meyers, C. F. (2011) 1-Deoxy-D-xylulose 5-phosphate synthase catalyzes a novel random sequential mechanism, *J. Biol. Chem.* 286, 36522-36531.
25. Nemeria, N., Chakraborty, S., Baykal, A., Korotchkina, L. G., Patel, M. S., and Jordan, F. (2007) The 1',4'-iminopyrimidine tautomer of thiamin diphosphate is poised for catalysis in asymmetric active centers on enzymes, *Proc Natl Acad Sci U S A* 104, 78-82.
26. Nemeria, N. S., Chakraborty, S., Balakrishnan, A., and Jordan, F. (2009) Reaction mechanisms of thiamin diphosphate enzymes: defining states of ionization and tautomerization of the cofactor at individual steps, *FEBS J.* 276, 2432-2446.
27. Xiang, S., Usunow, G., Lange, G., Busch, M., and Tong, L. (2007) Crystal structure of 1-deoxy-D-xylulose 5-phosphate synthase, a crucial enzyme for isoprenoids biosynthesis, *J. Biol. Chem.* 282, 2676-2682.
28. Arjunan, P., Sax, M., Brunskill, A., Chandrasekhar, K., Nemeria, N., Zhang, S., Jordan, F., and Furey, W. (2006) A thiamin-bound, pre-decarboxylation reaction intermediate analogue in the pyruvate dehydrogenase E1 subunit induces large scale disorder-to-order transformations in the enzyme and reveals novel structural features in the covalently bound adduct, *J. Biol. Chem.* 281, 15296-15303.
29. Kluger, R., and Pike, D. C. (1977) Active site generated analogues of reactive intermediates in enzymic reactions. Potent inhibition of pyruvate dehydrogenase by a phosphonate analogue of pyruvate1, *J. Am. Chem. Soc.* 99, 4504-4506.
30. Vinogradov, M., Kaplun, A., Vyazmensky, M., Engel, S., Golbik, R., Tittmann, K., Uhlemann, K., Meshalkina, L., Barak, Z., Hubner, G., and Chipman, D. M. (2005) Monitoring the acetohydroxy acid synthase reaction and related carbonylations by circular dichroism spectroscopy, *Anal. Biochem.* 342, 126-133.

31. Brammer, L. A., and Meyers, C. F. (2009) Revealing substrate promiscuity of 1-deoxy-D-xylulose 5-phosphate synthase, *Org. Lett.* *11*, 4748-4751.
32. Smith, J. M., Vierling, R. J., and Meyers, C. F. (2012) Selective inhibition of *E. coli* 1-deoxy-D-xylulose-5-phosphate synthase by acetylphosphonates(), *Medchemcomm* *3*, 65-67.
33. Jordan, F., and Nemeria, N. S. (2005) Experimental observation of thiamin diphosphate-bound intermediates on enzymes and mechanistic information derived from these observations, *Bioorg. Chem.* *33*, 190-215.
34. Nemeria, N. S., Korotchkina, L. G., Chakraborty, S., Patel, M. S., and Jordan, F. (2006) Acetylphosphinate is the most potent mechanism-based substrate-like inhibitor of both the human and *Escherichia coli* pyruvate dehydrogenase components of the pyruvate dehydrogenase complex, *Bioorg. Chem.* *34*, 362-379.
35. Sergienko, E. A., Wang, J., Polovnikova, L., Hasson, M. S., McLeish, M. J., Kenyon, G. L., and Jordan, F. (2000) Spectroscopic detection of transient thiamin diphosphate-bound intermediates on benzoylformate decarboxylase, *Biochemistry* *39*, 13862-13869.
36. Sergienko, E. A., and Jordan, F. (2002) New model for activation of yeast pyruvate decarboxylase by substrate consistent with the alternating sites mechanism: demonstration of the existence of two active forms of the enzyme, *Biochemistry* *41*, 3952-3967.
37. Shim da, J., Nemeria, N. S., Balakrishnan, A., Patel, H., Song, J., Wang, J., Jordan, F., and Farinas, E. T. (2011) Assignment of function to histidines 260 and 298 by engineering the E1 component of the *Escherichia coli* 2-oxoglutarate dehydrogenase complex; substitutions that lead to acceptance of substrates lacking the 5-carboxyl group, *Biochemistry* *50*, 7705-7709.
38. Hetalben Patel, D. J. S., Edgardo T. Farinas, Frank Jordan (2013) Investigation of the donor and acceptor range for chiral carbonylationcatalyzed by the E1 component of the 2-oxoglutarate dehydrogenase complex, *J. Mol. Catal. B: Enzym.* *98*, 42-45.
39. Balakrishnan, A., Nemeria, N. S., Chakraborty, S., Kakalis, L., and Jordan, F. (2012) Determination of pre-steady-state rate constants on the *Escherichia coli* pyruvate dehydrogenase complex reveals that loop movement controls the rate-limiting step, *J. Am. Chem. Soc.* *134*, 18644-18655.
40. Frank, R. A., Kay, C. W., Hirst, J., and Luisi, B. F. (2008) Off-pathway, oxygen-dependent thiamine radical in the Krebs cycle, *J. Am. Chem. Soc.* *130*, 1662-1668.

41. Reed, G. H., Ragsdale, S. W., and Mansoorabadi, S. O. (2012) Radical reactions of thiamin pyrophosphate in 2-oxoacid oxidoreductases, *Biochim. Biophys. Acta* 1824, 1291-1298.
42. Mansoorabadi, S. O., Seravalli, J., Furdui, C., Krymov, V., Gerfen, G. J., Begley, T. P., Melnick, J., Ragsdale, S. W., and Reed, G. H. (2006) EPR spectroscopic and computational characterization of the hydroxyethylidene-thiamine pyrophosphate radical intermediate of pyruvate:ferredoxin oxidoreductase, *Biochemistry* 45, 7122-7131.
43. Tittmann, K., Wille, G., Golbik, R., Weidner, A., Ghisla, S., and Hubner, G. (2005) Radical phosphate transfer mechanism for the thiamin diphosphate- and FAD-dependent pyruvate oxidase from *Lactobacillus plantarum*. Kinetic coupling of intercofactor electron transfer with phosphate transfer to acetyl-thiamin diphosphate via a transient FAD semiquinone/hydroxyethyl-ThDP radical pair, *Biochemistry* 44, 13291-13303.
44. Frank, R. A., Price, A. J., Northrop, F. D., Perham, R. N., and Luisi, B. F. (2007) Crystal structure of the E1 component of the *Escherichia coli* 2-oxoglutarate dehydrogenase multienzyme complex, *J. Mol. Biol.* 368, 639-651.
45. Muller, M., Gocke, D., and Pohl, M. (2009) Thiamin diphosphate in biological chemistry: exploitation of diverse thiamin diphosphate-dependent enzymes for asymmetric chemoenzymatic synthesis, *FEBS J.* 276, 2894-2904.
46. Kaplun, A., Binshtein, E., Vyazmensky, M., Steinmetz, A., Barak, Z., Chipman, D. M., Tittmann, K., and Shaanan, B. (2008) Glyoxylate carbonylase lacks the canonical active site glutamate of thiamine-dependent enzymes, *Nat. Chem. Biol.* 4, 113-118.
47. Mosbacher, T. G., Mueller, M., and Schulz, G. E. (2005) Structure and mechanism of the ThDP-dependent benzaldehyde lyase from *Pseudomonas fluorescens*, *FEBS J.* 272, 6067-6076.
48. Kokova, M., Zavrel, M., Tittmann, K., Spiess, A. C., and Pohl, M. (2009) Investigation of the carbonylase activity of thiamine diphosphate-dependent enzymes using kinetic modeling and NMR spectroscopy, *Journal of Molecular Catalysis B-Enzymatic* 61, 73-79.
49. Baykal, A., Chakraborty, S., Dodoo, A., and Jordan, F. (2006) Synthesis with good enantiomeric excess of both enantiomers of alpha-ketols and acetolactates by two thiamin diphosphate-dependent decarboxylases, *Bioorg. Chem.* 34, 380-393.
50. Sergienko, E. A., and Jordan, F. (2001) Catalytic acid-base groups in yeast pyruvate decarboxylase. 3. A steady-state kinetic model consistent with the

behavior of both wild-type and variant enzymes at all relevant pH values, *Biochemistry* 40, 7382-7403.

51. Nemeria, N., Tittmann, K., Joseph, E., Zhou, L., Vazquez-Coll, M. B., Arjunan, P., Hubner, G., Furey, W., and Jordan, F. (2005) Glutamate 636 of the *Escherichia coli* pyruvate dehydrogenase-E1 participates in active center communication and behaves as an engineered acetolactate synthase with unusual stereoselectivity, *J. Biol. Chem.* 280, 21473-21482.
52. Schlossberg, M. A., Bloom, R. J., Richert, D. A., and Westerfeld, W. W. (1970) Carboligase activity of alpha-ketoglutarate dehydrogenase, *Biochemistry* 9, 1148-1153.
53. Beigi, M., Waltzer, S., Fries, A., Eggeling, L., Sprenger, G. A., and Muller, M. (2013) TCA cycle involved enzymes SucA and Kgd, as well as MenD: efficient biocatalysts for asymmetric C-C bond formation, *Org. Lett.* 15, 452-455.
54. Jordan, F. (2003) Current mechanistic understanding of thiamin diphosphate-dependent enzymatic reactions, *Nat. Prod. Rep.* 20, 184-201.
55. Jordan, F., Nemeria, N. S., Zhang, S., Yan, Y., Arjunan, P., and Furey, W. (2003) Dual catalytic apparatus of the thiamin diphosphate coenzyme: acid-base via the 1',4'-iminopyrimidine tautomer along with its electrophilic role, *J. Am. Chem. Soc.* 125, 12732-12738.
56. Nemeria, N., Baykal, A., Joseph, E., Zhang, S., Yan, Y., Furey, W., and Jordan, F. (2004) Tetrahedral intermediates in thiamin diphosphate-dependent decarboxylations exist as a 1',4'-imino tautomeric form of the coenzyme, unlike the michaelis complex or the free coenzyme, *Biochemistry* 43, 6565-6575.
57. Jordan, F., Kudzin, Z. H., and Rios, C. B. (1987) Generation and Physical-Properties of Enamines Related to the Key Intermediate in Thiamin Diphosphate Dependent Enzymatic Pathways, *J. Am. Chem. Soc.* 109, 4415-4416.
58. Barletta, G., Huskey, W. P., and Jordan, F. (1992) Observation of a 2-Alpha-Enamine from a 2-(Methoxyphenylmethyl)-3,4-Dimethylthiazolium Salt in Water - Implications for Catalysis by Thiamin Diphosphate-Dependent Alpha-Keto Acid Decarboxylases, *J. Am. Chem. Soc.* 114, 7607-7608.
59. Barletta, G. L., Zou, Y., Huskey, W. P., and Jordan, F. (1997) Kinetics of C(2 alpha)-proton abstraction from 2-benzylthiazolium salts leading to enamines relevant to catalysis by thiamin-dependent enzymes, *J. Am. Chem. Soc.* 119, 2356-2362.
60. Chakraborty, S., Nemeria, N., Yep, A., McLeish, M. J., Kenyon, G. L., and Jordan, F. (2008) Mechanism of benzaldehyde lyase studied via thiamin

- diphosphate-bound intermediates and kinetic isotope effects, *Biochemistry* 47, 3800-3809.
61. Chakraborty, S., Nemeria, N. S., Balakrishnan, A., Brandt, G. S., Kneen, M. M., Yep, A., McLeish, M. J., Kenyon, G. L., Petsko, G. A., Ringe, D., and Jordan, F. (2009) Detection and time course of formation of major thiamin diphosphate-bound covalent intermediates derived from a chromophoric substrate analogue on benzoylformate decarboxylase, *Biochemistry* 48, 981-994.
 62. Kuo, D. J., and Jordan, F. (1983) Direct spectroscopic observation of a brewer's yeast pyruvate decarboxylase-bound enamine intermediate produced from a suicide substrate. Evidence for nonconcerted decarboxylation, *J. Biol. Chem.* 258, 13415-13417.
 63. Zeng, X., Chung, A., Haran, M., and Jordan, F. (1991) Direct Observation of the Kinetic Fate of a Thiamin Diphosphate Bound Enamine Intermediate on Brewers-Yeast Pyruvate Decarboxylase - Kinetic and Regiospecific Consequences of Allosteric Activation, *J. Am. Chem. Soc.* 113, 5842-5849.
 64. Merski, M., and Townsend, C. A. (2007) Observation of an acryloyl-thiamin diphosphate adduct in the first step of clavulanic acid biosynthesis, *J. Am. Chem. Soc.* 129, 15750-15751.
 65. Flournoy, D. S., and Frey, P. A. (1986) Pyruvate dehydrogenase and 3-fluoropyruvate: chemical competence of 2-acetylthiamin pyrophosphate as an acetyl group donor to dihydrolipoamide, *Biochemistry* 25, 6036-6043.
 66. Flournoy, D. S., and Frey, P. A. (1989) Inactivation of the pyruvate dehydrogenase complex of *Escherichia coli* by fluoropyruvate, *Biochemistry* 28, 9594-9602.
 67. Fadnavis, N. W., and Radhika, K. R. (2004) Enantio- and regiospecific reduction of ethyl 4-phenyl-2,4-dioxobutyrate with baker's yeast: preparation of (R)-HPB ester, *Tetrahedron-Asymmetry* 15, 3443-3447.
 68. Liu, M., Sergienko, E. A., Guo, F., Wang, J., Tittmann, K., Hubner, G., Furey, W., and Jordan, F. (2001) Catalytic acid-base groups in yeast pyruvate decarboxylase. 1. Site-directed mutagenesis and steady-state kinetic studies on the enzyme with the D28A, H114F, H115F, and E477Q substitutions, *Biochemistry* 40, 7355-7368.
 69. Gao, Y. (2000) Ph. D. Dissertation Rutgers University.
 70. Kneen, M. M., Pogozheva, I. D., Kenyon, G. L., and McLeish, M. J. (2005) Exploring the active site of benzaldehyde lyase by modeling and mutagenesis, *Biochim. Biophys. Acta* 1753, 263-271.

71. Brandt, G. S., Nemeria, N., Chakraborty, S., McLeish, M. J., Yep, A., Kenyon, G. L., Petsko, G. A., Jordan, F., and Ringe, D. (2008) Probing the active center of benzaldehyde lyase with substitutions and the pseudosubstrate analogue benzoylphosphonic acid methyl ester, *Biochemistry* 47, 7734-7743.
72. Balakrishnan, A., Gao, Y., Moorjani, P., Nemeria, N. S., Tittmann, K., and Jordan, F. (2012) Bifunctionality of the thiamin diphosphate cofactor: assignment of tautomeric/ionization states of the 4'-aminopyrimidine ring when various intermediates occupy the active sites during the catalysis of yeast pyruvate decarboxylase, *J. Am. Chem. Soc.* 134, 3873-3885.
73. Nemeria, N., Korotchkina, L., McLeish, M. J., Kenyon, G. L., Patel, M. S., and Jordan, F. (2007) Elucidation of the chemistry of enzyme-bound thiamin diphosphate prior to substrate binding: defining internal equilibria among tautomeric and ionization states, *Biochemistry* 46, 10739-10744.
74. Woodward, R. B. (1941) Structure and the Absorption Spectra of α,β -Unsaturated Ketones, *J. AM. Chem. Soc* 63, 1123-1126.
75. Fieser, L. F., Fieser, M. (1949) *Natural Products Related to Phenanthrene*, Reinhold.
76. Kuo, D. J., and Jordan, F. (1983) Active site directed irreversible inactivation of brewers' yeast pyruvate decarboxylase by the conjugated substrate analogue (E)-4-(4-chlorophenyl)-2-oxo-3-butenoic acid: development of a suicide substrate, *Biochemistry* 22, 3735-3740.
77. Jordan, F., Kuo, D. J., and Monse, E. U. (1978) A pH-rate determination of the activity-pH profile of enzymes. application to yeast pyruvate decarboxylase demonstrating the existence of multiple ionizable groups, *Anal. Biochem.* 86, 298-302.
78. Meyer, D., Neumann, P., Ficner, R., and Tittmann, K. (2013) Observation of a stable carbene at the active site of a thiamin enzyme, *Nat. Chem. Biol.* 9, 488-490.
79. Jordan, F., Zhang, Z., and Sergienko, E. (2002) Spectroscopic evidence for participation of the 1',4'-imino tautomer of thiamin diphosphate in catalysis by yeast pyruvate decarboxylase, *Bioorg. Chem.* 30, 188-198.

APPENDIX

CHAPTER 2

Results (unpublished)

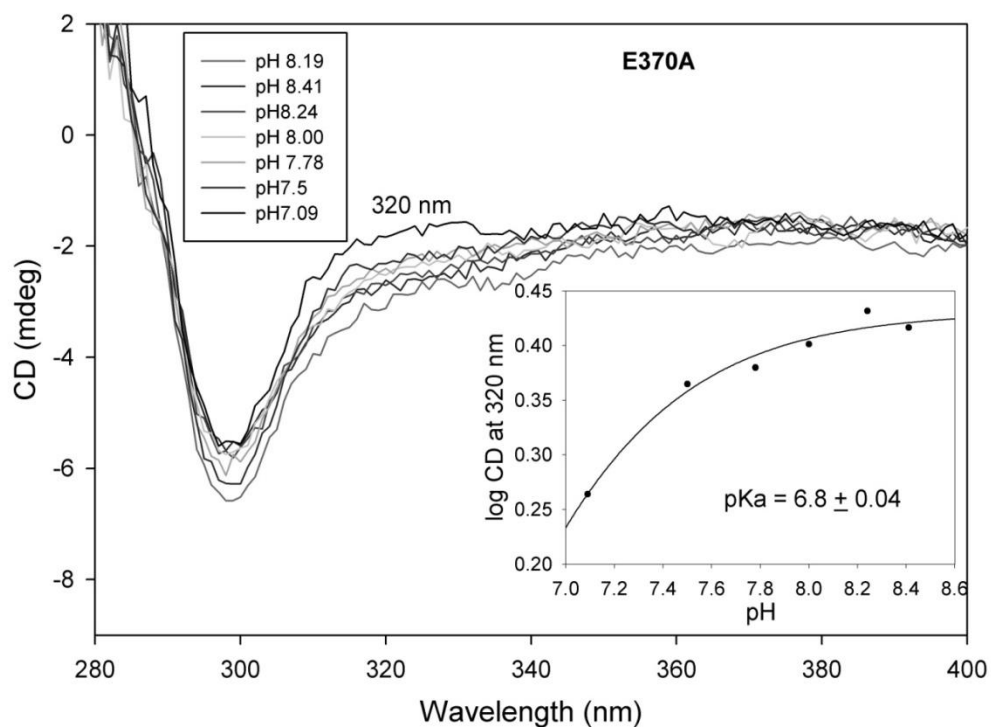
E370A DXP synthase

Figure A1 pH titration of the AP form of ThDP on E370A DXP synthase (22.2 μ M active centers) at 320 nm in triple pH buffer system containing 50 mM MES, 50 mM acetic acid and 100 mM Tris in the pH range 7.0 – 8.19 at 37 °C. (Inset) Dependence of the CD at 320 nm on pH. The data were treated using Eq 3 in Chapter 2.

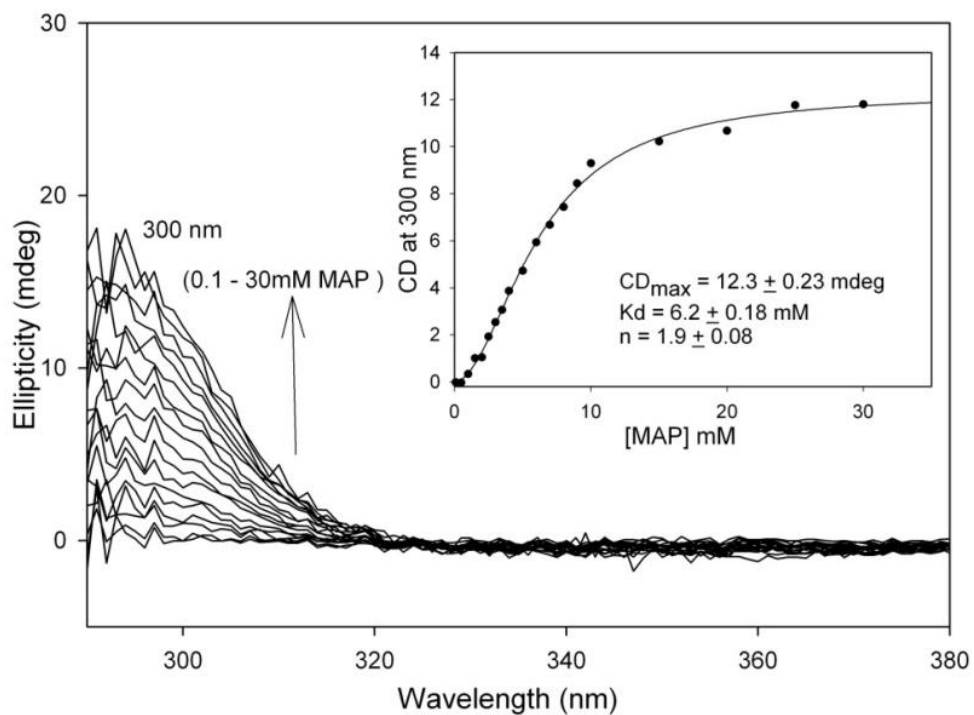


Figure A2. CD titration of E370A DXP synthase (44.8 μ M active site concentration) with MAP (0.001-30 mM) in buffer B (see Material and Methods section in Chapter 2) at 37 $^{\circ}$ C. The 1',4'-iminopyrimidinyl tautomer of phosphonolactylThDP is seen at 300 nm. (Inset) CD amplitude of IP form at 300 nm plotted against concentration of MAP using Eq 1 in Chapter 2.

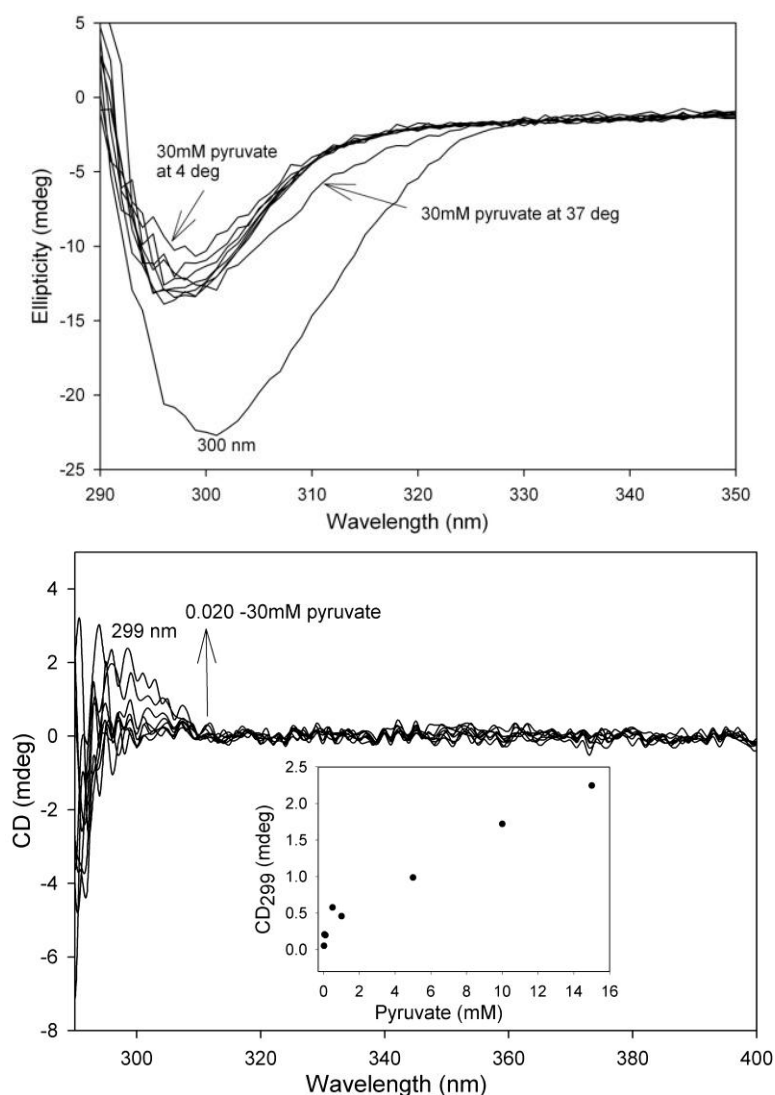


Figure A3 Top. E370A DXP synthase titration with pyruvate (0.02-30 mM) in buffer B (see Material and Methods section in Chapter 2) at 4 °C. Bottom. After subtraction of each recorded spectrum in the presence of pyruvate from the enzyme (Inset) CD changes at 299 nm. The CD spectrum of this variant appeared different from that of wild type DXP synthase, displaying a strong negative CD band at 298 nm and amplitude was reduced by addition of different concentrations of pyruvate (Top). Difference spectra revealed a positive CD band at 299 nm, but it did not display saturation (Bottom). Raising the temperature to 37 °C led to immediate formation of a negative CD band at 300 nm corresponding to (*R*)-acetolactate product.

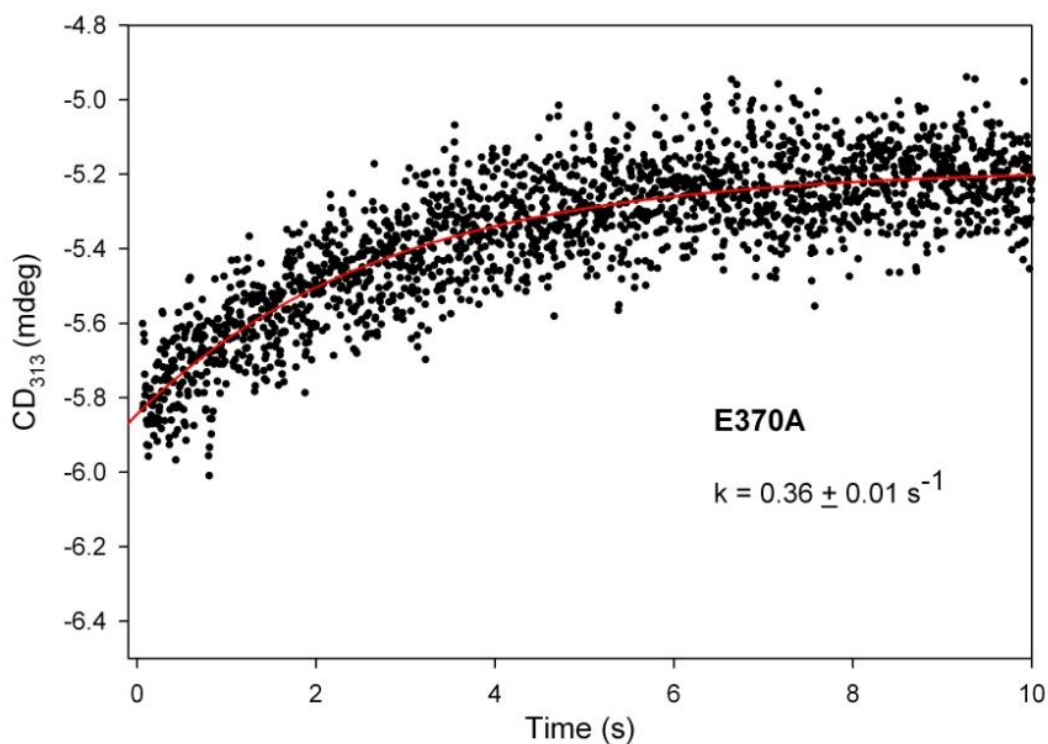


Figure A4 Pre-steady state formation of 1',4'-iminoLThDP. A solution of E370A DXP synthase (7.0 mg/ml, 103.3 μM active centers) in buffer B was placed in one syringe and an equal volume of pyruvate (30 mM) in the same buffer was placed in the second syringe. Spectra were recorded over a period of 10 s. Data were fit to a single-exponential model as in Eq 5, see Chapter 2).

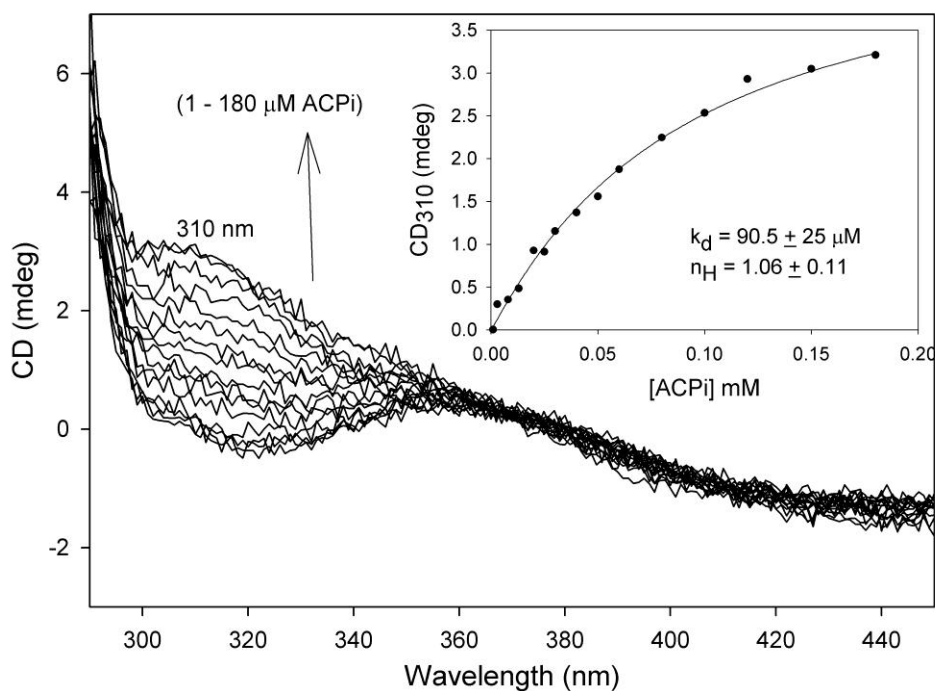
Y392F DXP synthase

Figure A5. CD titration of Y392F DXP synthase (29.6 μM active site concentration) with ACPi (0.001-30 mM) in buffer B (see Material and Methods section in Chapter 2). Formation of 1',4'-iminopyrimidinyl tautomer at 310 nm. (Inset) CD amplitude at 310 nm was plotted against [ACPi] using Eq 1 in Chapter 2.

Wt DXP synthase with D-glyceraldehyde

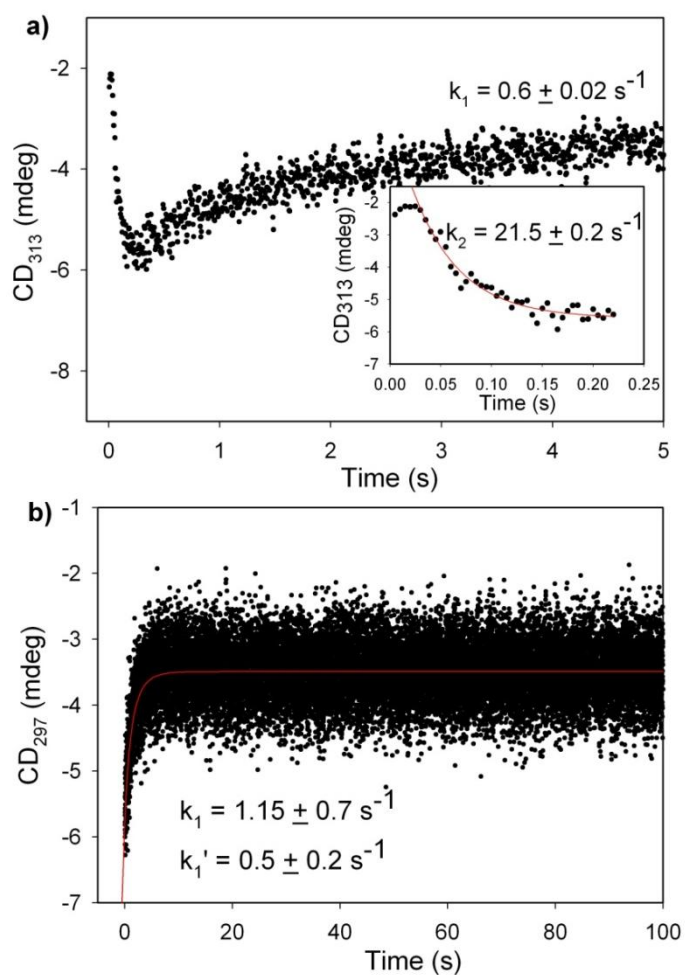


Figure A6. **a)** LThDP decarboxylation and re-synthesis at 313 nm was observed by mixing wt DXP synthase (47.5 μM active centers) with pyruvate (500 μM) to pre-form LThDP from one syringe with 30 mM D-glyceraldehyde placed in second syringe, both in 50 mM Tris (pH 8) containing 100 mM NaCl, 0.5 mM ThDP, 2 mM MgCl_2 , 1 mM DTT, 1 % glycerol. The reaction was monitored for 5 s at 8 $^\circ\text{C}$. **b)** DXS product formation was observed at 297 nm by mixing 1 μM wt DXP synthase from one syringe with 30 mM D-glyceraldehyde and 5 mM pyruvate from second syringe using same buffer as in **a)**. The reaction was monitored for 100 s at 8 $^\circ\text{C}$.

Wt DXP synthase with oxime inhibitors (GAP analogues).

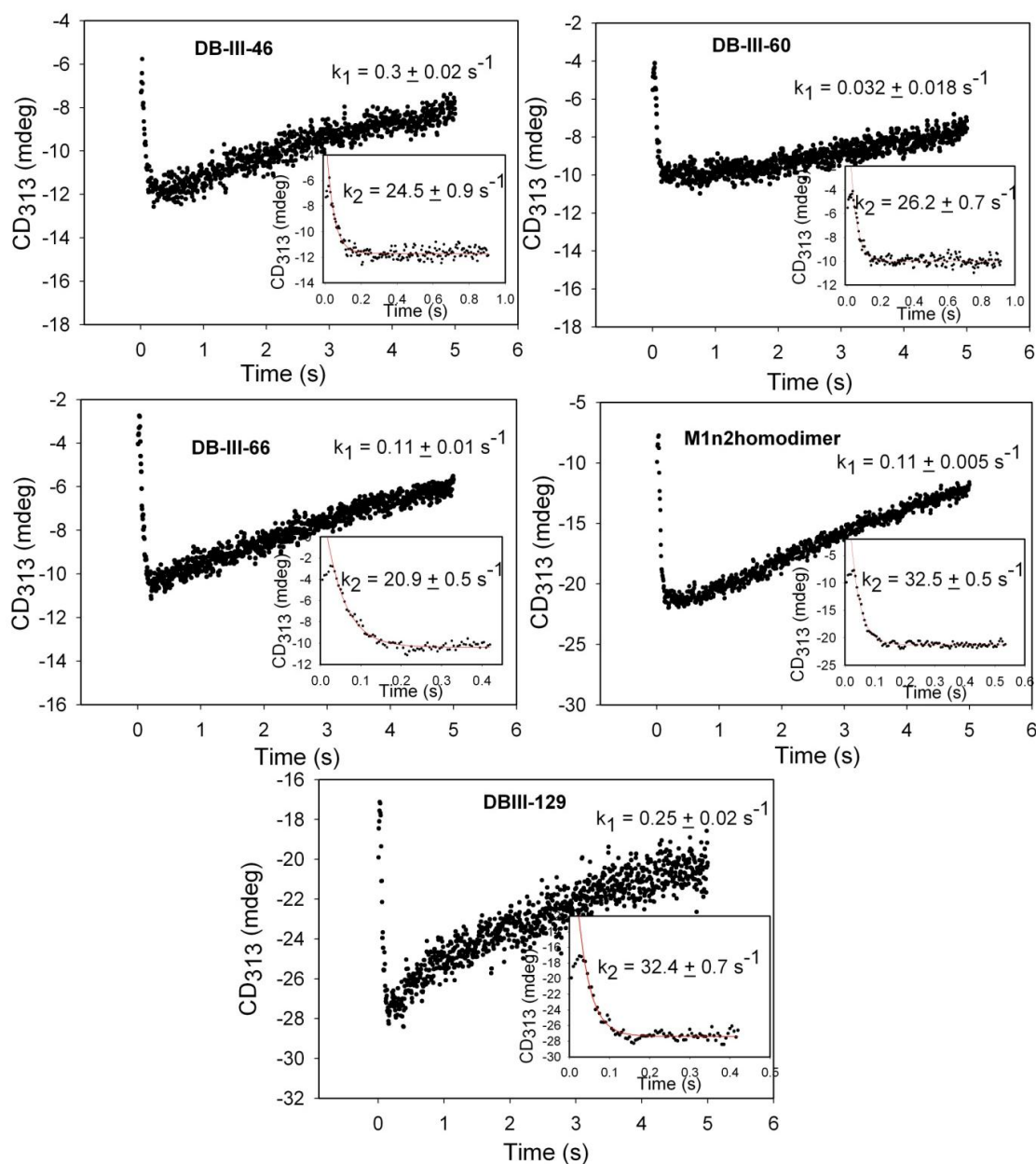
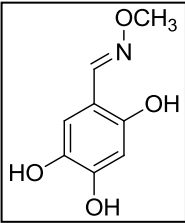
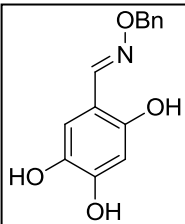
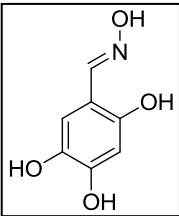
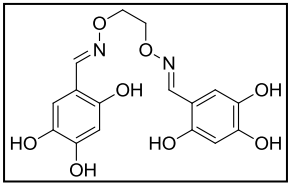
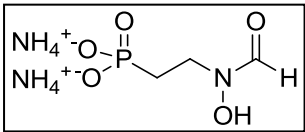


Figure A7. DXP synthase (36 μM active centers) mixed with pyruvate (200 μM) to pre-form LThDP in one syringe then rapidly mixed with an oxime [DB-III-46 (40 μM) or DB-III-60 (50 μM) or DB-III-66 (30 μM) or M1n2homodimer (20 μM) or DB-III-129 (5 mM)] placed in second syringe, both in 50 mM Tris (pH 8.0) containing 100 mM NaCl, 0.5 mM ThDP, 2 mM MgCl₂, 1 mM DTT, 1 % glycerol and 10% DMSO. The LThDP

decarboxylation was monitored at 313 nm for 5 s at 8 °C. **Note:** All of the oximes were first dissolved in DMSO (main stock) and for the experiment were diluted into buffer with 10% DMSO.

Table A1. Summary of pre-steady state rate determination on wt DXP synthase with oximes inhibitors at 313 nm.

Name	structure	LThDP decarboxylation (k_2 s ⁻¹)	LThDP resynthesis (k_1 s ⁻¹)
DB-III-46^a ($K_i = 3.2$ μM) ^b MWt:183.16		24.5 ± 0.9	0.3 ± 0.02
DB-III-60^a ($K_i = 4.5$ μM) ^b MWt:259.26		26.2 ± 0.7	0.032 ± 0.018
DB-III-66^a ($K_i = 2.1$ μM) ^b MWt:169.13		20.9 ± 0.5	0.11 ± 0.01
M1n2homodimer^a ($K_i = 0.9$ μM) ^b MWt:364.31		32.5 ± 0.5	0.11 ± 0.005
DB-III-129^a MWt:203.13		32.4 ± 0.7	0.25 ± 0.02

^aThe synthesized oximes with the given name codes were from JHU. ^b K_i measurements were performed by JHU group.

CHAPTER 3

Materials

The Wizard® Plus Minipreps DNA purification system was used for purification of DNA (Promega, Madison, WI). The QuikChange® II site-directed mutagenesis kit was used (Stratagene, La Jolla, CA). DNA sequencing was done at the Molecular Resource Facility of the New Jersey Medical School (Newark, NJ). *E. coli* BL21(DE3) cells were from Novagen (EMD Chemicals, Gibbstown, NJ). Primers were from Integrated DNA Technologies, Inc. (Coralville, IA).

The primer used to create E2o-ec didomain¹⁻¹⁷⁶:

5'-ctctggctgcacgtagtgaataacgtgtcccg-3'

Plasmid Purification

Plasmid purification was done based on protocol of Wizard® Plus Minipreps DNA purification kit from Promega. E2o-ec cells were spread on the LB agar plate containing 30 µg/ml chloramphenicol. Single colonies were chosen and grown overnight at 37 °C in 10 ml LB medium containing 30 µg/ml chloramphenicol followed by the plasmid purification protocol below:

1. Pellet 5-10 ml of cells by centrifugation at $1,400 \times g$ for 10 min. Pour off the supernatant and blot the tube upside-down on a paper towel to remove excess media.
2. Completely resuspend the cell pellet in 400 µl of Cell Resuspension Solution. Transfer the resuspended cells to a 1.5 ml microcentrifuge tube.
3. Add 400 µl of Cell Lysis Solution and mix by inverting the tube 4 times. The cell suspension should clear immediately.

4. Add 400 μ l of Neutralization Solution and mix by inverting the tube several times. Alternatively, if using an EndA+ strain, add 800 μ l of Neutralization Solution, mix by inverting the tube 4 times and incubate at room temperature for 10 min.
5. Centrifuge the lysate at 10,000 \times g in a microcentrifuge for 5 min. If a pellet has not formed by the end of the centrifugation, centrifuge an additional 15 min.
6. Pipet 1 ml of the resuspended resin into each barrel of the Minicolumn syringe assembly. (If crystals or aggregates are present, dissolve by warming the resin to 25-37 $^{\circ}$ C for 10 min. Cool to 30 $^{\circ}$ C before use). Thoroughly mix the Wizard[®] Minipreps DNA Purification Resin before removing an aliquot.
7. Carefully remove all the cleared lysate from each miniprep and transfer it to the barrel of the Minicolumn/syringe assembly containing the resin. No mixing is required at this stage. The resin and lysate should be in contact only for the time it takes to load the Minicolumns.
8. Open the stopcocks and apply a vacuum of at least 15 inches of Hg to pull the resin/lysate mix into the Minicolumn. When the entire sample has completely passed through the column, break the vacuum at the source.
If using an EndA+ strain, add 2 ml of 40% isopropanol/4.2M guanidine hydrochloride solution to each column. Apply a vacuum and continue it for 30 s after all of the solution has flowed through the columns. Note that this solution will flow through the column more slowly than the standard Column Wash Solution. After this wash proceed with the standard column wash procedure (Step 9).
9. Add 2 ml of the Column Wash Solution (containing 95% ethanol) to the Syringe Barrel and reapply the vacuum to draw the solution through the Minicolumn.

10. Dry the resin by continuing to draw a vacuum for 30 s after the solution has been pulled through the column. Do not dry the resin for more than 30 s. Remove the Syringe Barrel and transfer the Minicolumn to a 1.5 ml microcentrifuge tube. Centrifuge the Minicolumn at $10,000 \times g$ in a microcentrifuge for 2 min to remove any residual Column Wash Solution.

11. Transfer the Minicolumn to a new microcentrifuge tube. Add 50 μ l of nuclease-free water to the Minicolumn and wait 1 min. Centrifuge the tube at $10,000 \times g$ in a microcentrifuge for 20 s to elute the DNA. The DNA will remain intact on the Minicolumn for up to 30 min; however, prompt elution will minimize nicking of plasmids in the range of 20kb. For elution of large plasmids (≥ 10 kb), the use of water preheated to 65-70 °C may increase yields. For plasmids ≥ 20 kb, use water preheated to 80 °C.

12. Remove and discard the Minicolumn. DNA is stable in water without addition of buffer if stored at -20 °C or below. DNA is stable at 4 °C in TE buffer. To store the DNA in TE buffer, add 5 μ l of 10X TE buffer to the 50 μ l of eluted DNA.

13. The concentration of plasmids was measured using $\epsilon = 0.050$ at 260nm.

Plasmid Digestion

For plasmid digestion XhoI was used (vector PCA24N, molecular weight 5240 bp). The reaction medium contained in 1 μ l buffer 4, 5 μ l plasmid, 1 μ l BSA, 2 μ l distilled water and reaction was started by addition of 1 μ l of XhoI enzyme. The reaction was kept for overnight incubation at 37 °C and checked by Agarose gel.

Primer design

Primers were designed using program QuikChange Primer Design from Agilent Technologies.

- 1) Both mutagenic primers must contain the desired mutation and anneal to the same sequence on opposite strands of the plasmid.
- 2) Primers ideally should be between 25 and 45 bases in length, with a melting temperature (T_m) of ≥ 78 °C. Primers longer than 45 bases may be used, but using longer primers increases the likelihood of secondary structure formation, which may affect the efficiency of the mutagenesis reaction.
- 3) The desired mutation (deletion or insertion) should be in the middle of the primer with ~10–15 bases of correct sequence on both sides.
- 4) The primers optimally should have a minimum GC content of 40% and should terminate in one or more C or G bases.
- 5) The received primers and antiprimers were centrifuged for 6 min and dissolved in 100 μ l sterilized water which was centrifuged for 10 min. The concentration was measured using molar extinction coefficient (ϵ) = 0.033 at 260nm.

Mutagenesis

Mutagenesis was carried out using the QuikChange® II site-Directed mutagenesis kit.

[Stratagene Instruction manual Revision B (2007)]

1. Prepare the control reaction as indicated below:

5 μ l of 10 \times reaction buffer

2 μ l (10 ng) of pWhitescript 4.5-kb control plasmid (5 ng/ μ l)

1.25 μl (125 ng) of oligonucleotide control primer #1 [34-mer (100 ng/ μl)]

1.25 μl (125 ng) of oligonucleotide control primer #2 [34-mer (100 ng/ μl)]

1 μl of dNTP mix

38.5 μl of double-distilled water (ddH₂O) to a final volume of 50 μl

Then add

1 μl of *PfuTurbo* DNA polymerase (2.5 U/ μl)

2. Prepare the sample reaction(s) as indicated below:

5 μl of 10 \times reaction buffer

5–50 ng of dsDNA template (1 μl)

125 ng of oligonucleotide primer #1 (5 μl)

125 ng of oligonucleotide primer #2 (5 μl)

1 μl of dNTP mix

ddH₂O to a final volume of 50 μl

Then add 1 μl of *PfuTurbo* DNA polymerase (2.5 U/ μl)

3. [Note: If the thermal cycler to be used does not have a hot-top assembly, overlay each reaction with ~30 μl of mineral oil].

Set up cycling parameters for the site directed mutagenesis method

Segment 1: 1 cycle at 95°C for 30 seconds

Segment 2: 16 cycles at 95°C for 30 seconds, then 55°C for 1 minute, finally 68°C for 1 minute/kb of plasmid length

4. Cycle each reaction using the cycling parameter. For the control reaction, use a 5 minute extension time and run the reaction for 18 cycles.

5. Adjust segment 2 of the cycling parameters in accordance with the type of mutation desired. For single amino acid changes, 16 cycles can be used.

6. Following temperature cycling, place the reaction on ice for 2 minutes to cool the reaction $\leq 37\text{ }^{\circ}\text{C}$

7. *Dpn* I digestion of the amplification products

1. Add 1 μl of the *Dpn* I restriction enzyme (10 U/ μl) directly to each amplification reaction below the mineral oil overlay using a small, pointed pipet tip.

2. Gently and thoroughly mix each reaction mixture by pipetting the solution up and down several times. Spin down the reaction mixtures in a microcentrifuge for 1 minute and immediately incubate each reaction at 37°C for 1 hour to digest the parental supercoiled dsDNA

Transformation of XL1-Blue supercompetent cells

1. Gently thaw the XL1-Blue supercompetent cells on ice. For each control and sample reaction to be transformed, aliquot 50 μl of the supercompetent cells to a *prechilled* 14 ml BD Falcon polypropylene round-bottom tube.

2. Transfer 1 μl of the *Dpn* I-treated DNA from each control and sample reaction to separate aliquots of the supercompetent cells. As an optional control, verify the transformation efficiency of the XL1-Blue supercompetent cells by adding 1 μl of the pUC18 control plasmid (0.1 ng/ μl) to a 50 μl aliquot of the supercompetent cells. Swirl the transformation reactions gently to mix and incubate the reactions on ice for 30 minutes.

3. Heat pulse the transformation reactions for 45 seconds at $42\text{ }^{\circ}\text{C}$ and then place the reactions on ice for 2 minutes.

4. Add 0.5 ml of NZY+ broth preheated to 42 °C and incubate the transformation reactions at 37 °C for 1 hour with shaking at 225–250 rpm.
5. Plate the appropriate volume of each transformation reaction on agar plates containing the appropriate antibiotic for the plasmid vector. e. g. pWhitescript mutagenesis control: 250 µl, pUC18 transformation control: 5 µl in 200 µl of NZY+ broth, sample mutagenesis: 250 µl on each of two plates (entire transformation reaction). For the mutagenesis and transformation controls, spread cells on LB ampicillin agar plates containing 80 µg/ml X-gal (100 µl from 2 % stock) and 20 mM IPTG (100 µl from 10 mM stock).
6. Incubate the transformation plates at 37 °C for > 16 hours.

Transformation of AG1 competent cells

1. Pre-chill two 14-ml BD Falcon polypropylene round-bottom tubes on ice. Preheat SOC medium to 42°C.
2. Thaw the cells on ice, gently mix and add 100 µl to each polypropylene tubes.
3. Add 1.7 µl of the β-mercaptoethanol provided with kit to each aliquot of cells.
4. Swirl the tubes gently. Incubate the cells on ice for 10 minutes, swirling gently every 2 minutes. (note: do not need control here so two tubes can be used for sample plasmids)
5. Add 1-50 ng (1 µl) of experimental DNA.
6. Incubate the tubes on ice for 30 minutes.
7. Heat-pulse the tubes in a 42 °C water bath for 45 seconds. The duration of the heat pulse is critical.
8. Incubate the tubes on ice for 2 minutes.

9. Add 0.9 ml pre-heated SOC medium and incubate at 37 °C for 1 hour with shaking at 225-250 rpm.
10. Plate (5 µl+100 µl SOC, 50 µl+100 µl SOC, 150 µl plasmid) the transformation mixture on LB-ampicillin agar plates. Incubate the plates at 37 °C overnight.

Check expression

1. From the above plates 5 different colonies were chosen and grown overnight at 37 °C in 2 ml LB medium containing 30 µg/ml chloramphenicol.
2. Inoculated 0.2 ml overnight culture into 10 ml LB medium with 30 µg/ml chloramphenicol (50 times dilution) and incubated for 2 hour at 37 °C.
3. After addition of 1 mM IPTG cells were grown for additional 4-5 hour at 37 °C.
4. Cells were collected by centrifugation of 1 ml from each and stored at -20 °C. The expression was checked by SDS-PAGE.

Cells storage at -80 °C

Overnight culture of 10 ml LB medium containing 30 µg/ml chloramphenicol (5 tubes) was grown overnight at 37 °C. In small 1.5 ml tube (3 tubes from each culture) was taken 0.15 ml 70 % sterilized glycerol and 0.85 ml overnight culture and stored immediately in liquid nitrogen until it is ready to store at -20 °C.

His6-tag E2o-ec¹⁻¹⁷⁶ didomain purification

Protein expression

By using above cells 4 tubes with 10 ml of LB medium containing 30 µg/ml of chloramphenicol were grown at 37°C for overnight. Which was inoculated into 700 ml of LB medium containing 30 µg/ml of chloramphenicol and 0.30 mM lipoic acid from 0.3 M stock in ethanol (total 4 flasks volume of 2000 ml with 700 ml of LB medium in each).

Cells were grown for about 2-2.5 hours at 37°C to OD600 = 0.60-0.70. Then 0.50 mM IPTG was added, and cells were grown for 5-6 hours at 37°C and were collected and washed with 20 mM KH₂PO₄ (pH 7.0) containing 0.15 M NaCl. Cell pellets were stored at -20°C until purification.

Cell disruption

Cells were dissolved in 40-50 ml of the sonication buffer containing 50 mM KH₂PO₄ (pH 7.5), 0.3 M NaCl, 1 mM benzamidine HCl and 1 mM PMSF. Lysozyme was added to a final concentration of 0.60 mg/ml, and cells were incubated for 20 min on ice. Then sonication was performed by using 20" on 20" off 5 min and centrifugation at 18,000 rpm for 30 min. To avoid DNA contamination, 0.8 % streptomycin sulfate was added to the clear extract and cells were incubated an additional 20 min on ice to digest the DNA. Next the cell was treated by sonication as mentioned above until the clear cells extract was obtained.

Purification using Ni²⁺ Sepharose 6 fast flow column

His6-tag E2ec¹⁻¹⁷⁶ didomain was purified by using His6-tag Ni-NTA column. The column was equilibrated with 50 ml of sonication buffer and cell extract was applied in volume of 50 ml on the column. Then washed with 10 column volume binding buffer containing 50 mM KH₂PO₄ (pH 7.5), 0.3 M NaCl and 20 mM imidazole. The bound proteins were eluted using elution buffer containing 50 mM KH₂PO₄ (pH 7.5), 0.3 M NaCl and 200 mM imidazole. The fractions containing protein were dialyzed overnight in dialysis buffer containing 50 mM KH₂PO₄ (pH 7.5), 0.15 M NaCl and 1 mM benzamidine HCl. The enzyme was concentrated using a Millipore concentration unit.

Overexpression and purification of E1o. An *E. coli* frozen stock of the E1o harboring the plasmid [(transformed in BL21 (DE3))] was streaked on LB agar plates containing chloramphenicol (100 µg/ml) and incubated at 37 °C overnight. A single colony was used to inoculate 10 ml of LB medium containing chloramphenicol (100 µg/ml). The overnight culture was used to inoculate 700 ml of LB medium containing chloramphenicol (100 µg/ml). The culture was induced with 1 mM IPTG, 1 mM thiamin hydrochloride and 2 mM MgCl₂ and incubated at 20 °C with shaking overnight. The cells were precipitated at 4400 g at 4 °C, and stored at -20 °C. The cells were resuspended in 20 mM KH₂PO₄ (pH 7.0) containing 0.1 M NaCl, 2 mM MgCl₂, 1 mM ThDP, 1 mM benzamidine hydrochloride, 1 mM PMSF, 0.6 mg/ml lysozyme and incubated on ice for 20 min. The cells were sonicated for 6 min (10 s pulsar on and 10 s pulsar off) using the Sonic Dismembrator Model 550 from Fisher Scientific. The lysate was centrifuged at 30,000 g at 4 °C for 30 min. The supernatant was applied to a Ni Sepharose 6 Fast Flow Column and equilibrated with 20 mM KH₂PO₄ (pH 7.4) contained 0.1 M NaCl, 2 mM MgCl₂, 1 mM ThDP and 1 mM benzamidine hydrochloride. The enzyme was eluted with 20 mM KH₂PO₄ (pH 7.4) containing 0.5 M NaCl, 0.150 M imidazole, 2 mM MgCl₂, and 1 mM ThDP. Fractions with enzyme were combined, dialyzed against 20 mM KH₂PO₄ (pH 7.4) containing 2 mM MgCl₂, 1 mM ThDP and 1 mM benzamidine hydrochloride. Next, the enzyme was concentrated and stored at -20 °C with 20% glycerol. The purity was confirmed by SDS-PAGE.

Preparation of apo E1o. apo E1o was purified in the absence of thiamin during the protein over expression and also in the buffers during purification steps.

SDS-PAGE

Determination of the purity of protein fractions from the Ni²⁺ Sepharose 6 fast flow column was performed by using SDS PAGE. described in Mini-PROTEAN® 3 Cell Instruction Manual.

The procedure for gel casting (Mini-PROTEAN® 3 Cell Instruction Manual, bulletin # 4006157B)

1. For E1ec, 7.5 % Laemmli buffer system was used. 2.5 ml of 30 % acrylamide/ Bis stock solution in 4.85 ml of deionized water, 2.50 ml of 1.5 M Tris-HCl (pH 8.8), 100 µl of 10 % SDS and 50 µl of 10% APS were combined for making resolving gel. For E2o-ec, 12 % Laemmli buffer was used. 4.0 ml of 30 % acrylamide/ Bis stock solution and 3.35 ml of deionized water was used with same reagents as 7.5 % system.
2. 5.0 µl of TEMED was added into this mixture to initiate polymerization. This solution was added to the preassembled case immediately, and deionized water was overlaid. Then, the cast containing resolving gel solution was solidified for 30 min at room temperature.
3. After 30 min at room temperature, overlaid water was decanted from the cast, and 1.33 ml of 30 % acrylamide/ Bis stock solution in 6.10 ml of deionized water, 2.5 ml of 0.5 M Tris-HCl (pH 6.8), 100 µl of 10 % SDS and 50 µl of 10% APS was combined for making stacking gel.
4. 10.0 µl of TEMED was added into this mixture to initiate polymerization. This solution was poured on the top of solidified resolving gel, and sample combs were added on the stacking gel for making sample pockets. This cast containing stacking gel solution was solidified for 30 min at room temperature.

Sample preparation

Protein fractions from columns were diluted to 1-2 $\mu\text{g/ml}$ concentration. From that 5 μl sample was taken and added 50 μl of sample buffer containing 3.8 ml of deionized water, 0.5 M Tris-HCl (pH 6.8), 0.8 ml of glycerol, 10 % (w/v) SDS, 0.4 ml of 2-mercaptoethanol, and 1 % (w/v) bromophenol blue (8.0 ml total volume) and this mixture was heated for 3 min in boiling water bath.

Loading and running samples on SDS-PAGE

1. 15-20 μl of prepared samples were applied to the gel and allowed to run for 15 min at 100 volts and then for 40 min at 140 volts.
2. The gel was stained with staining solution containing 40 % methanol, 10 % acetic acid and 0.1 % Coomassie blue R-250 indicator for 15 min and destained with destaining solution (I) containing 50 % methanol and 10 % acetic acid for 10 min and (II) 5 % methanol and 7 % acetic acid for overnight.

Determination of Protein concentration by Bradford assay

The calibration of Bradford reagent

1. Prepare dye reagent by diluting 1 part Dye Reagent Concentrate (Bio-Rad catalog # 500-0006) with 4 parts deionized water. Filter through Whatman #1 filter (or equivalent) to remove particulates and store at 4 $^{\circ}\text{C}$. Every 2 weeks calibrate the Bradford reagent.
2. Prepare five to ten dilutions of a protein standard (BSA $\sim 2\text{mg/ml}$), which is representative of the protein solution to be tested. The linear range of the assay for BSA is 0.1 to 0.9 mg/ml .
3. Pipet 50 μl of each standard and sample solution into a clean, dry test tube. Protein solutions are normally assayed in duplicate or triplicate.

4. Add 2.5 ml of diluted dye reagent to each tube and vortex.
5. Incubate at room temperature for at least 5 min and measure absorbance at 595 nm.
6. Plot the absorbance as a function of standard (BSA) concentration to make a calibration curve from which concentration of similarly treated unknown could be determined.

The determination of protein concentration

1. Appropriately dilute protein (usually 5x or 10x dilution) and pipet 5 μ l and 10 μ l of diluted protein into clean and dry test tubes to 50 μ l of total volume with deionized water.
2. Add 2.5 ml of diluted dye reagent to each tube and vortex.
3. Incubate at room temperature for at least 5 min and measure absorbance at 595 nm.
4. Estimate protein concentration using the linear equation from the calibration of bradford dye reagent.

CURRICULUM VITAE

Date and place of birth: 22 nd April 1984, Gujarat, India	
B. Sc. , Chemistry, Saurashtra University, India	2004
M. Sc. , Organic Chemistry, Saurashtra University, India	2006
Quality Control Chemist , Mepro Pharmaceuticals Ltd., India	2006-2007
Research Associate , Jubilant Chemsys, India	2007-2008
Ph. D. , chemistry, Rutgers University, Newark, New Jersey	2009-2013

Awards and honors

Graduate student excellence award	2013
ASBMB Travel award	2013
Rutgers graduate student government association travel award	2013
Rutgers University graduate dissertation fellowship	2012

Publications

1. Synthesis of multifunctional chiral compounds with high enantiomeric excess using the E1 component of the 2-oxoglutarate dehydrogenase complex. Hetalben Patel, Da Jeong Shim, Edgardo T. Farinas and Frank Jordan. *J. Mol. Catal. B Enzym.*, **2013**, 98, 42-45.
2. Catalysis in enzymatic decarboxylations: Comparison of selected cofactor-dependent and cofactor-independent examples. Frank Jordan and Hetalben Patel. *ACS Catal.*, **2013**, 3, 1601–17 (**review**).
3. Observation of thiamin-bound intermediates and microscopic rate constants for their interconversion on 1-deoxy-d-xylulose 5-phosphate synthase: 600-fold rate acceleration of pyruvate decarboxylation by d-glyceraldehyde-3-phosphate. Hetalben Patel, Natalia S. Nemeria, Leighanne A. Brammer, Caren L. Freel Meyers and Frank Jordan. *J. Am. Chem. Soc.*, **2012**, 134, 18374-79.
4. Glyoxylate carboligase: a unique thiamin diphosphate-dependent enzyme that can cycle between the 4'-aminopyrimidinium and 1',4'-iminopyrimidine tautomeric forms in the absence of the conserved glutamate. Natalia Nemeria, Elad Binshtein, Hetalben Patel, Anand Balakrishnan, Ilan Vered, Boaz Shaanan, Ze'ev Barak, David Chipman, and Frank Jordan. *Biochemistry*, **2012**, 51, 7940-52.
5. Assignment of function to histidines 260 and 298 by engineering the e1 component of the escherichia coli 2-oxoglutarate dehydrogenase complex; substitutions that lead to acceptance of substrates lacking the 5-carboxyl group. Da Jeong Shim, Natalia S. Nemeria, Anand Balakrishnan, Hetalben Patel, Jaeyoung Song, Junjie Wang, Frank Jordan, and Edgardo T. Farinas. *Biochemistry*, **2011**, 50, 7705-09.